NONDESTRUCTIVE EVALUATION OF VENEER QUALITY BASED ON ACOUSTIC WAVE MEASUREMENTS

By

JIANHE WANG

B.Sc., Nanjing Forestry University, 1985

M.Sc., Nanjing Forestry University, 1988

A THESIS SUBMITTED IN PARTIAL FULFILLMENT OF

THE REQUIREMENTS FOR THE DEGREE OF

MASTER OF SCIENCE

in

FACULTY OF GRADUATE STUDIES

Department of Wood Science

We accept this thesis as conforming

to the required standard

THE UNIVERSITY OF BRITISH COLUMBIA

February, 1998

In presenting this thesis in partial fulfilment of the requirements for an advanced degree at the University of British Columbia, I agree that the Library shall make it freely available for reference and study. I further agree that permission for extensive copying of this thesis for scholarly purposes may be granted by the head of my department or by his or her representatives. It is understood that copying or publication of this thesis for financial gain shall not be allowed without my written permission.

Department of Wood Science

The University of British Columbia
Vancouver, Canada

Date March 5, 1998

DE-6 (2/88)

ABSTRACT

Veneer quality is critical to the performance of veneer based wood composites. In some engineered applications, lathe checks and knots have been identified as two most critical veneer grade factors affecting the shear strength which generally controls the load carrying capacity of these products. Currently, a nondestructive evaluation (NDE) method to detect veneer lathe checks and assess veneer overall quality is unavailable.

In this thesis, a NDE method for veneer overall quality assessment using stress wave and acousto-ultrasonic (AU) techniques has been developed. This method is based on the detection of lathe checks and knots with wave propagation in both parallel and perpendicular to grain directions. The sensitivity of stress wave and AU techniques for detecting lathe checks and knots through observed differences in the shape of waveforms, frequency components, stress wave timing (velocities) and attenuations was evaluated. The severity of lathe checks and size of knots were also quantified with wave parameters using multiple regression models. Further, an observed veneer overall quality criterion (Q) defined by averaged lathe check depth (LCD) and percentage of knot area (PKA) was established.

The significant findings of this research included: 1) wave propagation perpendicular to grain is sensitive to the presence of lathe checks, but cannot accurately detect the existence of knots; whereas wave transmission parallel to grain is sensitive to the existence of knots, but cannot reliably detect the presence of lathe checks; therefore to evaluate veneer overall quality based on the detection of both lathe checks and knots, measurements should be taken in both directions; 2) there is no significant difference in wave timing (or velocity) measurements between stress wave method and AU method with both methods showing strong promise to detect lathe checks and

knots; 3) wave timing and attenuation perpendicular to grain are strongly affected by averaged lathe check depth (LCD), but quantification of LCD cannot be significantly improved by incorporating both parameters into regression models; 4) a satisfactory NDE approach of knots in veneer has been achieved by using percentage of knot area (PKA) and incorporating wave parameters such as the standard deviation of parallel wave timings; 5) a regression model based on wave velocities in two orthogonal directions can predict the observed overall quality criterion (Q) with r^2 from 0.392 to 0.500 for the stress wave method, which shows promise to nondestructively evaluate the veneer quality for engineered applications.

TABLE OF CONTENTS

LIST OF TABLES

LIST OF FIGURES

LIST OF PHOTOGRAPHS

ACKNOWLEDGMENTS

I would like to express my sincere gratitude to my supervisor Dr. Frank Lam for his invaluable advice and patient guidance throughout this research.

My special appreciation goes to Dr. Jacek Biernacki for his advice and invaluable support during my research especially experimental setup and data processing. Also, gratitude is extended to Dr. J. D. Barrett and Dr. A. Akhtar for reviewing and providing feedback on the thesis while serving on the final examining committee.

I would like to thank Powertech Labs Inc. for their kind cooperation and permission allowing me to use their ultrasonic equipment. Thanks are also due to Mr. Bob Myronuk and Mr. David Kung for their technical assistance for the experimental setup. Dr. S. Avramidis is thanked for providing the stress wave timer.

The financial support from NSERC to the research grant of Dr. Frank Lam is gratefully acknowledged. Finally, my gratitude goes to my wife – Kaiyuan Wang for her encouragement during this research.

1. INTRODUCTION

Plywood, laminated veneer lumber (LVL) and laminated veneer panels (LVP) are structural veneer based wood composites. The structural performance of these products depends on factors such as veneer quality and processing variables.

The factors which affect veneer quality can be broadly classified as: 1) veneer machining defects such as lathe checks, roughness and thickness deviation and 2) veneer natural features such as species, thickness, knots, splits, density, grain angle, moisture content (MC) and growth ring characteristics. Although individual veneer defects and features can be assessed either visually or by veneer sample evaluation method, comprehensive grading methods capable of evaluating overall veneer structural quality are limited. Such evaluation of overall veneer quality could be achieved with assessing as many veneer factors as possible. However, it is not feasible to apply this type of time-consuming and labor-intensive procedures on production lines. Therefore, for engineered applications, the development of strength (or performance) based nondestructive evaluation (NDE) methods is necessary to determine veneer quality (Kunesh 1978; June 1979; Wilson 1992).

To provide quality assurance for LVL, stress wave or ultrasonic nondestructive testing (NDT) techniques are used to sort veneers into strength classes prior to assembly into end products. Such methods are based on the empirical relation between veneer modulus of elasticity (E) and the velocity at which waves travel along the veneer grain direction. The LVL constructed from NDT graded veneers yields clearly defined tension E groups but poorly defined strength groups (Kunesh 1978; June 1979; Jung 1982; Lam 1992; Metriguard Inc. 1995). In other veneer based wood composites such as plywood and LVP, however, rolling shear strengths may govern their applications (Chow 1970; Palka 1977; Bohlen 1975; ASTM D2718-95; Lam 1992). For example, rolling shear is particularly important for box beams, roof deckings, stress skin panels and concrete forms. It may also govern member design at low span-to-depth ratios encountered in some decking materials such as marine container floors. Existing NDT equipment may not provide the necessary parameters to assess the performance of plywood or LVP in cases where rolling shear properties are critical.

For a given veneer source, some veneer quality variables are constant if lathe settings and drying technology are regularly checked and maintained. Past research has identified the two most critical veneer grade factors in determining plywood or LVP rolling shear strength as lathe checks and knots (Chow 1970; Palka 1966; Palka 1970; Palka 1977; Hettiarachchi 1990).

It is well known that wave measurement in the direction parallel to grain is sensitive to the existence of knots (June 1979; Gerhards 1982). However, lathe checks are predominantly oriented in the parallel to grain direction; therefore, it is doubtful that wave transmission in this direction can also effectively detect their presence. In contrast, wave transmission in the perpendicular to grain direction may be sensitive to the presence of lathe checks and splits. This research focused on use of stress wave and acousto-ultrasonic (AU) techniques to detect and quantify the presence of lathe checks and knots and nondestructively evaluate veneer overall quality.

The objectives of this research were:

1) to investigate the sensitivity of using stress wave techniques and acousto-ultrasonic (AU) approach perpendicular to grain direction to veneer lathe checks and quantify their severity;

2) to establish a database and explore the inherent correlations between stress wave and AU parameters and veneer grade factors especially lathe checks and knots;
3) to establish an overall quality criterion for nondestructive evaluation (NDE) of veneer quality.

2. BACKGROUND

2.1. Veneer quality assessment

Veneers are commonly manufactured by a rotary-peeling process during which machining defects such as lathe checks, surface roughness and thickness deviation may be inadvertently introduced. Assuming the veneers are loaded as cantilever beams during peeling, checks will initiate when the bending stresses exceed the transverse modulus of rupture of the veneer. These checks occur on the knife side and predominantly run along the grain direction. They are termed lathe checks to distinguish them from occasional drying checks.

Veneer quality can be assessed either by visual grading or by sample evaluation method. Visual grading is based on appearance determined by size and location of various defects such as knots (dead knots, sound knots and holes), discoloration, splits, and decay *etc.* (Shupe *et al.* 1996). Six basic veneer grades are designated as N, A, B, C-plugged, C and D in order of decreasing quality following the American Plywood Association Standards. A and B grade veneers have better surface qualities than C and D grade veneers. One of the limitations of this method is that only exterior defects such as knots and open knotholes are considered in evaluating the veneer quality. Some other veneer grade factors such as lathe checks and thickness deviation are ignored, which may lead to the inaccurate quality evaluation of veneer for engineered applications. The sample evaluation method is based on checking machining defects such as roughness, thickness deviation and lathe checks of random samples from the production line. This time consuming method can only reflect the veneer random quality at any one time. It was reported that an on-line roughness measurement instrument is available for monitoring the veneer roughness change (George *et al.* 1970), but grading results based solely on roughness may not give accurate indication of veneer overall quality. Finally, the current stress wave or ultrasonic veneer grading method uses averaged wave velocity parallel to grain or stress wave E as an indicator of veneer quality. In this way, the veneer quality is estimated primarily based on tension E parallel to grain, grain angles and knots (June 1979).

Therefore, no known NDE method is available for detecting the presence of lathe checks and assessing overall veneer quality prior to assembly into veneer based wood composites.

2.2. Determination of veneer critical grade factors

Since no single NDE method can detect all veneer grade factors, it is important to identify the critical veneer grade factors which significantly influence the performance of plywood or LVP.

It was reported that rolling shear properties of plywood or LVP depend on veneer species, type, thickness, composing methods, gluing and drying process, and grade factors such as lathe checks, knots, roughness *etc.* (Palka 1966; Palka 1970; Chow 1970; Palka *et al.* 1977; Biblis *et al.* 1975; Biblis *et al.* 1982). Amongst all, it was found that lathe checks have a more pronounced influence on rolling shear properties of plywood or LVP than density which usually dominates clear wood properties (Chow 1970; Palka *et al.* 1977).

Loose veneer with deep lathe checks would not only cause significant degrade of plywood or LVP shear strength, but also cause reduced shear strength of LVL (Bohlen 1975).

Qualitatively, the effects of lathe checks on shear strength in plywood or LVP can be outlined as:

a) Lathe check in crossbands of plywood will decrease the effective load area;

b) Shear concentrations in the tips of lathe checks will facilitate the crack propagation at lower loads.

Quantitatively, the effect of lathe checks on shear strength of plywood or LVP can be summarized as follows (Chow 1970; Biblis *et al.* 1982; Palka *et al.* 1977; Palka 1966):

a) The average rolling shear strength of sawn veneer blocks (no lathe checks) was more than 2.5 times that of rotary-cut veneer blocks.

b) Every reduction of 1% in lathe check depth, by improved peeling or by forcing adhesive into lathe checks, would result in a shear strength increase of about 8.3 kPa when using lap-joint specimens (Chow 1970).

Knots and grain distortion are common natural characteristics that degrade the strength and appearance of veneer. Generally, knot sizes, shapes, locations and eccentricity need to be considered. In terms of tension strength properties parallel to grain, the larger the knot size, the greater the decrease in strength. Critical knot diameter and accumulative knot diameter have been proposed to characterize the existence of knots in veneers (Hettiarachchi 1990; Hettiarachchi *et al.* 1990). Since grain angle is seriously distorted around knots, critical grain angle effect can be incorporated into knot effect.

Rough veneers are also undesirable in plywood or LVP manufacture because they can reduce bond quality by as much as 33% compared with smooth veneers. Generally, rough veneers have more thickness deviation and are weaker in tension perpendicular to grain since roughness occurs mainly in this direction.

Veneer thickness deviation will affect proper adhesive distribution. The shear strength will be inversely affected since adhesive cannot be accepted evenly and sufficiently with a roll-type spreader if thickness deviation is large. However, if knife is kept sharp and the play in the bearings is maintained small, the effect of thickness deviation on shear strength can be safely ignored.

Moisture content has some unfavorable effects on rolling shear strength in plywood below the fiber saturation point (Palka *et al.* 1977). However, if veneer drying process is controlled reasonably, the variation of moisture content will be small during the manufacture process. So moisture content is not a critical factor.

Splits in veneer can be seen as a more serious effect of lathe checks. In this case, the lathe check depth is 100%. So their effect can be embodied in the lathe check effect.

In summary, veneer roughness and grain angle would mainly affect bonding or bending strength. Although lower bonding strength also inversely affects shear strength, their role in determining shear strength of plywood or LVP was limited (Palka *et al.* 1977; Chow 1970). Most of the reduction in strength in plywood and LVP could be attributed to lathe checks and knots; therefore, they are identified as the two critical veneer grade factors. When selecting NDE methods to assess veneer quality, attention should be paid to the sensitivity of NDE parameters to lathe checks and knots, which is addressed in this thesis.

2.3. Selection of veneer NDE methods

To improve quality assurance of wood products, the following categories of NDE techniques have been used (Ross *et al.* 1991):

a) Dynamic bending (MSR);

b) Transverse vibration techniques;

c) Acoustic methods (ultrasonic, acoustic-emission (AE), acousto-ultrasonic (AU), and impact-induced stress wave);

d) Electromagnetic radiation methods (X-ray, microwave, nuclear magnetic resonance and infrared spectroscopy); and

e) Optical methods (CCD camera, laser and video-laser systems).

To date, knot characterization by NDE mainly includes stress wave, ultrasonic and X-ray methods. However, information on presence of lathe checks is solely obtained from visual evaluation of veneer samples which is based on their depth and number (or frequency) (ASTM D2718-95).

Both X-ray and microwaves have shown promise for lumber grading on the production line. However, no report reveals that these methods have been used for NDE of veneer quality.

2.3.1. X-ray method

X-ray measurements can be used to grade lumber by providing excellent resolution of the density gradient in wood. High density wood absorbs more X-ray, generating lower detector current. The detector current is then converted to a voltage which can be calibrated to provide the density of wood materials. Instead of measuring bending E, X-ray grading method uses horizontal density profile as strength indicators (Hoag 1988; Suryoatmono *et al.* 1993). However, X-ray measurements can only give the total wood density (wood and moisture). Using currently available X-ray machine resolution, it is not possible to detect lathe checks in veneers. Also X-ray method does not assess any roughness and grain angle effects.

2.3.2. Microwave method

The microwave nondestructive testing (NDT) uses electromagnetic radiation at frequencies of a few hundred MHz to a few hundred GHz. The microwave method measures dielectric properties of wood materials, which can help detect density, moisture content (MC) and grain angle based on the wave phase change, attenuation, and degree of polarization. Although this method is noncontact and fast, it still requires cumbersome calibrations and data reductions due to considerable interactions between many parameters (James *et al.* 1985; Shen 1995; Martin 1987). Also grain angle can only be deduced reliably when the specimen thickness is large enough to introduce sufficient dielectric anisotropy to appreciably depolarize the incident wave. This method does not seem to be suitable for veneer testing because 1) many expensive sensors are needed to completely identify and model veneer grade factors especially lathe checks and knots; 2) the wavelength of microwave is large comparing with veneer thickness; 3) the relatively thin veneers will influence measurement accuracy and 4) the microwave method does not consider roughness effect.

2.3.3. Acoustic methods

Acoustic methods refer to the transmission and receiving of stress waves which encompass a frequency range approximately from 20 Hz to 50 MHz. Generally, acoustic methods comprise of impact-induced stress wave methods, ultrasonics, acoustic emissions (AE) and acoustic-ultrasonics (AU).

a. Impact-induced stress wave and ultrasonic methods

Both impact-induced stress wave and ultrasonic methods are based on the theory of acoustic wave propagation and usually differ only in the mode and frequency of excitation. No appreciable difference was found in velocities resulting from measurements with impact-induced and ultrasonic stress wave timing instruments (Gerhards 1978; June 1979). Both methods are convenient to use, and sensitive to most defects in wood. However, poor correlation of lumber or veneer MOR to NDE parameters and lack of non-contact techniques are two drawbacks shared by both methods. The stress wave method further includes drawbacks such as: 1) poor repeatability of the input signal; 2) lack of control over signal frequency.

The velocity of stress wave propagation in wood has the following characteristics:

1) it is about three times faster along the grain than across the grain in lumber (Gerhards 1982);

2) it decreases as grain angle, wood temperature or moisture content increase (Gerhards 1975; Armstrong *et al.* 1991);

3) it is not significantly affected by lumber width or veneer width when free of defects;

4) it is 10-25% slower in earlywood than in latewood or wholewood (Gerhards 1978);

5) it is reduced by the discontinuity, decay and cross grain associated with knots.

While stress wave velocity is reduced through a knot and the curved grain around a knot, a knot does not have much effect on the overall velocity of stress wave in wood when substantial straight grain exists near a knot, *i.e.*, the knot only results in a small localized increase in transit time. The correlation between knots area ratio (KAR) and acoustic wave transit time in lumber was generally weak since coefficient of determination (r^2) was as low as 5% (Gerhards 1982). Therefore, stress wave and ultrasonic techniques are capable of detecting the presence of knots, but are not very sensitive to the size of knots.

A commercial ultrasonic machine Model 2600FX veneer tester with 20-30 kHz piezoelectric transducers has been available to grade veneers at a rate of about a second per sheet to produce LVL (Metriguard Inc. 1995) with measurements along the grain direction of veneer. Based on a good correlation between modulus of elasticity (E) and averaged wave velocity or stress wave predicted E, veneers are sorted into several grades for tension E parallel to grain. However, this veneer grading method can only partly consider the knots effect because: 1) real-time veneer grading operation does not allow each sampling line to pass through knots area considering the grading speed and variations of knots dimensions, locations and shapes and 2) wave velocity is not an accurate indicator of knots size. Therefore, NDE of knots in veneer still remains a challenge.

Stress wave NDT techniques were also suggested to detect skips or voids in the gluelines of edge-glued red oak panels (Armstrong *et al.* 1991) by measuring transit time and amplitude of stress waves propagating from edge to edge of the panel, and detect wetwood by measuring wave velocities across the width of the boards (Ross 1994). Ultrasonic NDT methods were further suggested to detect lumber drying defects such as hidden honeycomb and closed surface check (Fuller 1995).

Other research topics included the detection of early stages of wood decay, the location of advanced decay, void and internal features, the anisotropy characterization of structural flakeboards, the monitoring of drying and the assessment of the structural integrity of members in situ (Wilcox 1988; Ross 1991).

To date, no research has been published on the relationship between lathe checks (splits) and surface conditions such as roughness and the characteristics of wave transmission signals.

b. Acoustic emission (AE) method

Acoustic emission (AE) is defined as acoustic waves generated in material when subjected to an external stimulus such as stress (Beattie 1993). AE signal processing methods generally measure the characteristic of the signal using feature extraction techniques. The current applications in wood industry includes monitoring of drying process, and prediction of fracture growth or failure (Noguchi *et al.* 1980; Porter *et al.* 1972; Knuffel 1988).

c. Acousto-ultrasonic (AU) method

Acousto-ultrasonic (AU) is the combination of acoustic emission (AE) and ultrasonic methods. It differs from ultrasonics in the type of sensors and signal processing methods. AU typically operates in a relatively low frequency range (generally less than 500 kHz). The lower frequency associated with AU testing is more desirable for veneer testing because high frequency could be attenuated rapidly in veneers. The acoustic energy during AU testing could propagate in three principal modes with different frequencies and velocities: 1) non-symmetric longitudinal waves; 2) anti-symmetric transverse (flexural) waves and 3) surface (or Rayleigh) waves. The major parameters measured for AU method are: 1) energy dissipation characteristics such as average signal level (root mean square) or attenuation, peak amplitude and frequency content and 2) energy storage characteristics such as wave velocity change. Root mean square (RMS) voltage is a measure of signal energy. A relative wave attenuation (ATT) can be assigned as the inverse of RMS voltage.

The AU method has been successfully used to assess wood and wood products such as monitoring the adhesive curing process and evaluating adhesion quality for parallel wood laminates, and panel evaluation *etc.* (Beall 1993; Beall *et al.* 1993; Biernacki *et al.* 1993; Lemaster *et al.*; Lemaster 1993). Results from those studies indicated that AU is sensitive to most of the typical wood strength reducing characteristics such as knots (holes), decay, splits and cross grains.

Acoustic wave propagation characteristics in the far-field (the ratio of propagation distance to thickness exceeds 20) of metal, maple veneer and hardwood have been experimentally examined with frequency range from 0 to over 1MHz (Hamstad *et al.* 1993). The results showed that the amplitude of resulting waveforms are dominated by the low frequency portion of first anti-symmetric flexural mode in the thin wooden plates like veneers. But no lathe checks and knots effect has been investigated.

Past experience showed that AU is capable of indicating diffuse flaw populations, internal damage, porosity and strength/MOE variation, and detecting defects throughout the entire volume of a material, which may be suitable for the characterization of lathe checks in veneer using velocity (or transit time) and attenuation of AU signals.

2.3.4. Selection of NDE methods for detection of lathe checks and knots

Based on above analyses, some comments can be made on NDE methods applied to wood products:

1) Existing veneer NDE methods mainly focus on ultrasonic or impact-induced stress wave methods;

2) Veneer sorting is solely based on wave transmission parallel to grain correlated with E;

3) No NDE method has been developed specifically to detect lathe checks in veneers;

It can be deduced that direct application of lumber NDE methods to veneer NDE may not be feasible since the critical factors being considered are drastically different. Considering the sensitivity to veneer critical factors, availability, on-line feasibility, safety, and cost of NDE methods, this research will target on use of stress wave and AU techniques to assess veneer quality based on the detection of lathe checks and knots.

3. EXPERIMENTAL PROCEDURES

3.1. Testing materials

Dried 2.5 mm thick Douglas-fir veneer specimens were obtained from a mill in British Columbia. Attention was paid to select veneer specimens with a range of veneer tightness which is usually correlated with seriousness of lathe checks. In total, sixty 1200 x 600 mm veneer sheets were selected. Among them, 40 sheets were randomly selected to be cut into eighty 320 x 320 mm specimens with two specimens in each sheet. The remaining 20 veneer sheets generated twenty 320 x 320 mm specimens with one specimen per sheet. In this way, a total of one hundred 320 mm squared veneer specimens were prepared. Owing to handling breakage of 2 veneer specimens, 98 specimens were used.

In this study, 40 x 40 mm grids were drawn on loose side (the side with lathe checks) of each veneer sheet with wave transmission distances 280 mm in both orthogonal directions. As shown in Figures 1 and 2, seven lines, 40 mm apart, were sketched in each direction leaving 40 mm at one edge for impact-induced stress wave testing and leaving 20 mm at two edges for AU testing to avoid boundary effects. The AU transmitting and receiving transducers were centered in the sampling points along the gridlines.

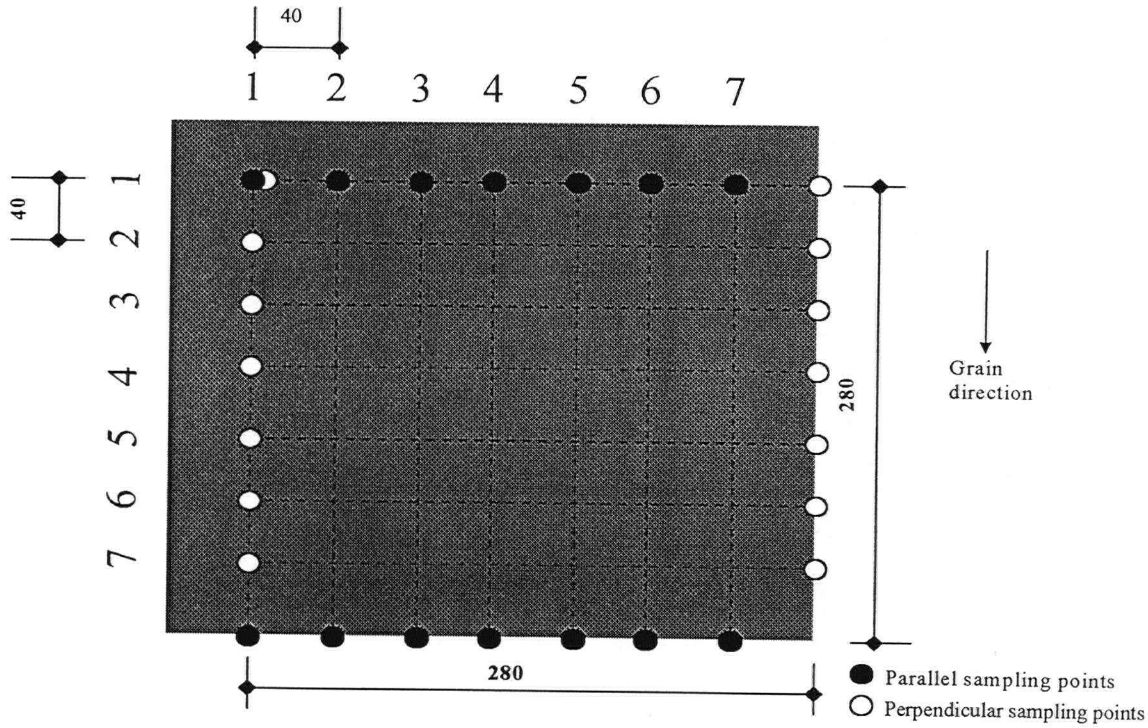

Fig. 1. Grids generated on a veneer sheet for stress wave testing (mm)

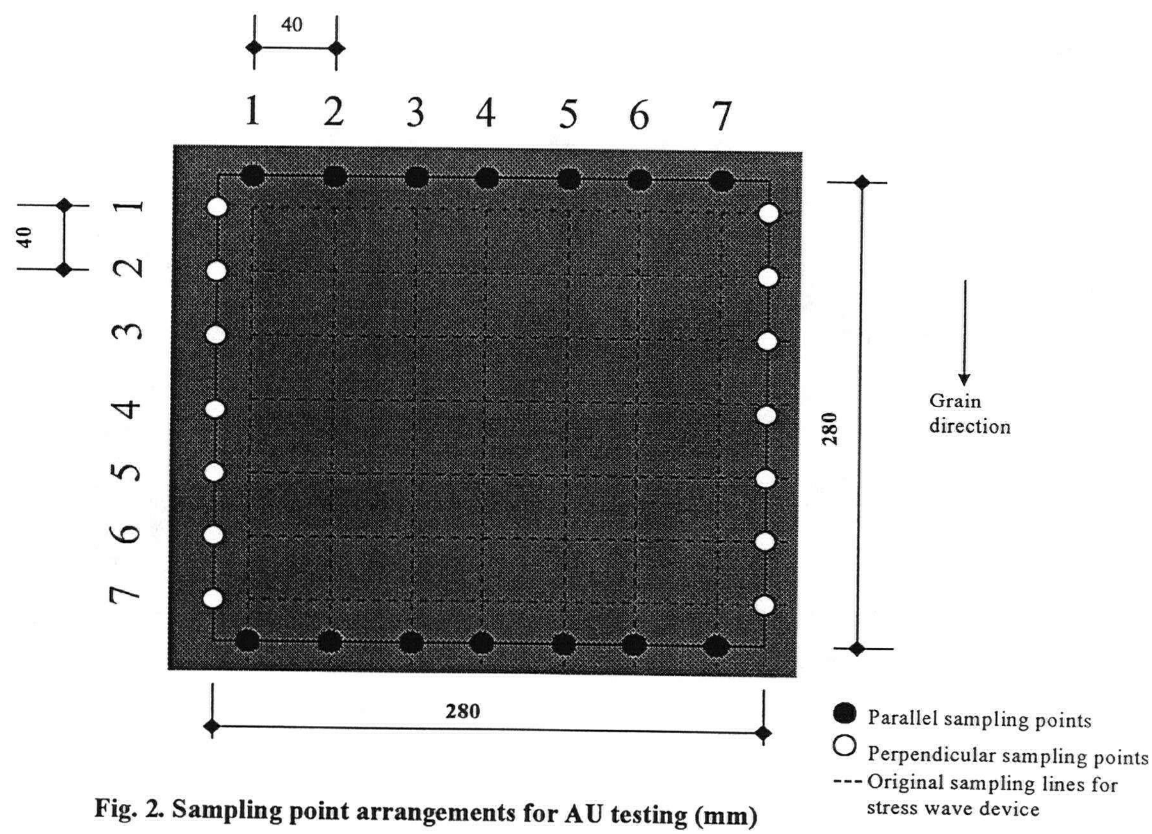

Fig. 2. Sampling point arrangements for AU testing (mm)

3.2. Measurement of veneer grade factors

The following veneer grade factors were measured:

a) Knots

A new knot criterion was introduced as Percentage of Knots Area (PKA) which is defined as the ratio of total knot area over the total area of the veneer sheet measured. The PKA of each specimen was established as:

$$PKA = A_K/A_T$$

Here A_K is the knot area within the area of 78,400 mm^2;

A_T is the total area of veneer sheet measured, *i.e.*, 78,400 (280 x 280) mm^2.

b) Mass density

The weight of each specimen was measured to calculate the mass density.

c) Average thickness and thickness deviation

Veneer thickness in each sheet was measured using a dial gauge. Twelve points in each sheet were measured and statistically analyzed as shown is Fig. 3. The average thickness and standard deviation were calculated.

d) Roughness

Veneer roughness in each specimen was assessed visually by assigning the specimen with one of the 7 grades (from 0 to 6) as:

0 ------ very smooth surface

1 ------ smooth surface

2 ------- smooth but small area (<5%) has rough surface

3 ------- smooth but small area (5 to15%) has rough surface

4 --------16 to 30% of area has rough surface

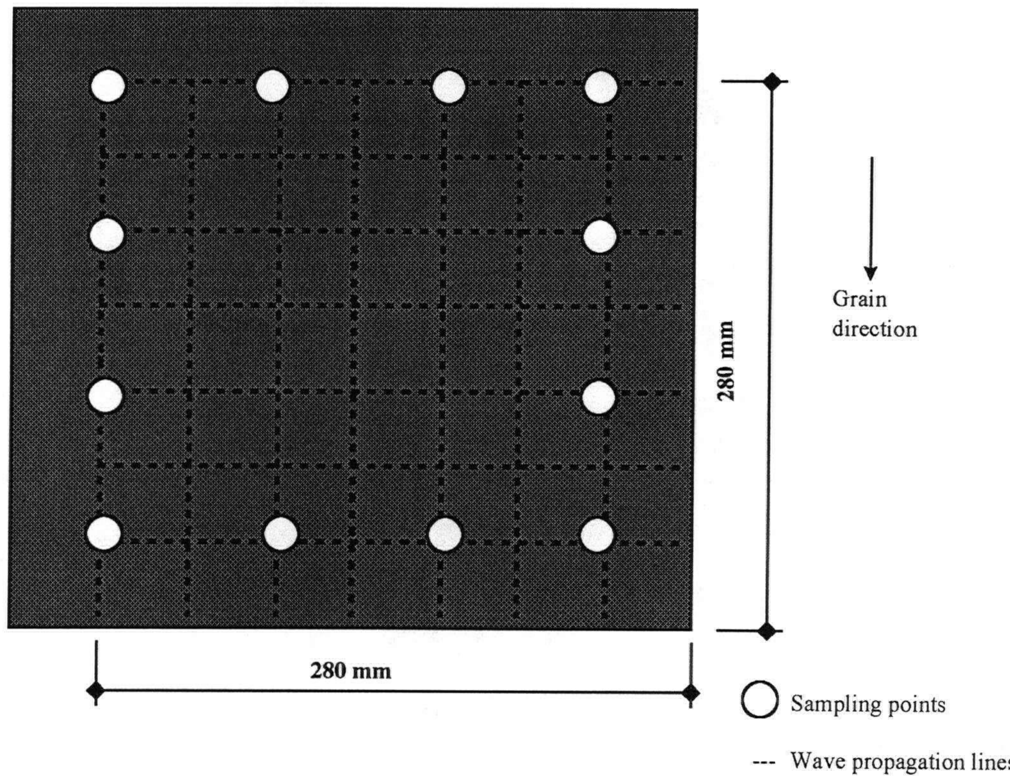

Fig. 3. Distribution of 12 sampling points for veneer thickness measurements

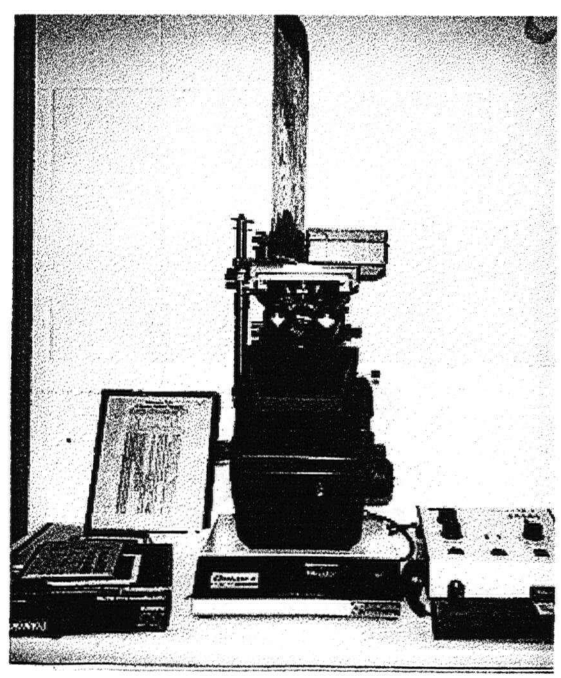

Photo 1. Microscope for veneer lathe check measurement

5 --------rough with larger rough area (31 to 60%)

6 --------very rough with large rough area (61 to 100%)

e) Grain angle

The grain angle in each specimen was also measured by scribing a mark using a ball-point pen in the grain direction over a distance of 240 mm. Seven grain angles with respect to seven straight sampling lines in each specimen were measured and averaged. The averaged angle was taken as the specimen grain angle.

f) Moisture content (MC)

Measurement of MC was taken using a portable Model RC-1C MC meter. The results showed that the MC for the 98 veneer sheets ranged from 6% to 9%. This variation in MC would cause about 3% variation of wave velocity (Sakai *et al.* 1990), which allowed us to ignore this variable for analysis.

g) Averaged lathe check depth (LCD) and total lathe check number (LCN)

After testing veneer with the stress wave device, two ends of specimens were soaked in water-soluble dye for half an hour and air-dried for 48 hours. Then, a table saw was used to crosscut the two ends of each veneer specimen perpendicular to grain to establish a clear view of lathe checks in two cross sections. To measure lathe checks, each cross section was divided into seven 40 mm wide portions which were equivalent to the intervals of grids. The lathe check depths in each of these seven portions were measured and averaged as a percentage of veneer thickness using a microscope with scale as shown in Photo.1. The lathe check depth in each cross section was obtained by averaging these seven averaged depths of lathe checks. Finally, the averaged lathe check depth (LCD) of each veneer specimen was obtained by averaging the lathe check depths in two cross sections. Also the total lathe check number (LCN) in two cross sections was counted for each specimen. LCN can be easily converted into lathe check frequency, *i.e.*, the number of lathe checks per millimeter. The experimental results of veneer grade factors are summarized in Table 1 (Appendix A).

3.3. Experimental apparatus

3.3.1. Stress wave timer

The Metriguard 239A stress wave timer, a portable instrument designed for laboratory use, was adopted to investigate the possibility of using the stress wave method to detect the presence of lathe checks. As shown in Photo 2, its application involved placing start and stop accelerometer transducers against the veneer to be tested. A stress wave was introduced into the veneer by a pendulum impact. Timing was started when the stress wave reached the start accelerometer coupled with the pendulum set and stopped when it was transmitted to the stop accelerometer. Ninety-eight specimens were tested with wave transmission in both directions with ten repetitions of pendulum hits for each sampling line. Timings were repeatable in the parallel to grain direction but not very consistent in the perpendicular to grain direction. Eight out of 98 specimens showed very large and inconsistent timings perpendicular to the grain. This phenomenon could be explained by: 1) those 8 specimens were rather loose and the wave amplitudes attenuated very rapidly and 2) a higher threshold (0.2 V) was set originally for the stress wave timer, which was inappropriate for wave measurements perpendicular to the grain. By culling those 8 specimens, the correlation between averaged lathe check depth (LCD) and wave timings perpendicular to grain was generated with coefficient of determination $r^2 = 0.394$ as shown in Fig. 4, which showed a possibility of using stress wave techniques to detect lathe checks.

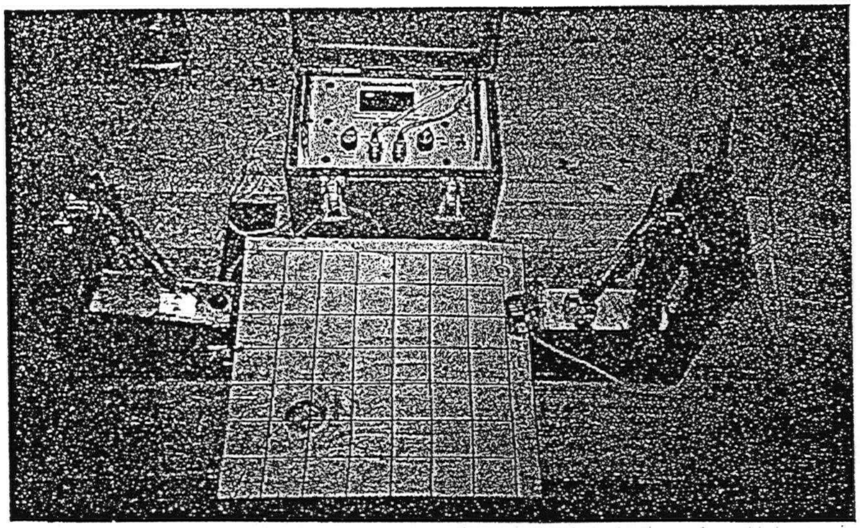

a) Parallel to grain

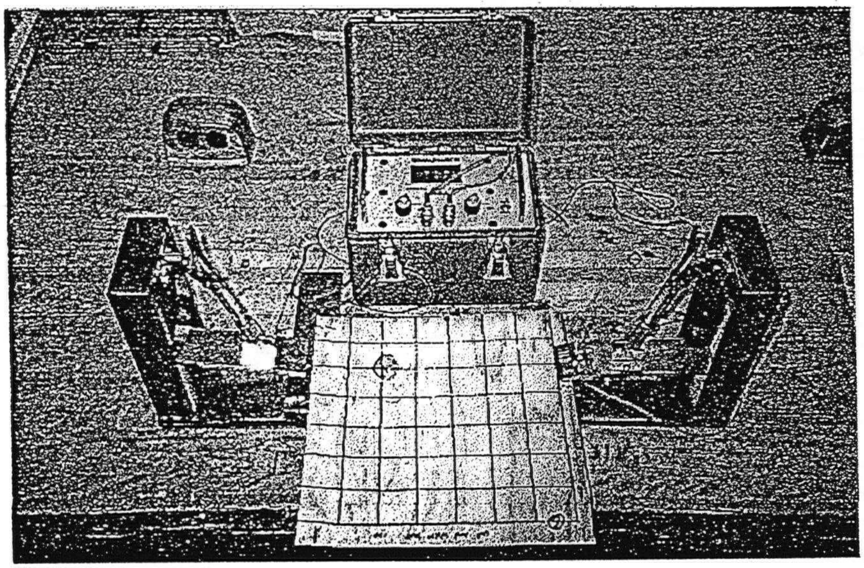

b) Perpendicular to grain

Photo 2. Veneer testing with stress wave timer

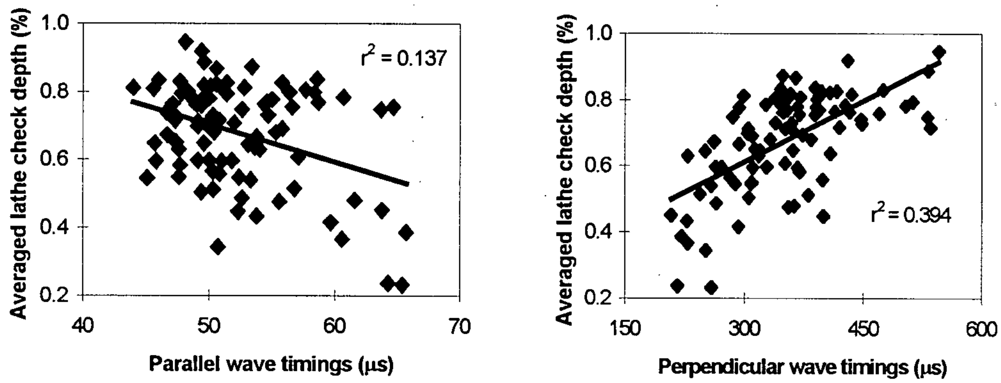

Fig. 4. The relationships between stress wave timings and LCD (90 specimens)

3.3.2. Stress wave device setup

In the first phase of this research, a Metriguard 239A stress wave generator (without an algorithm viewer) coupled with a Tektronix 2232 digital oscilloscope was set up as shown in Photo 3. The schematic of setup is shown in Fig. 5.

In the impact-induced stress wave testing, the time-domain waveform received by the transducer on the "non-impact" side was monitored and displayed on the oscilloscope with each pendulum hit. Only selected waveforms were plotted. Since the oscilloscope display was triggered by the impact-side transducer, a time lag existed which was represented by a relatively flat line at the beginning of the received waveform. This was the transit time of the stress wave.

The maximum background noise level of the "flat" portion was established by a moving cursor. The transit time of the stress wave was recorded when the voltage just crossed the maximum background noise level. Further, the signal was continuously traced to record the first peak amplitude and the time of its occurrence.

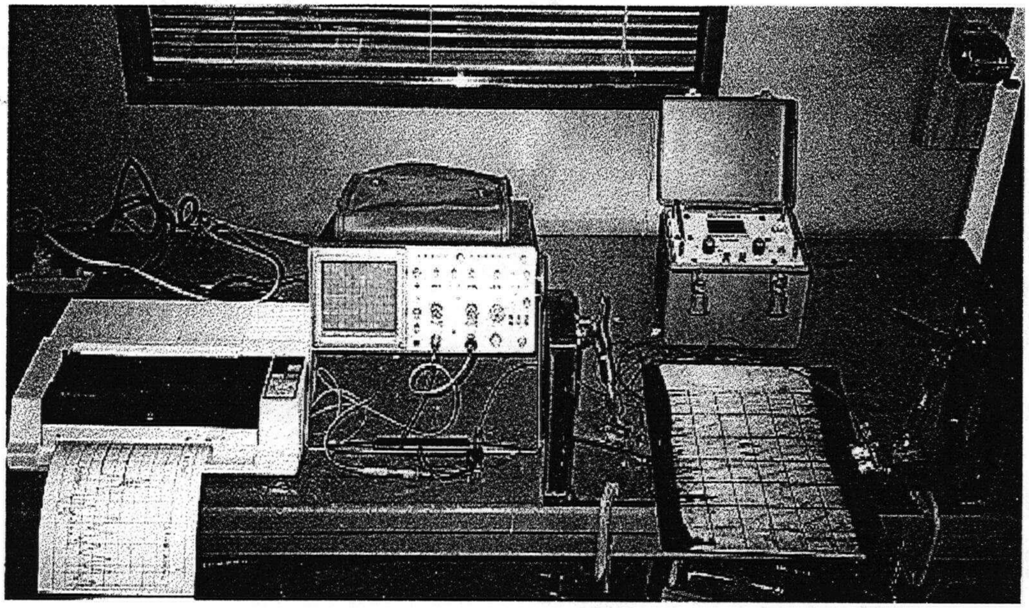

Photo 3. Veneer stress wave device setup

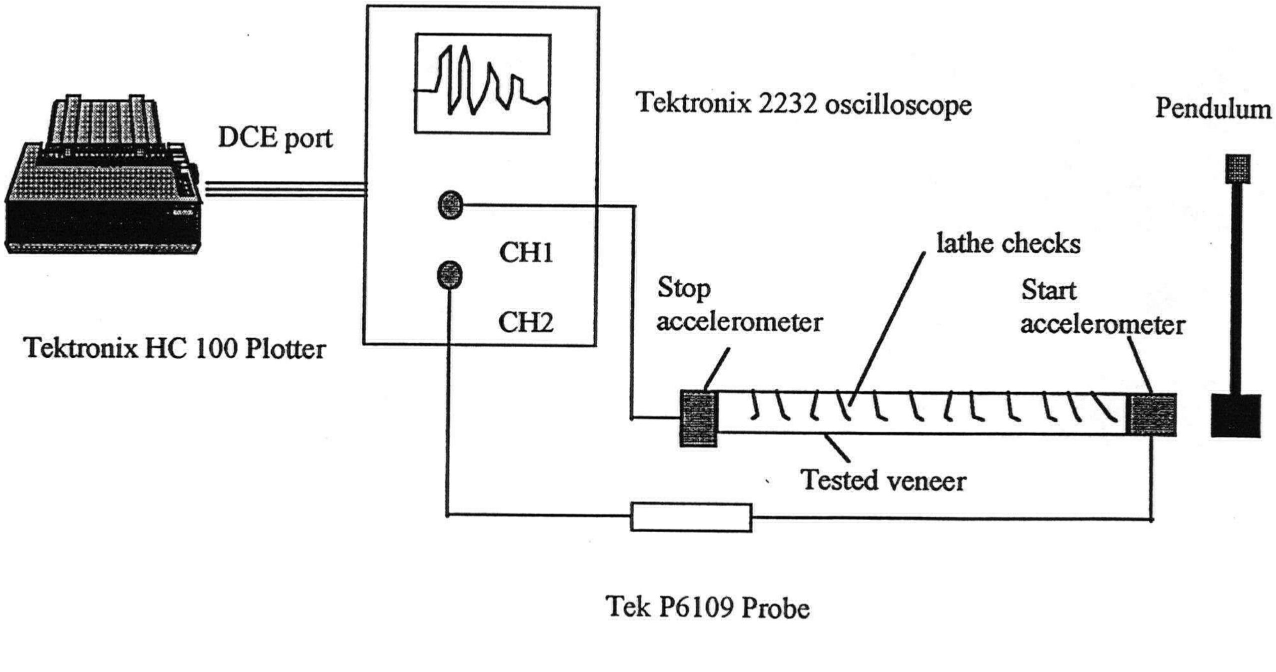

Fig. 5. Impact-induced stress wave device setup

3.3.3. Ultrasonic equipment setup (AU approach)

In the second phase of this research, a control test was conducted to compare the small impact-induced stress wave device and ultrasonic equipment (AU approach). Fifty out of 98 stress-wave tested veneer specimens were chosen for testing again with ultrasonic equipment. An acousto-ultrasonic (AU) testing of veneers was performed on a Matec immersion ultrasonic inspection system. This system includes a SR-9000 Pulser / Receiver Card and a Model STR* 8100D high speed analog-to-digital converter (A/D) board. The SR-9000 Pulser / Receiver Card was used as a pulser providing a spike with amplitude of 300 V. The STR* 8100D A/D board, an advanced software package, was used to display the signal (voltage/time information) on a computer monitor and to store the digital signal on a computer hard drive at a rate of 100 MHz with a resolution of 8 bits. The ultrasonic testing setup for veneers is shown in Photo 4.

AU testing of veneer was performed in same-side through transmission mode with veneer loose side face up. Two 50 kHz resonant piezoelectric transducers were attached to the veneer surface with high vacuum silicon grease and held in place with a transducer holder. A thick plastic foam was used to isolate the veneer specimen from the testing platform. To improve coupling, a 1.0 kg weight was applied to each transducer as shown in Photo 5 and high vacuum grease was applied on the veneer at the sampling points. The wave transmission distance (center–to–center spacing between transducers) was maintained as 280 mm.

Figure 6 shows a schematic representation of the AU experimental setup. A 300 V spike pulse, created by the pulse generator, was sent to a transmitting transducer through the veneer to be captured by the receiving transducer. The received signal was amplified by a preamplifier with a 20 kHz to 100 kHz bandpass filter and a gain of 60 dB. The analog

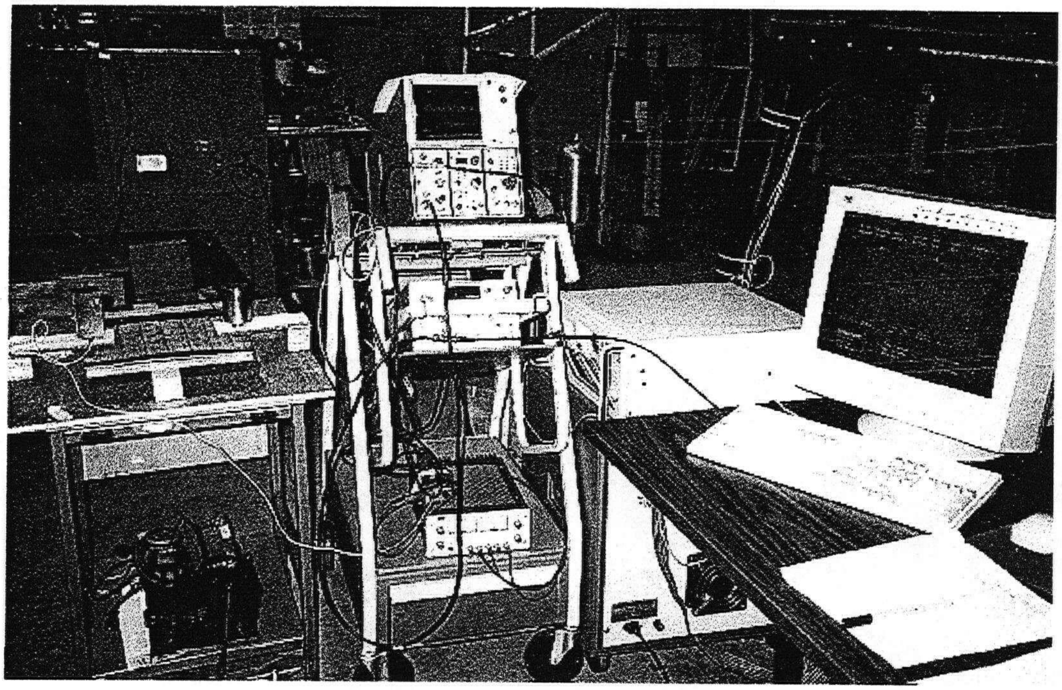

Photo 4. Veneer AU testing setup

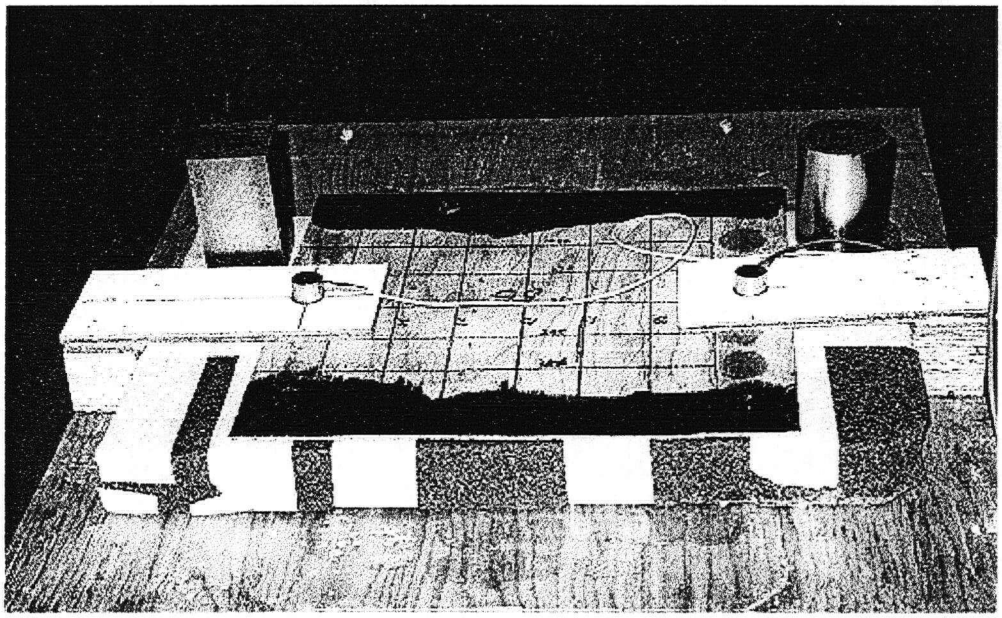

Photo 5. Transducers attached in veneer AU testing

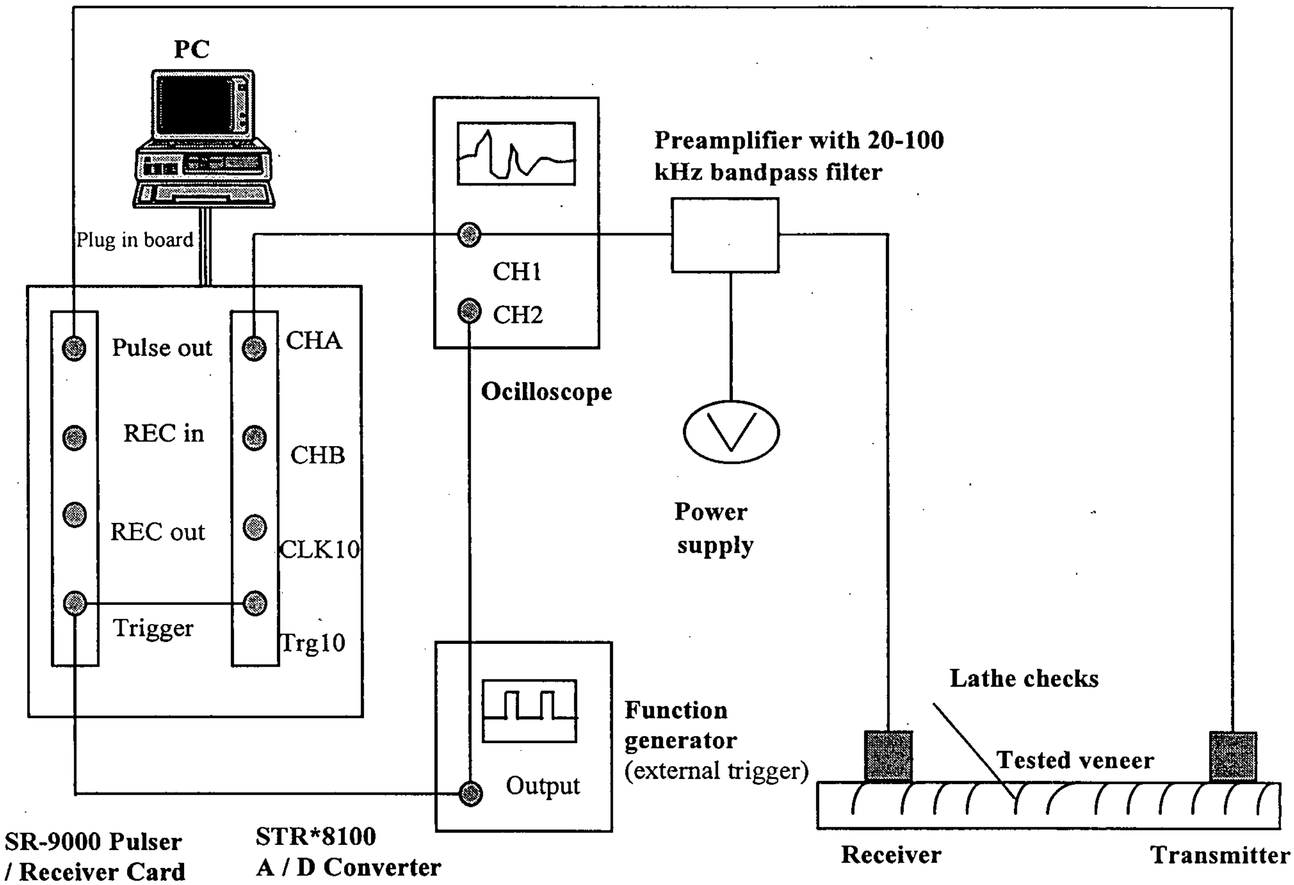

Fig. 6. Veneer AU testing setup

signal was digitized by the A/D converter and saved into a computer hard driver. A sampling rate of 0.78125 MHz was used to establish an interval of 1.28 μs for consecutive points collected. To avoid waveform overlapping, the function generator was set with a repetition pulse rate of 100 Hz to trigger the signals. To reduce noise effects, the software was set to obtain an ensemble average of 128 x 31 and 128 x 5 AU waveforms in the perpendicular and parallel to grain directions respectively. Each ensemble averaged AU signal was saved using 2048 points (waveform length was 2.62 ms), and could be stored in two data types: 1) ASCII and 2) binary forms. ASCII data were used to generate time domain waveforms by inputting into a Microsoft Excel™ spreadsheet; and the binary data were further processed using a specialized waveform analysis software Wind-vd2 developed by Biernacki (1994) to extract wave features in both time and frequency domains. The wave parameters extracted by the software included RMS voltage of the signal, transit time, duration time, counts, and moments of the power spectrum.

4. EXPERIMENTAL RESULTS

4.1. Experimental results on wave parameters

4.1.1. Data processing and waveform analysis

4.1.1.1. Stress wave device

By displaying the waveforms as shown in Fig. 7, the wave timing (transit time) could be easily attained. Other observations were also made on some of the displayed waveforms including: wave timing consistencies, effects of subsequent hits, output voltage and frequency information, effect of the presence of knots and the effect of artificially induced

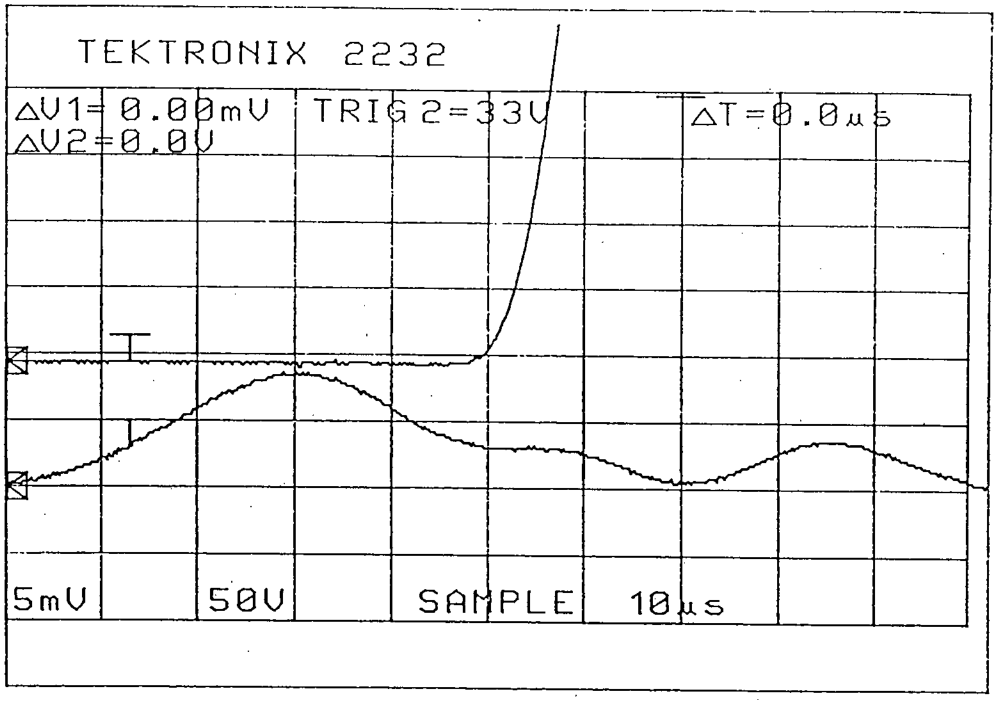

a) Parallel to grain

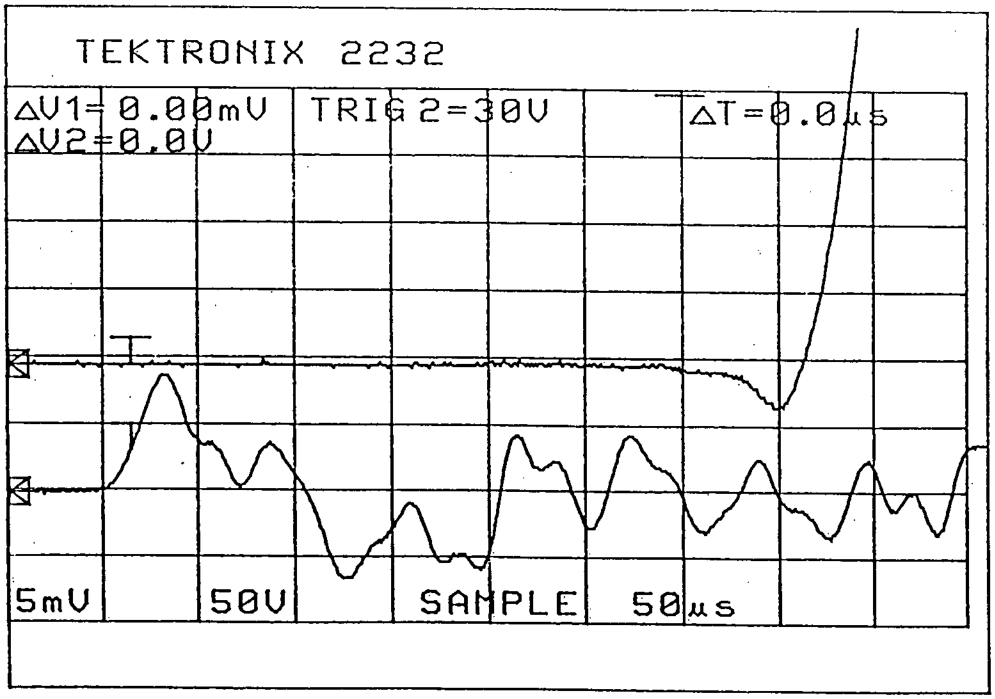

b) Perpendicular to grain

Fig. 7. Timing for stress wave device in both directions (specimen 4, point 4)

checks. Details of these observations are available in Appendix B. The following is a brief summary of the key observations.

Comparisons of wave timing information obtained directly from Metriguard 239A stress wave timer and from analysis of waveform indicates that the Metriguard 239A stress wave timer threshold level of 0.2 V seemed to be too high which can sometimes yield inconsistent wave timing results especially in the perpendicular to grain direction.

The effects of subsequent hits on the waveform were not significant. Although the waveform changes slightly from subsequent hits, the wave timing was not affected and the first peak amplitude was less affected compared to the amplitudes of other peaks. The inverse of the first peak amplitude was therefore selected as a relative criterion of attenuation (ATT). An example of this analysis is shown in Fig. 24 in Appendix B.

Impedance of wave propagation in the parallel to grain direction by knots was observed by comparing waveforms of knot containing material and neighboring knot free material. An example is shown in Fig. 27 in Appendix B. However, for wave propagation in the perpendicular to grain direction the observations were inconclusive.

Finally, the waveforms of several specimens were measured prior to the introduction of artificial checks. The waveforms were re-measured and compared to the original data. The wave timing was clearly influenced by the introduction of artificial checks whereas the influence of first peak amplitude was inconclusive. Therefore, wave timing may be a better parameter than the first peak amplitude to characterize the effect of lathe checks.

4.1.1.2. Ultrasonic equipment (AU approach)

The threshold level was determined based on the product of maximum noise level of the signal within selected noise points and a desired threshold factor. By trial and error, it was found to be appropriate to set 1) the noise points as 40 points (51.2 μs) and 150 points (192 μs) for the parallel and perpendicular to grain directions respectively and 2) the threshold factor as 1.25 for both directions. However, wave timings parallel to grain were found to be inconsistent if the noise was absent for some specimens. To extract waveform features not supported by Wind-vd2, a modified algorithm was developed using MS Excel with Visual Basic code. An additional 0.2 V was added to maximum absolute noise level in the first 40 points to establish the threshold level as shown in Fig. 31 (Appendix C). The wave timings and root mean square (RMS) voltages with a highlight on first 100 points were computed, which was found to be well applicable to all of the specimens.

1) <u>Lathe check effects on time domain waveform and power spectrum</u>

Specimens 56, 29 and 96 were typical examples with different averaged lathe check depths (LCD) of 23.6%, 51.1% and 76.1% respectively and percentage of knots area (PKA) of 0.26%, 0% and 0.47%, respectively (all sampling lines were free of knots in both directions). Mass densities for those three specimens were 0.456, 0.419 and 0.516 g/cm^3, respectively. Details of the lathe check influence on time domain waveform and power spectrum in both parallel and perpendicular to grain directions are shown in Appendix D.

In summary, the significant difference between amplitudes in two directions in the same specimen was strongly related to the magnitude of LCD. Owing to the cross grain propagation and existence of lathe checks, the amplitude in the perpendicular to grain direction was attenuated 10 to over 100 times comparing with that in the parallel to grain direction.

Averaged lathe check depth (LCD) clearly exerted an influence on the displayed waveform, amplitude and RMS voltage in the perpendicular to grain direction. But in the parallel to grain direction, its influence was not clearly identified.

Another interesting observation was that the main frequencies focused on 25 kHz and/or 95 kHz regardless of directions measured and seriousness of lathe checks throughout all the specimens tested.

2) Knot effects on time domain waveform and power spectrum

Specimen 77 contained a knot (PKA 1.66%) in the intersection of parallel sampling line 4 and perpendicular sampling line 4. The knot chord along the parallel sampling line was 47 mm, and the knot chord along the perpendicular sampling line was 42 mm as shown in Fig. 8. The LCD and mass density of this specimen were 77.65% and 0.580 g/mm^3 respectively.

In the parallel to grain direction, there existed remarkable differences between knot-free and knot-containing sampling lines in wave timings and RMS voltages as shown in Figures 9 and 10 respectively. Therefore, existence of knots definitely affected the wave propagation parallel to grain not only in wave velocity but also in wave attenuation. Also signal energy was mainly concentrated on a higher frequency zone such as 95 kHz instead of low frequency zone such as 25 kHz, and a high frequency component centered at 145 or 165 kHz appeared in knot-containing sampling line and adjoining knot-free sampling line as shown in Figures 34 a) and b) in Appendix E. This suggested that a higher frequency over 95 kHz is also capable of characterizing knots and adjoining detoured grain area.

In the perpendicular to grain direction, the influence of knots on the wave timing, RMS voltage was inconclusive as shown in Figures 11 and 12, respectively, which demonstrated that the wave propagation was not sensitive to the existence of knots. Also

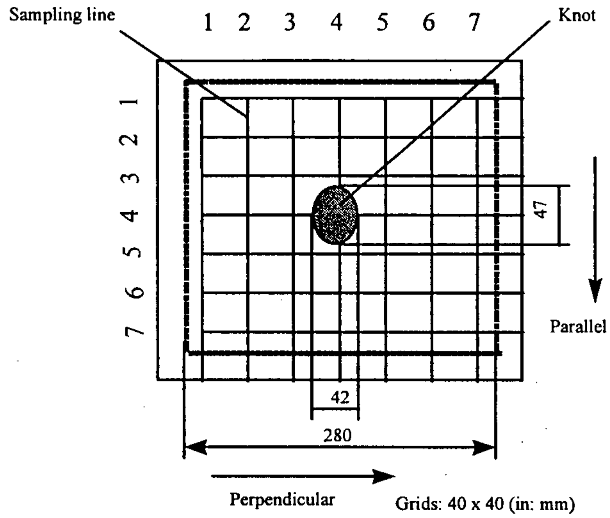

Fig. 8. Knot presented at the intersection of parallel sampling line 4
and perpendicular sampling line 4 for specimen 77

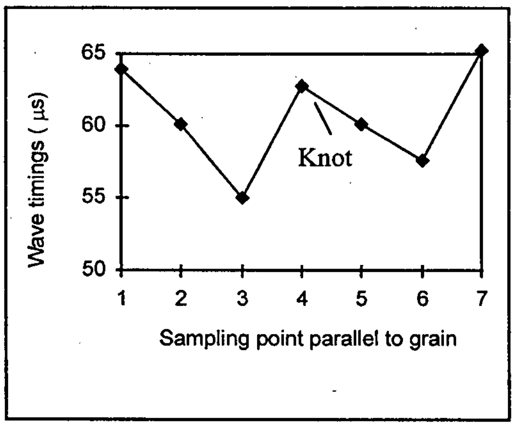

Fig. 9. Knot effect on parallel wave timings

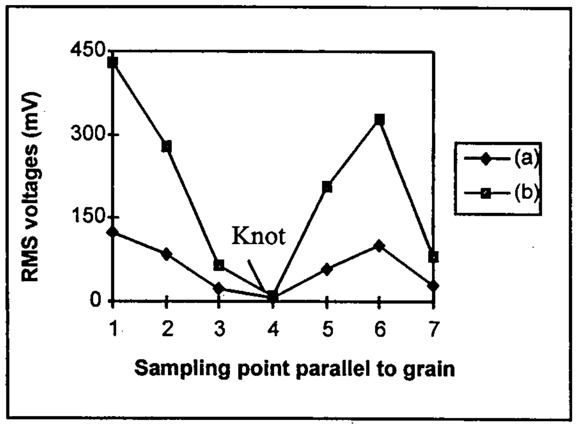

Fig. 10. Knot effect on parallel RMS voltages
a) based on an entire waveform
b) based on first 100 data points

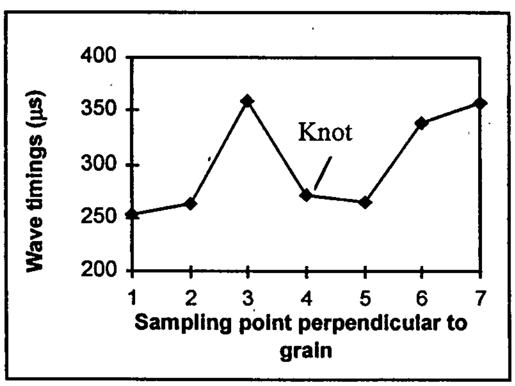

Fig. 11. Knot effect on perpendicular wave timings

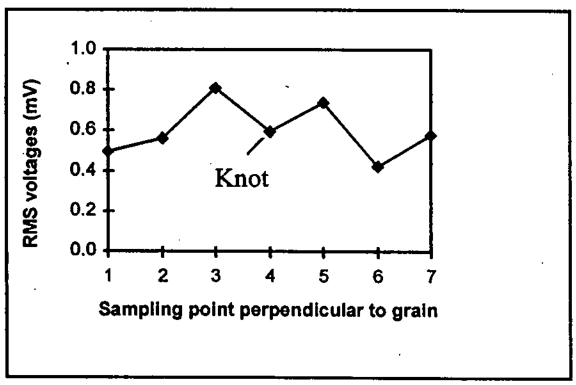

Fig. 12. Knot effect on perpendicular RMS voltages

the waveform amplitude in knot-containing sampling line retained almost the same level comparing to that in neighboring knot-free sampling line, and the signal energy was concentrated on low frequency zone centered at 25 kHz as shown in Figures 35 a) and b) in Appendix E. This indicated that lower frequency can penetrate loose veneer much easier than higher frequency, and the signal energy is predominately affected by the lathe checks rather than knots in this direction.

In summary, wave transmission in the parallel to grain direction was sensitive to the presence of knots. Both wave timings and RMS voltages (or attenuations) in this direction were affected by the existence of knots. In contrast, wave propagation in the perpendicular to grain direction was not sensitive to the presence of knots considering the responses of wave timings, amplitudes or RMS voltages to the existence of knots.

The acoustic transducer with frequency centered at 50 kHz being used in this study was appropriate since it was capable of characterizing both lathe checks and knots very well throughout all the veneer specimens tested.

4.1.2. Calculation of wave parameters

For impact-induced stress wave method, seven measurements of wave timings (or velocities) and first peak amplitudes in each specimen were statistically analyzed to get their averages and standard deviations, and an inverse of the averaged first peak amplitude perpendicular to grain was seen as a wave attenuation criterion (ATT). The results are summarized in Table 2 as shown in Appendix F.

Owing to the crosscut of specimens for measuring the lathe checks, five out of 50 AU testing specimens did not have sufficient sampling points in the direction perpendicular to grain, while twenty-four specimens in the direction parallel to grain also lacked sufficient sampling points. These specimens were not included in the regression analysis of AU method in the relevant direction. The AU wave timing and RMS voltage were statistically analyzed to get their averages and standard deviations, respectively. An inverse of averaged RMS voltage was seen as a wave attenuation criterion (ATT) for individual veneer specimens. The results are summarized in Table 3.1 for parallel to grain direction and Table 3.2 for perpendicular to grain direction as shown in Appendix G.

4.2. Correlations between wave parameters and veneer grade factors

4.2.1. Stress wave measurements

4.2.1.1. Correlation matrix for wave parameters and veneer grade factors

As shown in Table 1 and Table 2 in Appendix A and F, total 13 wave parameters and veneer grade factors were measured. A correlation matrix was generated to see how those 13 variables correlated with each other as shown in Table 4 .

In Table 4:

X_1--------Wave timings in the parallel to grain direction (parallel wave timings)

X_2------- Wave timings in the perpendicular to grain direction (perpendicular wave timings)

X_3--------Wave attenuations in the perpendicular to grain direction (perpendicular wave attenuations) ATT

X_4 ------- Mass density

X_5 ------ Averaged thickness

X_6 -------Thickness deviation

Correlations	*X1*	*X2*	*X3*	*X4*	*X5*	*X6*	*X7*	*X8*	*X9*	*X10*	*X11*	*X12*	*X13*
X1	1.0000												
X2	-0.4924	1.0000											
X3	-0.2132	0.1844	1.0000										
X4	0.2588	-0.2560	-0.0101	1.0000									
X5	0.1025	0.0203	-0.0673	-0.2091	1.0000								
X6	0.2383	0.0646	-0.0747	0.0679	0.2573	1.0000							
X7	0.2671	-0.0221	-0.0720	0.0103	0.1348	0.3345	1.0000						
X8	0.2142	0.0418	-0.0691	0.0255	0.4244	0.3758	0.4890	1.0000					
X9	0.1921	-0.0607	0.0915	0.0276	0.3082	0.1450	0.2076	0.2810	1.0000				
X10	-0.2929	0.6892	0.3347	0.1468	-0.3016	0.0301	0.0389	-0.0345	-0.1186	1.0000			
X11	-0.1357	0.1776	0.0813	0.2976	-0.3485	0.0479	-0.0991	-0.2728	-0.1582	0.3739	1.0000		
X12	0.4999	-0.0480	-0.1163	0.1565	0.0905	0.2527	0.5828	0.2354	0.3007	-0.0089	-0.0657	1.0000	
X13	-0.1478	0.3225	-0.1729	-0.1736	0.3135	0.0190	0.1202	0.1522	0.0890	-0.0021	-0.0909	-0.0240	1.0000

Table 4. Correlation matrix for wave parameters and veneer grade factors

X_7--------Percentage of knot area (PKA)

X_8--------Roughness grade (RG)

X_9--------Grain angle (GA)

X_{10}-------Averaged lathe check depth (LCD)

X_{11}------ Total lathe check number in one veneer specimen (LCN)

X_{12} ------Standard deviation of wave timings in the parallel to the grain direction (parallel timing stdev.)

X_{13} ------Standard deviation of wave timings in the perpendicular to the grain direction (perpendicular timing stdev.)

From Table 4, the important variables in an ascending or descending order to a given variable could be identified based on the magnitude of correlation coefficient r.

Note that the correlations between wave timings and mass density were weak in both directions with $r^2 \approx 0.066$, which demonstrated that, unlike X-ray method, stress wave method cannot accurately deliver veneer density information.

Note also that there existed no relationship between averaged lathe check depth (LCD) and percentage of knot area (PKA), which showed that the lathe checks and knots do not have an inherent correlation.

4.2.1.2. Correlation between wave timings in two directions

As shown in Fig. 13, parallel wave timings and perpendicular wave timings were negatively correlated with $r^2 = 0.243$. Although the correlation was not very strong, it might indicate that a higher wave velocity (shorter wave timing) in one direction is probably associated with a slower wave velocity (longer wave timing) in the other direction.

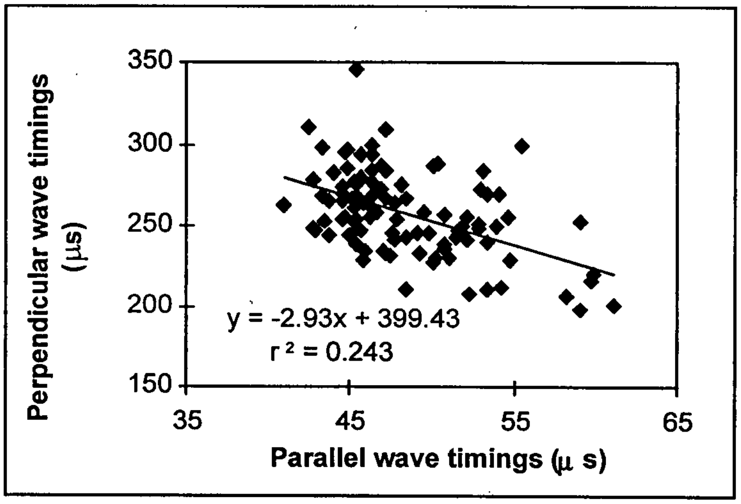

Fig. 13. Correlation between wave timings in two directions

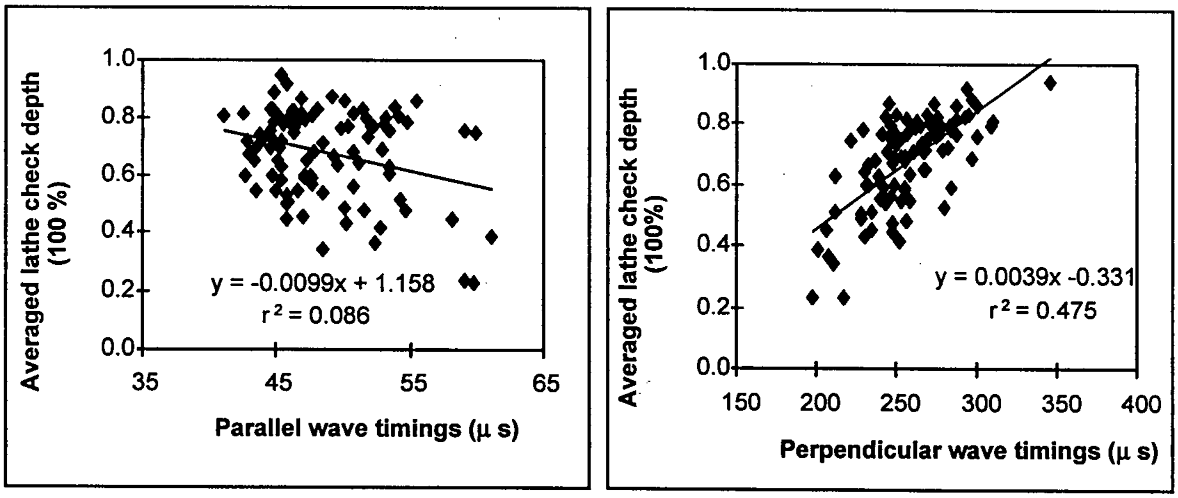

a) Parallel to grain

b) Perpendicular to grain

Fig. 14. The relationships between wave timings and averaged lathe check depth (LCD)

4.2.1.3. Characterization of lathe checks with multivariate regression methods

4.2.1.3.1. Averaged lathe check depth (LCD)

As shown in Fig. 14, a good correlation was found with $r^2 = 0.475$ between wave timings and averaged lathe check depth (LCD) in the perpendicular to grain direction, which suggested that wave propagation perpendicular to grain is sensitive to the presence of lathe checks. In contrast, a weak but negative correlation was found between parallel wave timings and LCD with $r^2 = 0.086$, which indicated that the wave propagation in the parallel to grain direction can not reliably detect the existence of lathe checks.

To best characterize the interrelations of LCD, mass density (X_4) and wave parameters such as perpendicular wave timings (X_2), wave attenuations (X_3), multivariate linear regression analyses and response surface method (RSM) were introduced to investigate the relationships between LCD and wave parameters and mass density. The RMS model has the following general form:

$$F(x_1, x_2, \ldots, x_m) = b_0 + \sum_{j=1}^{m} b_j x_j + \sum_{\substack{i=1 \\ i<j}}^{m-1} \sum_{j=2}^{m} b_{ij} x_i x_j + \sum_{j=1}^{m} b_{jj} x_j^2 \quad (4.1)$$

Here: x_1, x_2, ….., x_m are independent variables; b_0, b_j, b_{ij} and b_{jj} are constants determined by regression analysis.

The results are summarized in Table 5.

Table 5. The regression results for LCD using impact-induced stress wave method

Independent variables	r^2	SEE*	Regression models for LCD	Remarks
<u>All combinations</u>				
X_2, X_3, X_4	0.626	0.093	$-0.977 + 0.004\ X_2 + 0.155\ X_3 + 1.014\ X_4$	(4.2)
X_2, X_3	0.520	0.105	$-0.331 + 0.00369\ X_2 + 0.165\ X_3$	(4.3)
X_2, X_4	0.589	0.097	$-0.992 + 0.00440\ X_2 + 1.038\ X_4$	(4.4)
X_3, X_4	0.135	0.141	$0.356 + 0.258\ X_3 + 0.451\ X_4$	
X_2	0.475	0.109	$-0.331 + 0.00392\ X_2$	Shown in Fig. 14
X_3	0.112	0.142	$0.5873 + 0.257\ X_3$	
X_4	0.022	0.149	$0.4514 + 0.440\ X_4$	
<u>Elimination</u>				
X_2, X_3, X_4	0.626	0.093	$-0.977 + 0.004\ X_2 + 0.155\ X_3 + 1.014\ X_4$	
X_2, X_4	0.589	0.097	$-0.992 + 0.0044\ X_2 + 1.038\ X_4$	Step 1, final
<u>RSM Model</u> **(elimination)**				
$X_2, X_3, X_4,$ $X_2X_3, X_2X_4, X_3X_4,$ X_2^2, X_3^2, X_4^2	0.677	0.089	$-4.421 + 0.027\ X_2 + 0.182\ X_3 + 3.249\ X_4$ $-0.0024\ X_2X_3 - 0.0183\ X_2X_4 + 1.01X_3X_4$ $-0.00002\ X_2^2 + 0.109\ X_3^2 + 1.906\ X_4^2$	X_2, X_2X_4, X_2^2 are significant, initial expression
X_2, X_3X_4, X_4^2	0.630	0.092	$-0.703 + 0.0042\ X_2 + 0.313\ X_3X_4$ $+ 0.897\ X_4^2$	Step 6, final

* SEE refers to the standard error of estimate of regression model

Comparing (4.3) with (4.4), it can be seen that, coupled with perpendicular wave timings (X_2), mass density (X_4) is a better variable than perpendicular wave attenuation (X_3) to quantify LCD. The regression model (4.2) was significantly improved over (4.3) with the incorporation of mass density.

4.2.1.3.2. Lathe check number (LCN)

The multivariate regression method was also used to characterize LCN using perpendicular wave timings (X_2), perpendicular wave attenuations (X_3) and mass density (X_4) as independent variables.

1) Using X_2, X_3, X_4 as independent variables

The multiple linear regression equation was

$$LCN = 39.567 + 0.218\, X_2 + 4.013\, X_3 + 158.622\, X_4 \qquad (4.5)$$

with $r^2 = 0.1588$ and SEE = 20.142.

2) Using RSM model of X_2, X_3, X_4

Response surface method (RSM) model showed that the significant variables are X_2, X_3, and $X_2 * X_3$ with $r^2 = 0.2810$ and SEE = 19.246.

Combining 1) with 2), no satisfactory model could be found to predict LCN; *i.e.*, wave parameters were not very sensitive to the number of lathe checks.

4.2.1.4. Identification of a better criterion and NDE model for characterizing knots

Individual wave timing information in both parallel and perpendicular to grain directions were chosen as individual sampling lines pass through knot area in the 98 specimens. Also the corresponding knot chord in both parallel and perpendicular to grain directions were recorded for these sampling lines. The correlations between wave timings and knot chords in both parallel and perpendicular to grain directions were generated and shown in Figures 15 and 16 which indicated weak correlations. Note that the slope of regression line in Fig. 16 was negative, which suggested that existence of knots did not impede the wave propagation perpendicular to grain.

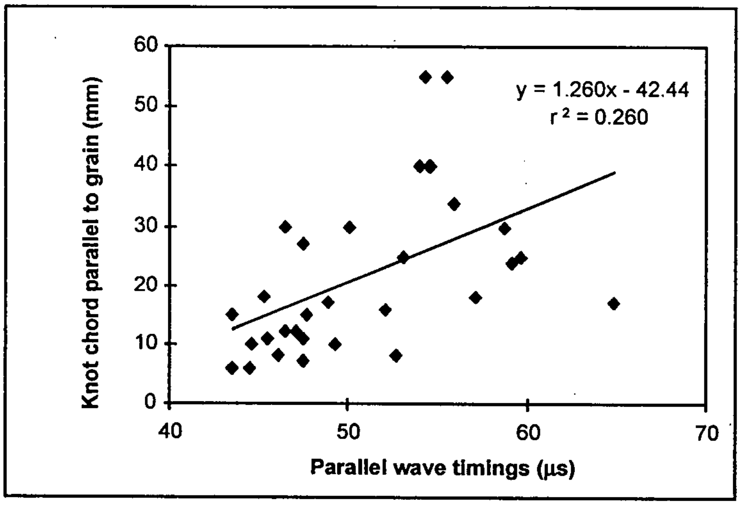

Fig. 15. The relationship between parallel wave timings and knot chord parallel to grain

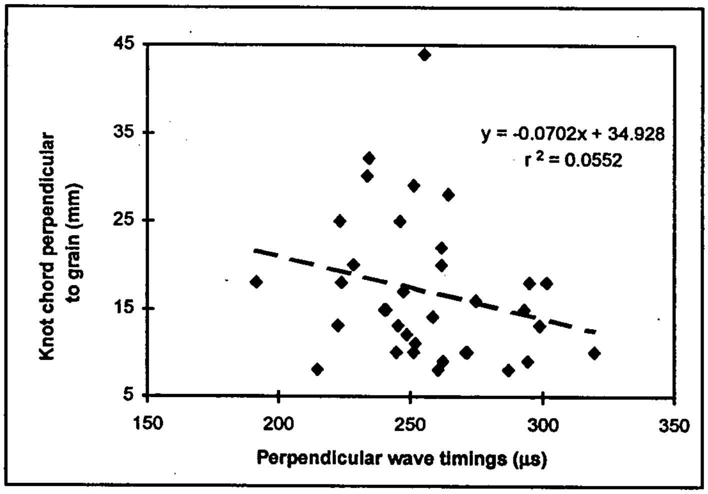

Fig. 16. The relationship between perpendicular wave timings and knot chord perpendicular to grain

Furthermore, considering the practicality issue, it was also inappropriate to simply use knot chord as a criterion to quantify the existence of knots because knot chord estimate would vary with the location of sampling lines; *i.e.*, localized knot effects rather than knot effects in an entire veneer sheet was identified.

In addition to Percentage of Knot Area (PKA), Cumulative Knots Diameter in the parallel (CKD_1) and perpendicular (CKD_2) to the grain directions were introduced for quantifying the presence of knots in an entire veneer specimens. CKD_1 or CKD_2 was the cumulative maximum diameter for an entire veneer sheet in the parallel or perpendicular to grain direction respectively. CKD_1 (or CKD_2) was equivalent to Knots Area Ratio (KAR) if knot diameter was seen as constant throughout the veneer thickness. This assumption might not cause much difference between CKD_1 (or CKD_2) and KAR since veneer specimen is usually very thin. The knot criteria such as PKA, CKD_1 and CKD_2 were correlated with the averaged wave timing in each veneer specimen respectively to see which criterion is the best for acoustic wave methods to quantify the existence of knots.

Based on regression analyses of wave timings and PKA, CKD_1, and CKD_2 in both directions, it can be shown that the acoustic wave method is not sensitive to the size of knots with $r^2 < 0.10$ for 98 veneer specimens tested. In the following analyses, PKA rather than CKD_1 and CKD_2 was chosen to quantify the existence of knots since PKA was non - directional and more perceivable.

From Table 4 and Table 6 it can be noted that PKA correlated well with the standard deviation of parallel wave timings (X_{12}) with $r^2 = 0.340$, which indicated that parallel wave timing standard deviation is a much better parameter than parallel wave timings to characterize the presence of knots in veneer specimens. This would provide a means to greatly improve the knot quantification using acoustic wave techniques.

Multiple linear regression and RSM methods were used to establish the relationships between PKA and wave timing characteristics such as parallel wave timings (X_1) and parallel wave timing standard deviation (X_{12}) as shown in Table 6.

Table 6. The regression results for PKA using impact-induced stress wave method

Independent variables	r^2	SEE	Regression models for PKA	Remarks
<u>All combinations</u>				
X_1, X_{12}	0.341	0.845	$-0.0782 - 0.00754 X_1 + 0.438 X_{12}$	X_{12} is significant
X_1	0.071	0.998	$-2.545 + 0.0622 X_1$	
X_{12}	0.340	0.841	$-0.419 + 0.426 X_{12}$	
<u>Elimination</u>				
X_1, X_{12}	0.341	0.845	$-0.0782 - 0.00754 X_1 + 0.438 X_{12}$	
X_{12}	0.340	0.841	$-0.419 + 0.426 X_{12}$	Step 1, final
<u>RSM model</u> (elimination)				
$X_1, X_{12}, X_1X_{12}, X_1^2, X_{12}^2$	0.508	0.742	$-11.830 + 0.575 X_1 - 2.418 X_{12} + 0.0515 X_1X_{12} - 0.0068 X_1^2 + 0.0295 X_{12}^2$	X_{12}, X_1X_{12} are significant, initial expression
$X_1, X_{12}, X_1X_{12}, X_1^2$	0.505	0.740	$-13.190 + 0.656 X_1 - 3.022 X_{12} + 0.0671 X_1X_{12} - 0.0079 X_1^2$	Step 1
X_{12}, X_1X_{12}, X_1^2	0.489	0.748	$2.754 - 2.481X_{12} + 0.0569X_1X_{12} - 0.00128 X_1^2$	Step 2, final (4.6)

The equation (4.6) could be used to quantify the existence of knots in veneers. Unlike wave attenuation (ATT), wave timing characteristics could be easily attained; hence, this model showed promise for real-time NDE of the existence of knots.

4.2.2. Ultrasonic equipment (AU approach)

4.2.2.1. Correlations between AU timings in two directions

The AU timings in both directions were negatively correlated with $r^2 = 0.385$ for 26 veneer specimens as shown in Fig. 17. The results again confirmed the finding from stress wave methods discussed in section 4.2.1.2.

4.2.2.2. Multiple regression models for characterizing lathe checks

1) Averaged lathe check depth (LCD)

As shown in Fig. 18, in the perpendicular to grain direction, the AU timings and LCD were positively correlated with $r^2 = 0.425$, SEE = 0.123 for 45 specimens, which demonstrated that AU method is also sensitive to the presence of lathe checks. However, in the parallel to grain direction, a relatively weak but negative correlation was found between LCD and AU timings with $r^2 = 0.276$, SEE = 0.148 for 26 specimens, which again illustrated that the parallel wave transmission cannot reliably detect the presence of lathe checks.

As shown in Fig. 19, a good corrrelation was found between AU attenuation perpendicular to grain and LCD with $r^2 = 0.393$, which suggested that AU attenuation (inverse of perpendicular RMS voltages) perpendicular to grain is also a good indicator of LCD. The result also suggested that this attenuation criterion is better than the inverse of the first peak amplitude (stress wave method) since this RMS voltage is an indicator of attenuation characteristics based on the entire signal.

Several multiple regression analyses were performed to investigate how AU parameters such as perpendicular wave timings (X_2) and perpendicular wave attenuation

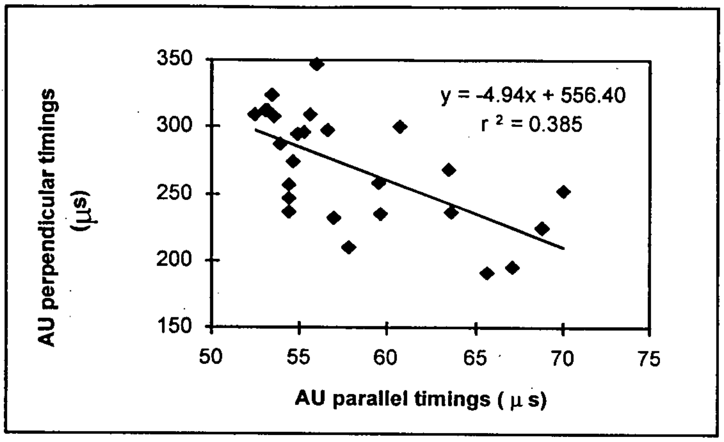

Fig. 17. Correlation between AU timings in two directions (26 specimens)

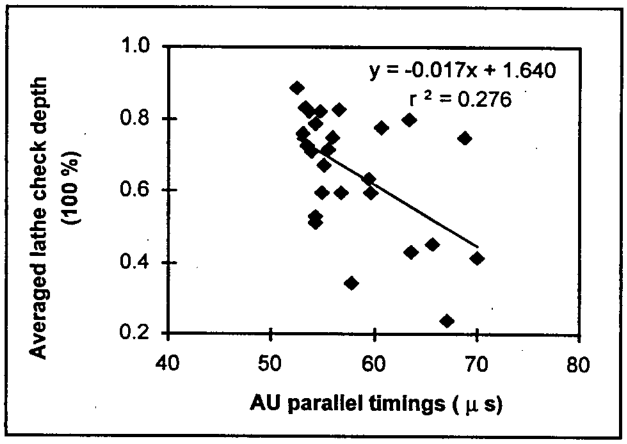

a) Parallel to grain (26 specimens)

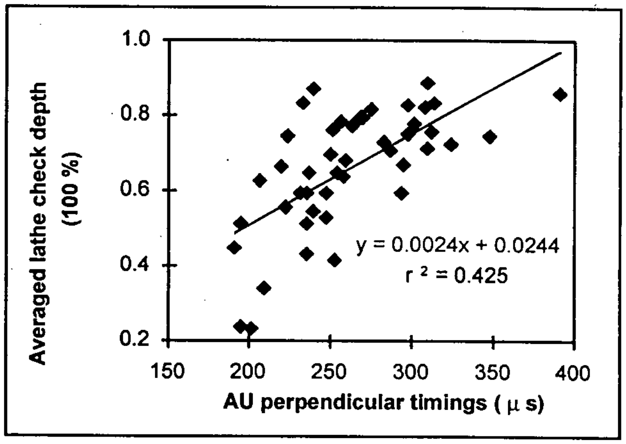

b) Perpendicular to grain (45 specimens)

Fig. 18. The relationships between AU timings and averaged lathe check depth (LCD)

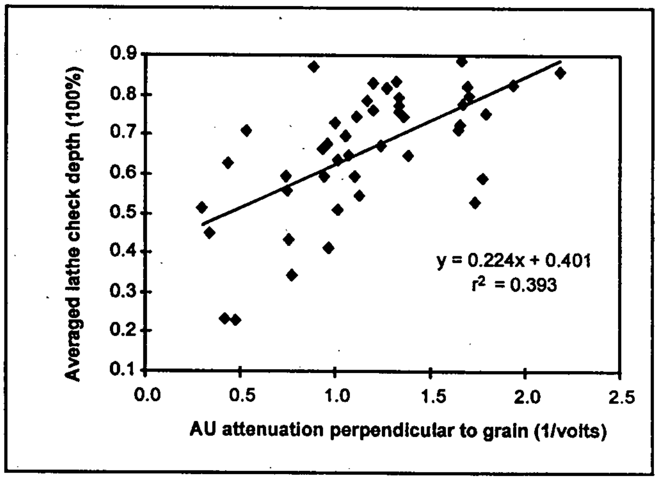

Fig. 19. Correlation between LCD and AU attenuation perpendicular to grain

(X_3) and mass density (X_4) contribute to the explanation of averaged lathe check depth (LCD) as shown in Table 7.

Table 7. The regression results for LCD using AU method for 45 specimens

Independent variables	r^2	SEE	Regression models for LCD	Remarks
All combinations				
X_2, X_3, X_4	0.516	0.116	$-0.239 + 0.0018X_2 + 0.092X_3 + 0.619X_4$	X_2 is significant (4.7)
X_2, X_3	0.474	0.119	$0.121 + 0.00155X_2 + 0.115X_3$	(4.8)
X_2, X_4	0.487	0.118	$-0.377 + 0.00251X_2 + 0.729X_4$	(4.9)
X_3, X_4	0.413	0.126	$0.191 + 0.219\,X_3 + 0.412\,X_4$	
X_2	0.425	0.123	$0.0244 + 0.00243\,X_2$	Shown in Fig. 18
X_3	0.393	0.127	$0.401 + 0.224\,X_3$	Shown in Fig. 19
X_4	0.037	0.160	$0.368 + 0.562\,X_4$	
Elimination				
X_2, X_3, X_4	0.516	0.116	$-0.239 + 0.00180X_2 + 0.092X_3 + 0.619X_4$	
X_2, X_4	0.487	0.118	$-0.377 + 0.00251X_2 + 0.729\,X_4$	Step 1
X_2	0.425	0.123	$0.0244 + 0.00243\,X_2$	Step 2, final
RSM Model (elimination)				
X_2, X_3, X_4, X_2X_3, X_2X_4, X_3X_4, X_2^2, X_3^2, X_4^2	0.652	0.106	$-4.581 + 0.022X_2 + 0.111X_3 + 7.083X_4 + 0.0012X_2X_3 - 0.018X_2X_4 - 0.449X_3X_4 - 2.2\text{E-}05X_2^2 - 0.0515X_3^2 - 1.342X_4^2$	No variable is significant, initial expression
X_2, X_4, X_2X_4, X_2^2	0.619	0.104	$-3.956 + 0.0211\,X_2 + 5.109\,X_4 - 0.0172\,X_2X_4 - 0.00002\,X_2^2$	Step 5 (4.10)
X_2, X_4, X_2^2	0.573	0.109	$-1.770 + 0.0126\,X_2 + 0.809\,X_4 - 0.00002\,X_2^2$	Step 6 (4.11)
X_2, X_2^2	0.497	0.117	$-1.208 + 0.0117\,X_2 - 0.00002\,X_2^2$	Step 7 (4.12)
X_2	0.425	0.123	$0.0244 + 0.00243\,X_2$	Step 8, final (4.13)

Comparing (4.8) with (4.9), it was seen that mass density (X_4) is a better variable than perpendicular wave attenuation (X_3) to characterize the averaged lathe check depth (LCD) coupling with perpendicular wave timings (X_2), which showed the same results with the stress wave method. Although perpendicular wave attenuation (X_3) correlated with LCD well with $r^2 = 0.393$, it did not contribute to the model improvement significantly coupling with perpendicular wave timings (X_2). This demonstrated that a similar mechanism between wave timings and wave attenuations may exist for characterizing LCD; *i.e.*, a change in wave timings means a change in wave attenuation. This was also proved by regression model (4.7) which only give slightly improved correlation compared to equations (4.9).

2) <u>Lathe check number (LCN)</u>

From Table 4 a weak correlation was found between AU attenuation perpendicular to grain and LCN with $r^2 = 0.0902$. But no correlation was found between AU perpendicular timings and LCN ($r^2 = 0.011$), which suggested that AU method is also not very sensitive to LCN.

The multivariate linear regression model was established to account for lathe check number (LCN) using perpendicular wave timings (X_2), perpendicular wave attenuation (X_3) and mass density (X_4). The model was:

$$LCN = 122.84 - 0.091X_2 + 20.42X_3 + 98.09X_4 \qquad (4.14)$$

with $r^2 = 0.172$ and SEE = 21.35

Therefore, there was no strong relationship between lathe check number (LCN) and AU parameters.

3) Summary results of lathe check effects

Similar to the stress wave method, AU method was also sensitive to averaged lathe check depth (LCD) but not sensitive to lathe check number (LCN). The established model for explaining LCD was shown to be acceptable using just perpendicular wave timings and mass density. In on-line veneer quality assessment using AU method, mass density and perpendicular wave timings could be more conveniently attained than perpendicular wave attenuations, which showed promise for real-time monitoring of lathe checks in veneer.

4.2.2.3. Knots characterizing using AU parameters

The correlation matrix for parallel wave parameters, mass density and PKA was established for 26 veneer specimens as shown in Table 8.

Table 8. Correlation matrix for AU parameters, density and PKA

Correlations	*Parallel timings*	*Par. timing stdev.*	*Parallel ATT*	*Par. ATT stdev.*	*Density*	*PKA*
Parallel timings	1.0000					
Par. timing stdev	0.5481	1.0000				
Parallel ATT	0.3780	0.1166	1.0000			
Parallel ATT stdev.	0.3911	0.2054	0.8837	1.0000		
Density	0.1356	0.3117	-0.2270	-0.1228	1.0000	
PKA	0.0571	0.3369	0.0709	0.2273	-0.1320	1.0000

From Table 8 it can be found that parallel wave timings and parallel wave attenuation were not very sensitive to the size of knots, but wave timing standard deviation and wave attenuation standard deviation parallel to grain are much more sensitive to PKA than wave timings and wave attenuations parallel to grain respectively. This conclusion agreed with that from the stress wave method. Using these 5 variables listed in Table 8, a multiple linear regression model for PKA was generated with $r^2 = 0.302$ and SEE = 0.604. Since only 26 specimens were used and 16 specimens contained knots, the correlation was not strong enough as expected. It was believed that the knots characterizing with AU methods can be significantly improved with the increase of veneer specimens and the incorporation of more wave parameters.

4.3. Comparison between stress wave and acousto-ultrasonic (AU) methods

4.3.1. Comparison between parallel wave timings

As seen from Fig. 20, the correlation between AU parallel timings and stress wave parallel timings was very good since the r^2 reached 0.820. It was found that the AU parallel timings are generally larger than stress wave parallel timings because: First the sampling points for AU testing and stress wave testing were not exactly the same (see Figures 5 and 6) and secondly the two ends of AU testing specimens were once soaked into water-soluble dye for measuring the lathe checks before AU testing. In this case, the moisture content in veneer specimens were increased, which was considered to be unfavorable to the wave transmission in both directions. Therefore, there existed no significant difference between AU timings and stress wave timings in the parallel to grain direction.

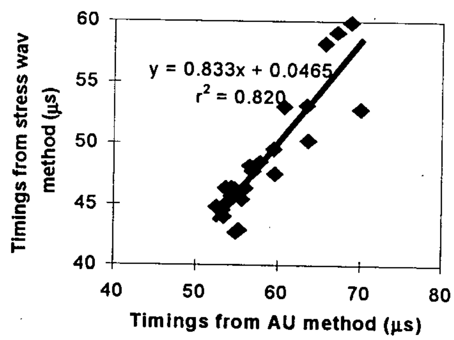

Fig. 20. Comparison of parallel wave timings (26 specimens)

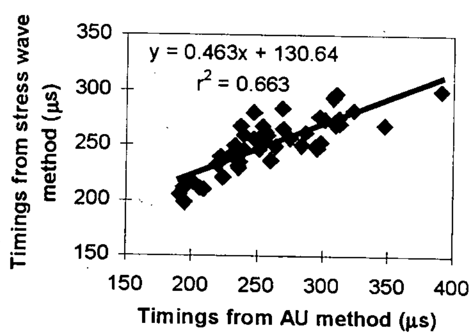

Fig. 21. Comparison of perpendicular wave timings (45 specimens)

4.3.2. Comparison between perpendicular wave timings

As seen from Fig. 21, the correlation between AU perpendicular timings and stress wave perpendicular timings was also good (r^2 = 0.663). Therefore, there also existed no significant difference between AU timings and stress wave timings in the perpendicular to grain direction.

4.4. Establishment of veneer quality criterion

To evaluate veneer overall quality based on the detection of both lathe checks and knots, wave measurements should be taken in both orthogonal directions since wave propagation in only one direction cannot reliably detect the existence of lathe checks and knots simultaneously.

One way to implement veneer grading is to define a single parameter that includes overall veneer quality. Actual grading could be then accomplished by setting specific limits on this parameter for different grades. For this purpose a quality criterion (Q) of each veneer specimen was defined to evaluate veneer overall quality based on the existence and severity of lathe checks and knots. Since there existed no significant difference in the wave timings between the stress wave and AU methods, the establishment of Q was based on the database collected with the stress wave device which contained more tested specimens.

An observed overall quality criterion (Q) for each veneer specimen can be described as:

$$Q_i = w_1 (LCD)_{Ni} + w_2 (PKA)_{Ni} \qquad (i = 1 \cdots\cdots 98) \qquad (4.15)$$

where $(LCD)_{Ni}$ and $(PKA)_{Ni}$ are the normalized averaged lathe check depth and percentage of knot area of each veneer specimen, and w_1 and w_2 are the weighted factors (positive values) based on the relative importance of the LCD and PKA.

Defining the LCD_{Ni} and PKA_{Ni} of each veneer specimen as:

$$LCD_{Ni} = (LCD_i - LCD_{min})/(LCD_{max} - LCD_{min}) \qquad (i = 1 \cdots\cdots 98) \qquad (4.16)$$

$$PKA_{Ni} = (PKA_i - PKA_{min})/(PKA_{max} - PKA_{min}) \qquad (i = 1 \cdots\cdots 98) \qquad (4.17)$$

where LCD_{max}, LCD_{min} and PKA_{max}, PKA_{min} are the upper and lower limits of the LCD and PKA based on experimental results shown in Table 1, respectively. This normalization method can balance the numerical levels of LCD and PKA and eliminate their unit difference. The smaller the Q value, the better the quality of the veneer specimen as shown in Table 2 (Appendix F).

One way to estimate Q from nondestructive measurements is using averaged wave velocities in the directions parallel to grain (V_1) and perpendicular to grain (V_2) in each veneer specimen. In terms of different combinations of weighted factors, the established regression models for Q using V_1 and V_2 were listed in Table 9.

Table 9. Regression results for Q using V_1 and V_2

Weight combinations	r^2	SEE	Regression equations
w_1=1 and w_2=1	0.392	0.206	$Q=3.473-0.00016V_1-0.00167V_2$ (1)
w_1=2 and w_2=1	0.478	0.329	$Q=5.970-0.00021V_1-0.00309V_2$ (2)
w_1=3 and w_2=1	0.500	0.465	$Q=8.460-0.00027V_1-0.00452V_2$ (3)

Based on the predicted Q from model (1) in Table 9, the correlation between the observed Q and the predicted Q was generated as shown in Fig. 22a which indicated that the combination of averaged wave velocities in two orthogonal directions can account for 39.2 % of the variation of both lathe checks and knots in veneer specimens if the lathe checks and knots are assumed to have equal importance to the performance of veneer based products. The accuracy of this model was affected by the weak correlation between V_1 and PKA. The model would be significantly improved if more weight was assigned to the lathe checks than knots as shown in Table 9 and Fig. 22b. In the practical application, the weighted factors could be adjusted according to the relative importance of lathe checks and knots to the different veneer based products. Further research is needed to find this information to evaluate veneer overall quality and grade veneers with an aim to enhance shear strength of these products.

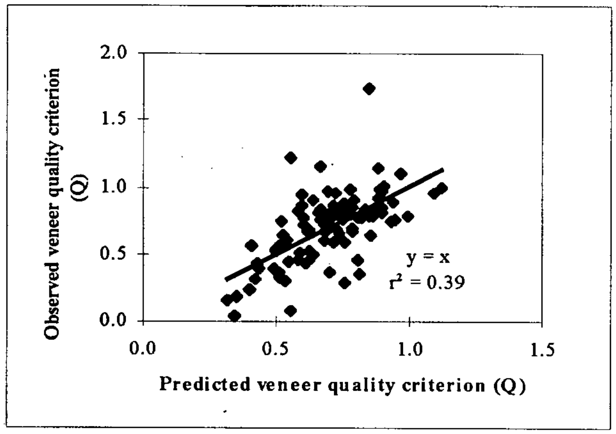

a) w_1=1 and w_2=1

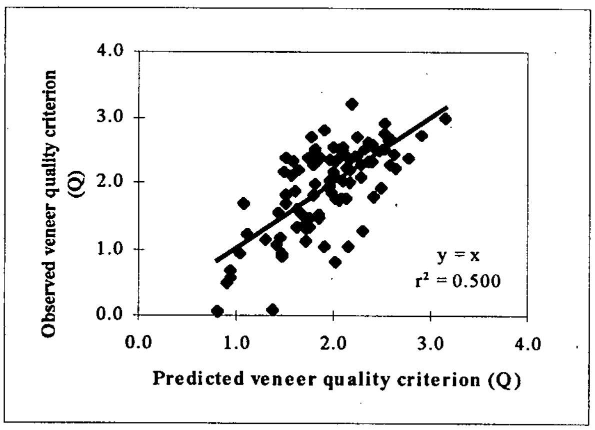

b) w_1=3 and w_2=1

Fig. 22. The correlation between observed Q and predicted Q

5. CONCLUSIONS

Based on above analyses and results, the following conclusions were made:

1. Acoustic wave propagation in the perpendicular to grain direction is sensitive to the averaged lathe check depth (LCD) based on stress wave or AU techniques, but cannot detect the presence of knots effectively.
2. The suitability of using wave propagation parallel to grain to detect the presence of knots was confirmed in this research. However, such a method cannot effectively detect the presence of lathe checks.
3. The severity of lathe checks (LCD) and size of knots (PKA) can be successfully quantified with multiple regression methods using wave parameters such as wave timings, attenuations and mass density.
4. To evaluate overall veneer quality using a stress wave or AU method based on the detection of both lathe checks and knots, the measurement of wave velocities in both directions is necessary. Three regression based models were developed for this purpose which can predict veneer overall quality defined by LCD and PKA with r^2 ranging from 0.392 to 0.500. Such techniques show promise as the NDE method to assess veneer quality for engineered applications.

6. FUTURE STUDY

The above conclusions have shown strong promise to apply the stress wave or AU method in NDE of veneer quality. However, there still exist several areas where improvements can be made such as:

1) Effects of some factors on wave signals

In this research, sampling lines (lines of wave propagation) of some specimens did not pass through knots areas, so the averaged parallel wave velocity was overestimated. The wood natural variability effect such as component difference of earlywood and latewood in veneer specimens, the growth ring angle (dive angle) effect on wave propagations perpendicular to grain have not been considered.

2) Improvement of prediction of veneer overall quality

Although the prediction model for the veneer overall quality criterion developed in this research shows promise, further improvement is possible through a detailed evaluation of the waveform to better characterize lathe checks and knots. Future work should consider the feature extraction of waveform to improve the prediction model of veneer quality.

3) Development of on-line AU testing

Future research is needed to refine AU veneer testing setup and develop feasible on-line scanning method such as a) modifying transducer coupling and test configurations and b) using air-coupled or wheeled transducers.

4) Verification of the veneer overall quality approach

The reliability of the veneer overall quality approach needs to be verified by examining failure modes and testing strength properties of laminated veneer products.

7. BIBLIOGRAPHY

Antonucci, R., R. Giacchetti and P. Munafo. 1996. Nondestructive evaluation of structural parameters in wooden beams. In: Proceedings of International Wood Engineering Conference. 3:218-225

Armstrong, J. P. and D. W. Patterson. 1991. Evaluation of a stress wave NDT techniques for detecting skips in the gluelines of edge-glued red oak panels. Forest Prod. J. 41(11/12):61-66

ASTM D 2718 - 95. 1995. Standard test method for structural panels in planar shear (rolling shear). Annual book of ASTM. Vol 04.10.

ASTM D1038 - 83. 1993. Standard Terminology relating to veneer and plywood. Annual book of ASTM. Vol 04.10.

ASTM E 1495 - 92. 1992. Standard guide for acousto-ultrasonic assessment of mechanical properties of composites, laminates, and bonded joints. Annual book of ASTM. Vol 03.03.

Beall, F. C. 1993. Overview of Acousto-ultrasonics applied to wood and wood-based products. In: Proceedings of Second International conference on Acousto-Ultrasonics. Hyatt Regency Atlanta, Atlanta, GA

Beall, F. C. and J. Biernacki. 1993. Monitoring the adhesive curing process for parallel wood laminates. In: Proceedings of Second International conference on Acousto-Ultrasonics. Hyatt Regency Atlanta, Atlanta, GA

Beattie, A. G. 1983. Acoustic Emission, Principles and Instrumentation. Journal of Acoustic Emission. 2(1/2):95-127

Bendtsen, B. A. 1976. Rolling shear characteristics of nine structural softwoods. Forest Prod. J. 26(11):51-56

Bethel, F. K. 1986. Use of the Metriguard Model 239A stress wave timer. Instruction material. 8pp

Biblis, E. J., W. Chen and W. Lee. 1982. Rolling shear properties of southern pine plywood and unidirectionally laminated veneer. Forest Prod. J. 32(2):45-50

Biblis, E. J. and Y. Chiu. 1975. Effect of reversing the loose and tight sides of surface veneer on flexural and shear properties of Southern Pine plywood. 25(10):33-37

Biernacki, J. M. and F. C. Beall. 1993. Development of an acousto-ultrasonic scanning system for nondestructive evaluation of wood and wood laminates. Wood and Fiber Science. 25(3):289-297

Biernacki, J. M. and F. C. Beall. 1993. Evaluation of the quality of adhesive bonding in parallel wood laminates. In: Proceedings of Second International conference on Acousto-Ultrasonics. Hyatt Regency Atlanta, Atlanda, GA

Bohlen, J. C. 1975. Shear strength of Douglas-fir laminated veneer lumber. Forest Prod. J. 25(2):16-23

Booth, L. G. 1990. Predicting the bending strength of structural plywood (Part 1). J. Inst. Wood Sci. 12(1): 14-47

Bucur, V. and F. Feeney. 1992. Attenuation of ultrasound in solid wood. Ultrasonics. 30(2):76-81

Chow, S. 1970. Lathe-check influence on plywood shear strength. VP-X-122, Forestry Service, Environment Canada. 14pp.

Faust, T. D. 1987. Real time measurement of veneer surface roughness by image analysis. Forest Prod. J. 37(6): 34 -40

Fox, R. L. 1972. Optimization methods for engineering design. Addison-Wesleg Publishing.

Fuller, J. J., R. J. Ross and J. R. Dramm. 1995. Nondestructive evaluation of honeycomb and surface checks in Red Oak lumber. Forest Prod. J. 45(5):42-44

George, P. and D. G. Miller. 1969. Detection of roughness in moving Douglas-fir veneer. Forest Prod. J. 20(&):53-59

Gerhards, C. C. 1974. Stress wave speed and MOE of sweetgum ranging from 150 to 15 percent MC. Forest Prod. J. 25(4):51-57

Gerhards, C. C. 1978. Effect of earlywood and latewood on stress wave measurements parallel to grain. Wood Sci. 11(2):69-72

Gerhards, C. C. 1982. Longitudinal stress waves for lumber stress grading: factors affecting applications: state of art. Forest Prod. J. 32(2):20-25

Gerhards, C. C. 1980. Effect of cross grain on stress waves in lumber. Research Paper FPL 368. Forest Service, USDA. 8pp

Gerhards, C. C. 1982. Effect of knots on stress waves in lumber. Research Paper FPL 384. Forest Service, USDA. 14pp

Hailey, J. R. T. and M. K. Robert. 1980. Optimizing veneer yield and quality: A comparison of industrial and laboratory lathes. Forest Prod. J. 30(4):43-47

Hailey, J. R. T., W. V. Hancock, and W. G. Warren. 1980. The effect of lathe parameters on veneer yield and quality. Wood Sci. 12(3):141-148

Hamstad, M. A. and S. L. Quarles. 1993. Experimental far-field wideband acoustic waves in wood rods and plates. In: Proceedings of Ninth International Symposium on Nondestructive Testing of Wood. Madison, Wisconsin, USA. 30-44

Hettiarachchi, M. T. P. 1990. Predicting the bending strength of structural plywood. In: Proceedings of 1990 International Timber Engineering Conference. Tokyo. 215-221

Hettiarachchi, M. T. P. 1990. Predicting the bending strength of structural plywood (Part 3): Incorporating the effect of knots. J. Inst. Wood Sci. 12(2): 83-92

Hoag, M. L. and R. L. Krahmer. 1991. Polychromatic X-ray attenuation characteristics and wood densitometry applications. Wood and Fiber Science. 23(1) 23-31

Hoag, M. and M. D. McKimmy. 1988. Direct scanning X-ray densitometry of thin wood sections. Forest Prod. J. 38(1)23-26

James, W. L., Y. You-Hsin and J. K. Ray. 1985. A microwave method for measuring moisture content, density, and grain angle of wood. Research Note FPL-0250. Forest service, USDA. 9pp

June, J. 1979. Stress-wave grading techniques on veneer sheets. FPL-GTR-27, Forest Service, USDA. 10pp.

Jung, J. 1982. Properties of parallel-laminated veneer from stress-wave-tested veneers. Forest Prod. J. 32(7):30-35

Kaiserlik, J. H. and R. F. Pellerin. 1977. Stress wave attenuation as an indicator of lumber strength. Forest Prod. J. 27(6): 39-43

Knuffel, W. E. 1988. Acoustic emission as strength predictor in structural timber. Holzforchung. 42(3): 195-198

Kunesh, R. H. 1978. Using ultrasonic energy to grade veneer. In: Proceedings of 4th NDT of wood symposium. The Inn at the Quay, Vancouver, Washington. 275-277

Lam, F. 1992. Performance of laminated veneer wood plates in decking systems. Ph.D. dissertation. UBC, Vancouver. 239pp.

Lemaster, R. L. and D. A. Dornfeld. 1987. Preliminary investigation of feasibility of using AU to measure defects in lumber. Journal of Acoustic Emission. 6(3): 157-165

Lemaster, R. L. 1993. The use of acousto-ultrasonics to detect decay in wood -based products. In: Proceedings of Second International conference on Acousto-Ultrasonics. Hyatt Regency Atlanta, Atlanta, GA

Martin, P., R. Collet, P. Barthelemy and G. Roussy. 1987. Evaluation of wood characteristics: Internal scanning of the material by microwaves. Wood Science and Technology. 21: 361-371

McAlister, R. H. 1976. Modulus of elasticity distribution of Loblolly Pine veneer as related to location within the stem and specific gravity. Forest Prod. J. 26(10): 37-39

Metriguard Inc. 1995. Precision testing equipment for wood. Instruction book. 80pp.

Munthe, B. P. and R. L. Ethington. 1968. Method for evaluating shear properties of wood. Research Note FPL-0195. Forest Service, USDA. 8pp

Noguchi, M., Y. Kagawa and J. Katagiri. 1980. Detection of Acoustic Emission during Hardwood Drying. Mokuzai Gkkashi 26(9):637-638

Palka, L. C. 1966. Factors affecting the strength properties of Douglas-fir plywood normal to the glueline. Forest Prod. J. 16(3): 44-52

Palka, L. C. 1970. Rolling shear properties of single-species Canadian softwood plywoods. VP-X-177, Environmental Management Service, Fisheries and Environment Canada. 26pp.

Palka, L. C. and W. G. Warren. 1977. Grouping of Canadian veneer species based on plywood rolling shear properties. Information Report VP-X-163. Western Forest Products Lab. Canadian Forestry Service.

Palka, L. C. and J. Hejjas. 1977. Effect of moisture content on the mechanical properties of Douglas-fir plywood in rolling shear. Forest Prod. J. 27(4): 49-53

Porter, A. W., M. L. El-Osta and D. J. Kusec. 1972. Prediction of Failure of Finger Joints using Acoustic Emissions. Forest Prod. J. 22(9):74-82

Ross, R. J., J. C. Ward and A. TenWolde. 1994. Stress wave nondestructive evaluation of wetwood. Forest Prod. J. 44 (7/8): 79-83.

Ross, R. J. and R. F. Pellerin. 1991. Nondestructive testing for assessing wood members in structures: A review. FPL-GTR-70, Forest Service, USDA.27pp.

Ross, R. J. and R. F. Pellerin. 1988. NDE of wood-based composites with longitudinal stress waves. Forest Prod. J. 38 (5):39-45

Ross, R. J. 1991. NDE of green material with stress waves: preliminary results using dimension lumber. Forest Prod. J. 41(6):57-59

Ross, R. J., C. D. Rodney, J. N. William, K. L. Patricia. 1996. Stress wave NDE of biologically degraded wood. In: Proceedings of International Wood Engineering Conference. 3:213-217

Sakai, H., A. Minamisawa and K. Takagi. 1990. Effect of moisture content on ultrasonic velocity and attenuation in woods. 28(6): 382-385

Sandoz, J. L. J. 1993. Valorization of forest products as building materials using nondestructive testing. In: Proceedings of Ninth International Symposium on Nondestructive Testing of Wood. Madison, Wisconsin, USA. 105-109

Schmoldt, D. L. and J. C. Duke. 1993. Application of ultrasound nondestructive evaluation to grading pallet parts. In: Proceedings of Ninth International Symposium on Nondestructive Testing of Wood. Madison, Wisconsin, USA. 183-190

Shen, J. 1995. Wood property measurements using microwaves. Ph.D. dissertation. UBC. 118pp

Shupe, T. F., Y. H. Chung, H. G. Leslie and T. C. Elvin. 1996. Effect of veneer grade layup on bending properties of Lobolly Pine LVL. In: Proceedings of International Wood Engineering Conference. Louisiana. 526-530

Suryoatmono, B., Y. S. Cramer and K. A. McDonald. 1993. Within-board lumber density variations from digital X-ray images. In: Proceedings of Ninth International Symposium on Nondestructive Testing of Wood. Madison, Wisconsin, USA. 168-175

Szymani, R. and A. M. Kent. 1981. Defect detection in lumber: state of art. Forest Prod. J. 31(11): 34 -44

Walker, N. K. and S. D. Richard. 1988. Calculation of wood density variation from X-ray densitometer data. Wood and Fiber Science. 20(1):35-43

Wilcox, W. W. 1988. Detection of early stages of wood decay with ultrasonic velocity. Forest Prod. J. 38(5):68-73

Wilson, J. B. 1992. Nondestructive testing and product quality. Wood and fiber science 24(2): 111-112

Appendix A

Table 1. Experimental results of veneer grade factors

Specimen No.	Density	Thickness Average	Thickness Stdev	Lathe Checks LCD	Lathe Checks LCN	Knots PKA	Knots CKD_1	Knots CKD_2	Grain Angle	Roughness Grade
	(g/mm^3)	(mm)		(100 * %)		(%)	(mm)	(mm)	(degree)	
1	0.476	2.51	0.047	0.8000	171	0	0	0	2.020	0
2	0.460	2.56	0.055	0.5820	191	0	0	0	1.687	0
3	0.436	2.54	0.071	0.8860	190	0	0	0	1.555	0
4	0.527	2.46	0.113	0.7930	220	0	0	0	1.350	0
5	0.525	2.39	0.115	0.7145	235	0	0	0	1.084	0
6	0.517	2.71	0.088	0.5285	172	0.28	30	31	2.576	3
7	0.479	2.50	0.123	0.6785	175	2.12	47	70	1.493	0
8	0.573	2.44	0.075	0.7750	183	0.65	48	43	1.187	1
9	0.472	2.35	0.103	0.8145	187	0.26	13	17	1.923	0
10	0.545	2.59	0.171	0.8605	158	0.54	23	25	1.902	4
11	0.551	2.49	0.054	0.8250	194	0	0	0	1.984	0
12	0.644	2.52	0.065	0.7825	208	0	0	0	1.902	1
13	0.538	2.48	0.065	0.7965	187	0	0	0	1.064	0
14	0.533	2.61	0.076	0.6645	167	0	0	0	1.718	1
15	0.555	2.35	0.054	0.8720	201	0	0	0	1.677	0
16	0.451	2.60	0.070	0.2305	104	0.54	27	28	1.636	3
17	0.495	2.68	0.150	0.7535	161	2.79	39	46	2.535	2
18	0.538	2.48	0.094	0.5035	170	0.06	9	16	0.962	0
19	0.485	2.61	0.078	0.5395	169	0	0	0	1.923	0
20	0.512	2.58	0.122	0.9180	164	0.09	6	12	1.657	4
21	0.443	2.55	0.068	0.7285	167	0	0	0	1.289	0
22	0.528	2.67	0.146	0.7110	165	0.53	32	34	2.188	4
23	0.505	2.46	0.090	0.8080	171	0.12	8	11	1.882	0
24	0.514	2.52	0.109	0.6930	158	0.21	13	20	1.555	0
25	0.516	2.54	0.064	0.7145	201	1	42	41	1.411	2
26	0.480	2.57	0.093	0.7785	173	0.61	36	35	1.207	0
27	0.432	2.46	0.070	0.4145	143	0.19	0	0	3.311	1
28	0.578	2.55	0.053	0.6715	161	0.15	11	12	1.800	1
29	0.419	2.56	0.102	0.5110	181	0	0	0	2.433	1
30	0.517	2.42	0.046	0.7800	176	0	0	0	0.573	1
31	0.483	2.40	0.064	0.7680	196	0	0	0	0.982	1
32	0.502	2.63	0.082	0.9450	174	0	0	0	1.657	2
33	0.520	2.65	0.157	0.4750	162	0.16	9	17	1.371	1
34	0.562	2.58	0.073	0.5965	196	0.07	5	8	1.146	2
35	0.571	2.55	0.161	0.3855	173	0.11	10	11	0.511	1
36	0.494	2.54	0.095	0.7605	182	0	0	0	1.432	1
37	0.541	2.61	0.120	0.8040	183	1.15	43	44	2.249	2
38	0.516	2.55	0.156	0.5485	205	0	0	0	1.207	1
39	0.483	2.67	0.146	0.7055	161	0	0	0	2.045	2
40	0.488	2.53	0.079	0.4860	180	0.04	6	8	1.800	1
41	0.465	2.52	0.049	0.7630	168	0.2	0	0	0.941	1
42	0.434	2.55	0.075	0.5450	166	0.08	8	10	0.675	1
43	0.431	2.52	0.081	0.8285	185	0	0	0	0.552	1
44	0.495	2.58	0.105	0.6880	190	0	0	0	0.675	2
45	0.560	2.38	0.104	0.8060	253	0	0	0	0.982	0
46	0.544	2.80	0.172	0.4790	197	0	0	0	3.780	6
47	0.584	2.36	0.085	0.7680	174	1.61	37	40	1.064	1
48	0.539	2.48	0.066	0.8105	182	0.47	39	38	0.777	2
49	0.474	2.44	0.123	0.8110	191	0	0	0	0.716	2
50	0.541	2.37	0.098	0.7390	176	0.08	11	20	0.614	1
51	0.555	2.45	0.098	0.8250	199	0	0	0	0.511	1
52	0.684	2.51	0.103	0.7465	192	0	0	0	2.842	5

Appendix A

Table 1. Experimental results of veneer grade factors

Specimen No.	Density	Thickness		Lathe Checks		Knots			Grain Angle	Roughness Grade
		Average	Stdev	LCD	LCN	PKA	CKD_1	CKD_2		
	(g/mm^3)	(mm)		(100 * %)		(%)	(mm)	(mm)	(degree)	
53	0.557	2.41	0.062	0.8665	194	0.11	15	14	1.330	2
54	0.574	2.57	0.157	0.7855	179	0	0	0	0.900	3
55	0.544	2.39	0.066	0.7930	210	0.05	7	8	0.143	1
56	0.456	2.61	0.082	0.2360	133	0.26	18	23	1.084	1
57	0.435	2.53	0.210	0.7965	167	2.07	74	70	1.084	4
58	0.546	2.51	0.057	0.5950	150	0.15	11	13	0.552	1
59	0.458	2.58	0.064	0.4320	152	0.15	11	22	1.391	1
60	0.543	2.48	0.046	0.8320	166	0.1	9	12	1.882	2
61	0.413	2.65	0.081	0.7105	148	0	0	0	1.350	5
62	0.553	2.51	0.050	0.3425	164	0	0	0	0.880	2
63	0.487	2.49	0.022	0.8175	155	2.3	83	83	0.593	3
64	0.535	2.52	0.090	0.5965	142	0.36	19	15	1.002	4
65	0.527	2.59	0.082	0.7570	173	0.97	29	31	0.716	2
66	0.491	2.55	0.115	0.7460	169	0.29	28	34	0.184	1
67	0.466	2.48	0.067	0.3645	128	0	0	0	2.331	1
68	0.550	2.60	0.119	0.6965	164	0.06	7	7	3.107	4
69	0.399	2.60	0.055	0.4535	172	0.06	7	11	1.166	3
70	0.479	2.44	0.074	0.7790	195	0.14	7	18	0.900	2
71	0.484	2.43	0.056	0.6890	206	0.06	8	8	0.839	1
72	0.475	2.67	0.057	0.8590	178	0.08	9	8	0.430	2
73	0.454	2.68	0.123	0.5930	147	1.91	55	34	0.675	6
74	0.581	2.53	0.052	0.5930	172	0.05	10	12	0.921	3
75	0.588	2.53	0.095	0.4500	166	0	0	0	1.207	1
76	0.466	2.52	0.116	0.8215	172	0.14	11	16	0.900	1
77	0.580	2.56	0.135	0.7765	179	1.66	47	42	0.675	4
78	0.533	2.53	0.062	0.6355	198	0.2	17	15	0.471	0
79	0.496	2.51	0.071	0.7250	185	0	0	0	0.491	1
80	0.466	2.58	0.084	0.6070	176	1.56	65	56	1.514	5
81	0.472	2.70	0.056	0.7675	171	0.08	8	14	0.614	1
82	0.470	2.60	0.079	0.4465	172	1.47	44	41	1.636	5
83	0.547	2.56	0.085	0.6290	186	0	0	0	0.532	0
84	0.580	2.55	0.090	0.5140	180	0.21	10	10	0.491	0
85	0.493	2.56	0.043	0.6500	211	0	0	0	2.249	0
86	0.575	2.57	0.111	0.7540	167	6.89	100	90	3.576	6
87	0.523	2.51	0.070	0.5645	221	0.4	20	40	0.532	0
88	0.496	2.60	0.058	0.6465	177	0	0	0	1.227	0
89	0.503	2.60	0.263	0.6430	210	4.4	86	64	1.452	4
90	0.499	2.64	0.095	0.6790	189	0.31	9	9	0.962	2
91	0.530	2.45	0.141	0.7290	169	1.8	50	44	0.552	4
92	0.570	2.51	0.104	0.6465	164	0.14	10	16	1.105	0
93	0.586	2.47	0.075	0.6290	208	0	0	0	0.900	1
94	0.493	2.55	0.068	0.5945	176	0	0	0	1.432	2
95	0.544	2.55	0.096	0.5575	193	0	0	0	0.552	0
96	0.516	2.49	0.054	0.7610	177	0.47	24	24	0.389	1
97	0.494	2.57	0.073	0.5465	182	3.61	60	60	1.555	4
98	0.493	2.45	0.147	0.8350	185	0	0	0	0.552	3
Average	0.513	2.535	0.092	0.677	178.22	0.476	15.51	16.34	1.317	1.684
Stdev	0.050	0.085	0.039	0.150	21.618	1.030	21.96	20.75	0.737	1.616

Appendix B

1) Comparison of wave timings with different thresholds

Not only the signal amplitude but also the detection threshold can affect the wave timings. For instance, in specimen 6 at parallel sampling point 4, if the threshold level is set at 0.8 mV just above maximum noise level 0.6 mV as shown in Figure 23 a), the timing would be 44 μs. However, if setting the threshold level as 200 mV as shown in Figure 23 b), the timing would be 59 μs which agrees with that displayed directly by Metriguard 239A timer which sets the fixed threshold level as 200 mV. A high threshold level would also cause timings inconsistent especially in the perpendicular to grain direction, which is not suitable for weak wave signals encountered in veneer testing.

2) Output voltage range and frequency components

The comparison of first peak amplitudes with subsequent pendulum hits was shown in Fig. 24. By observing all of the waveforms, it was clear that the main frequency range is approximately from 1.5 to 4.0 kHz; *i.e.*, low frequencies dominated in the whole waveform in both directions. Typical waveforms in both parallel and perpendicular to grain directions are shown in Fig. 25. Note that the output voltage range of the signal in the parallel to grain direction was slightly higher than that in the perpendicular to grain direction. This suggested that lower frequency signals can penetrate veneer easily with a relative small signal attenuation. Note also that the transition of frequency components in an entire waveform was from the lowest to high then to lower again. But at the beginning of waveform, there might exist some high frequency components mixed with lowest frequency components as shown in Fig. 26. This demonstrated that wave propagation in the veneer is rather complicated and affected by multiple reflections from interfaces in the stress wave path.

3) Knots effect on wave timings

Wave propagation parallel to grain impeded by knots was illustrated by comparing knot-containing and neighboring knot-free sampling lines as shown in Fig. 27. However, no consistent conclusion could be drawn in the perpendicular to grain direction although timing differences were observed between knot-containing and knot-free sampling lines.

4) Artificial check effects on wave propagation

By introducing artificial checks in the veneer specimens, the lathe check effects on wave propagation were explored preliminarily with additional veneer specimens. The waveforms perpendicular to grain direction before and after introducing 5 artificial checks (80% depth) were compared as shown in Fig. 28. It could be seen that the signal voltage level after introducing checks was considerably attenuated.

The first several peaks of perpendicular wave signals before and after introducing 5 artificial checks were also compared as shown in Fig. 29. Clearly both the wave timing and the first peak amplitude were affected; *i.e.*, the wave timing was increased, and the first peak amplitude was decreased. A comparison was further made by introducing additional 5 more checks as shown in Fig. 30. The original first peak disappeared in the lower Figure, which resulted in the significant increases of both the timing and the first peak amplitude.

In summary, an increase of the wave timing was clearly identified after introducing several checks whose depths are deeper than the averaged lathe check depth (LCD) of veneer specimens, but no consistent conclusion could be drawn for the effect of the introduced checks on the first peak amplitude. This might indicate that the wave timing is a better wave parameter than the first peak amplitude to characterize the effect of lathe checks.

a) Timing 44 μs (threshold level 0.8 mV)

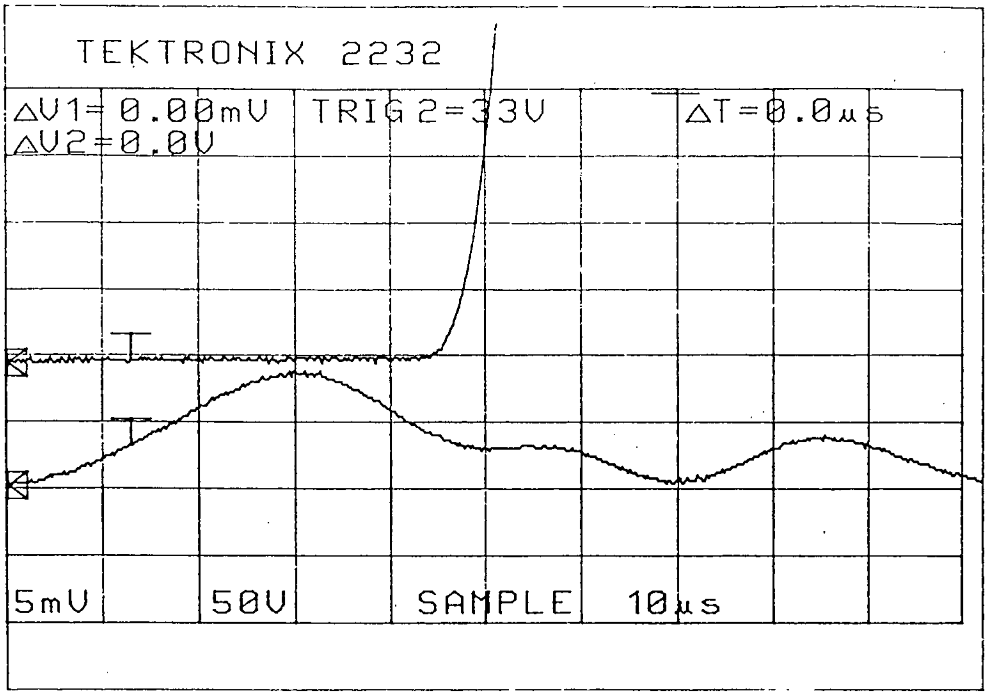

b) Timing 59 μs (threshold level 0.2 V)

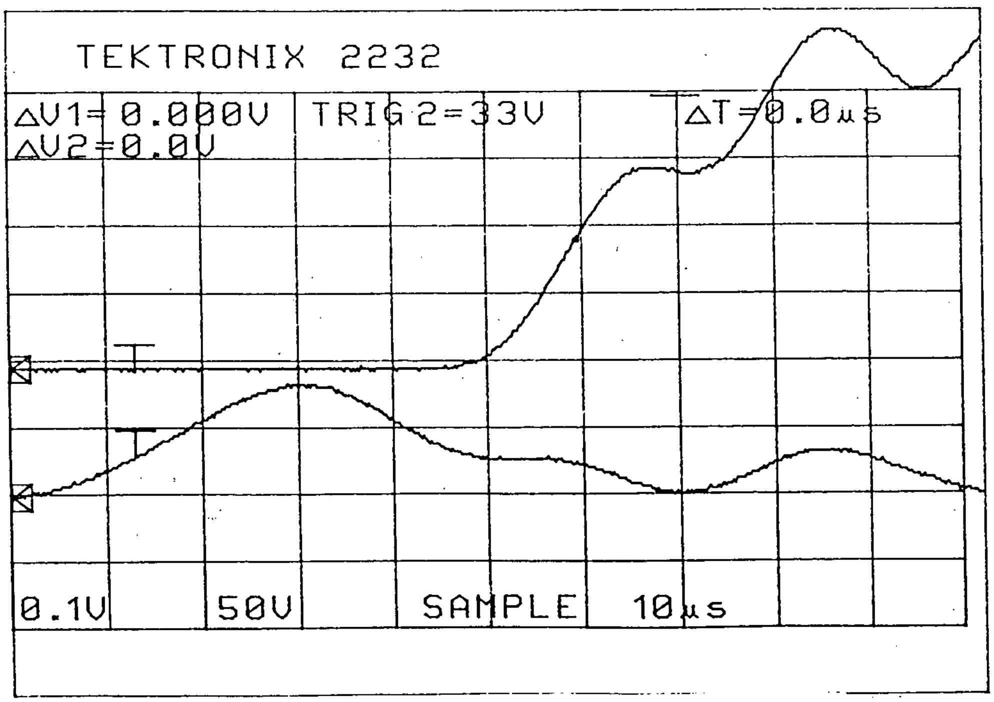

(specimen 6, point 4) in the parallel to grain direction

Fig. 23. Comparison of timings with different thresholds

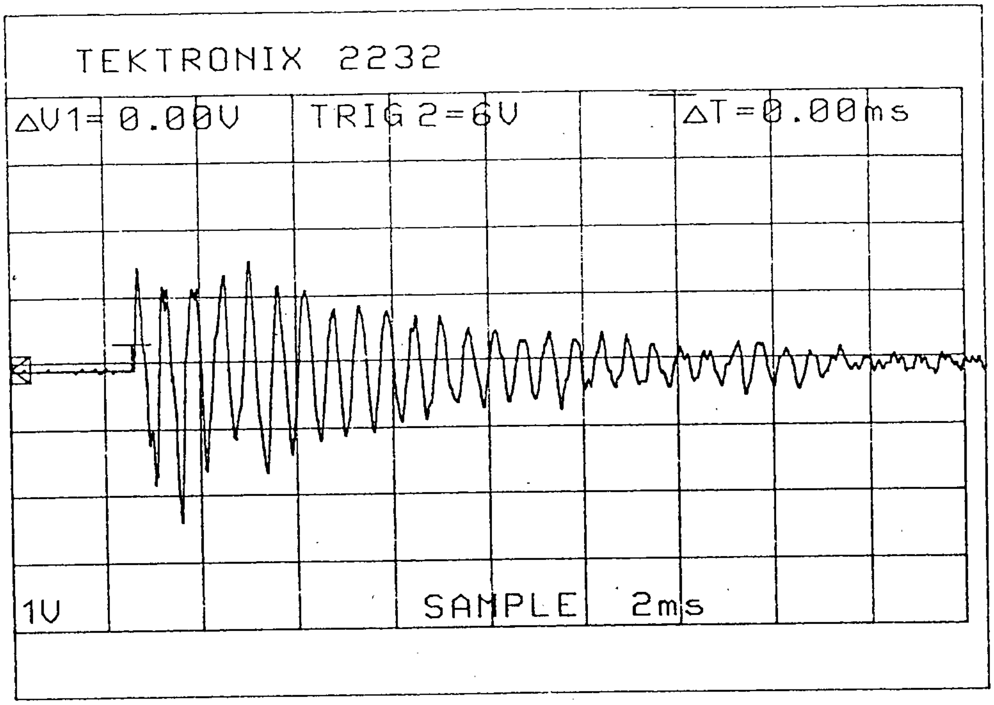

a) First pendulum hit

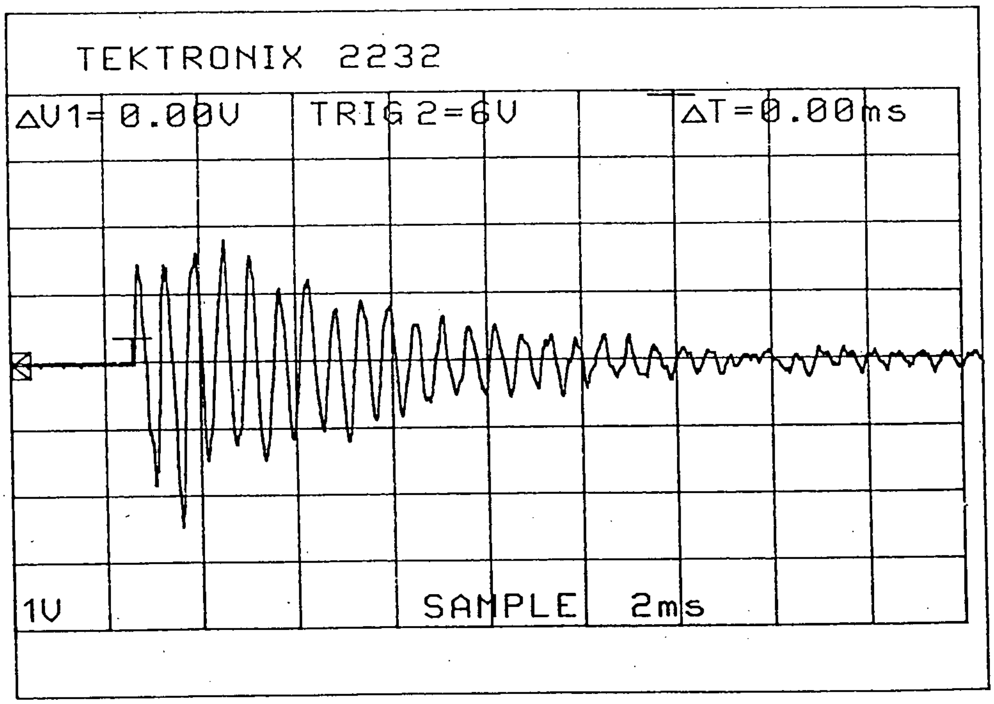

b) Second pendulum hit

Fig. 24. Comparison of first peak amplitudes with subsequent pendulum hits

a) Parallel to grain direction

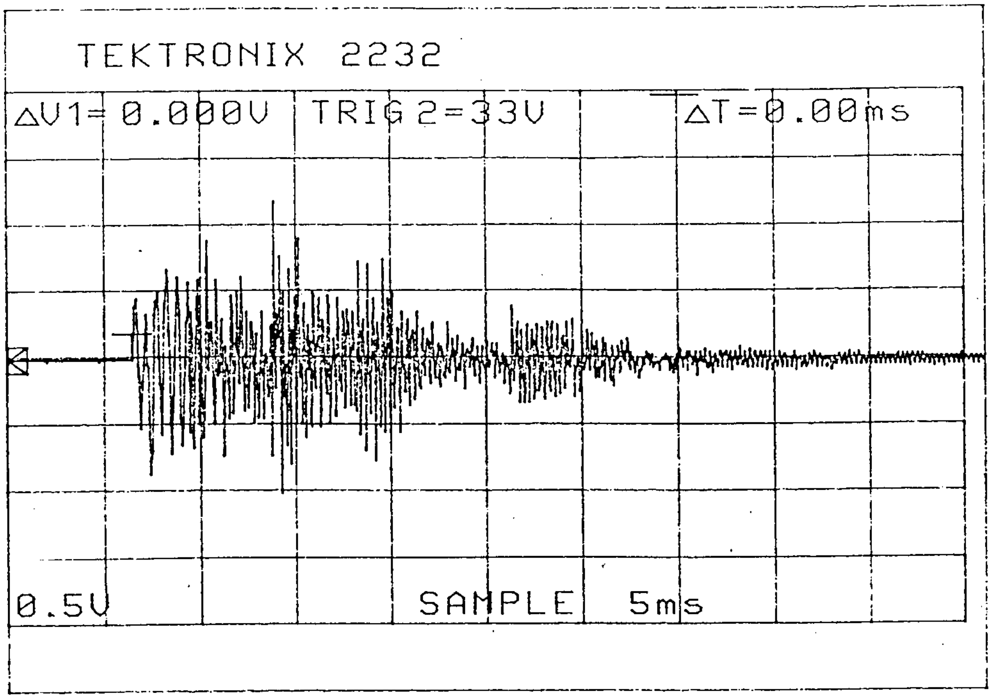

b) Perpendicular to grain direction

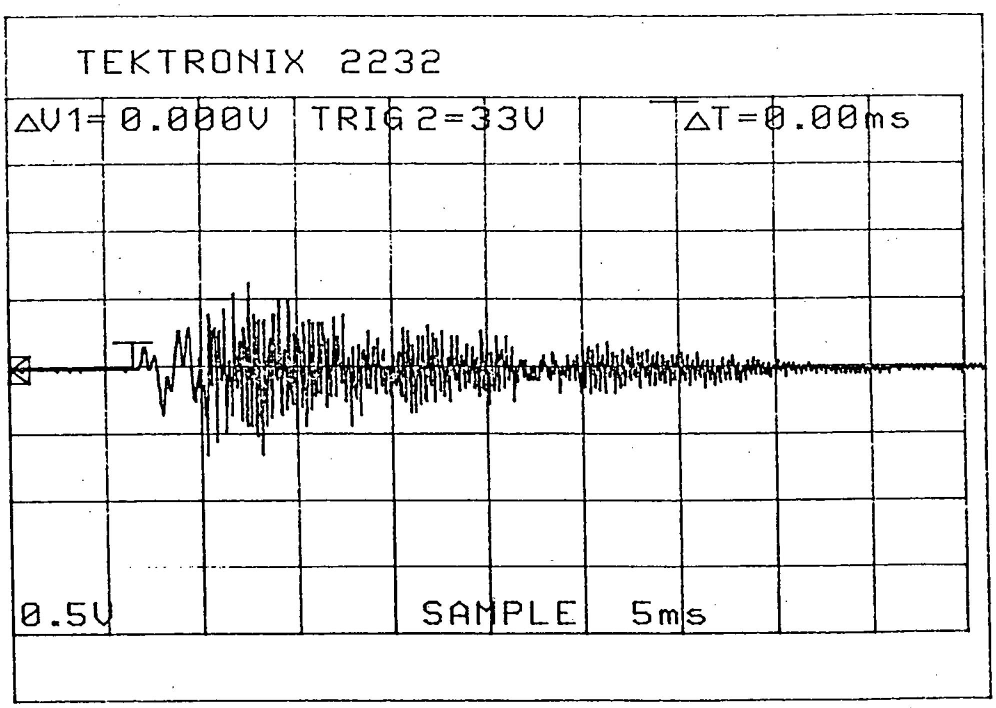

Fig. 25. Waveform comparison for stress wave device in both directions

(specimen 12, point 4)

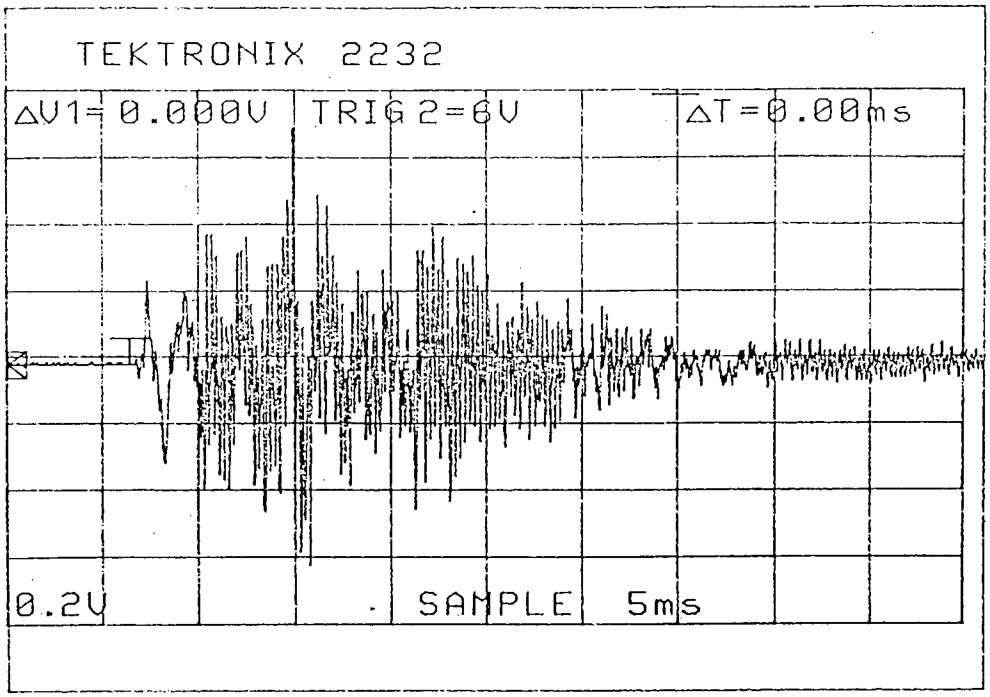

a) Entire waveform

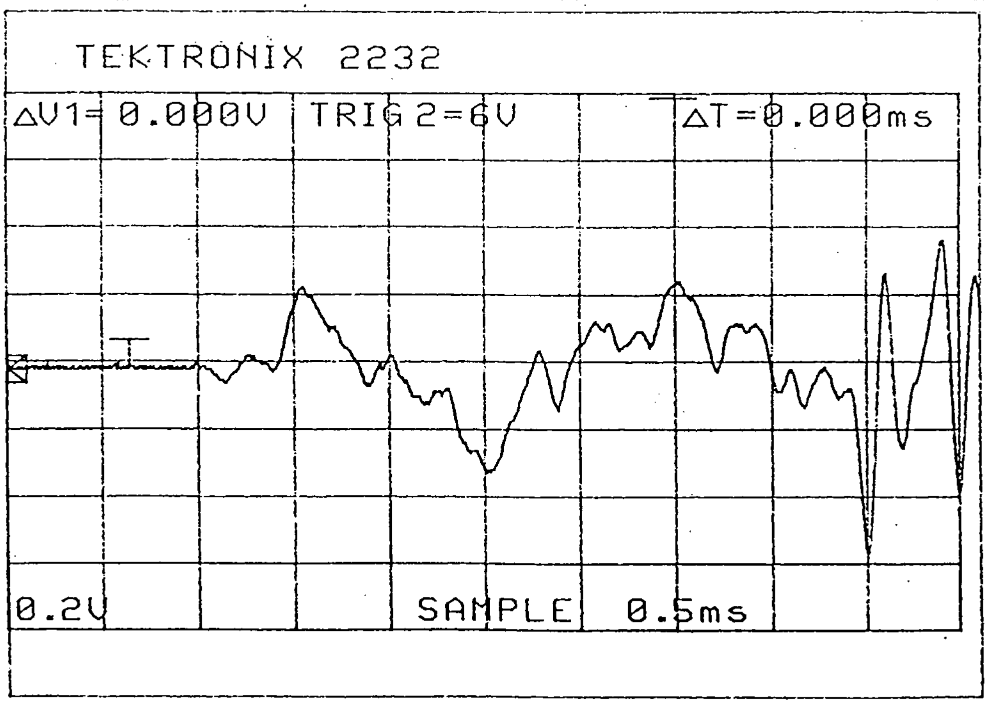

b) Enlargement of first several peaks

Fig. 26. Waveform in the perpendicular to grain direction (specimen 1, point 7)

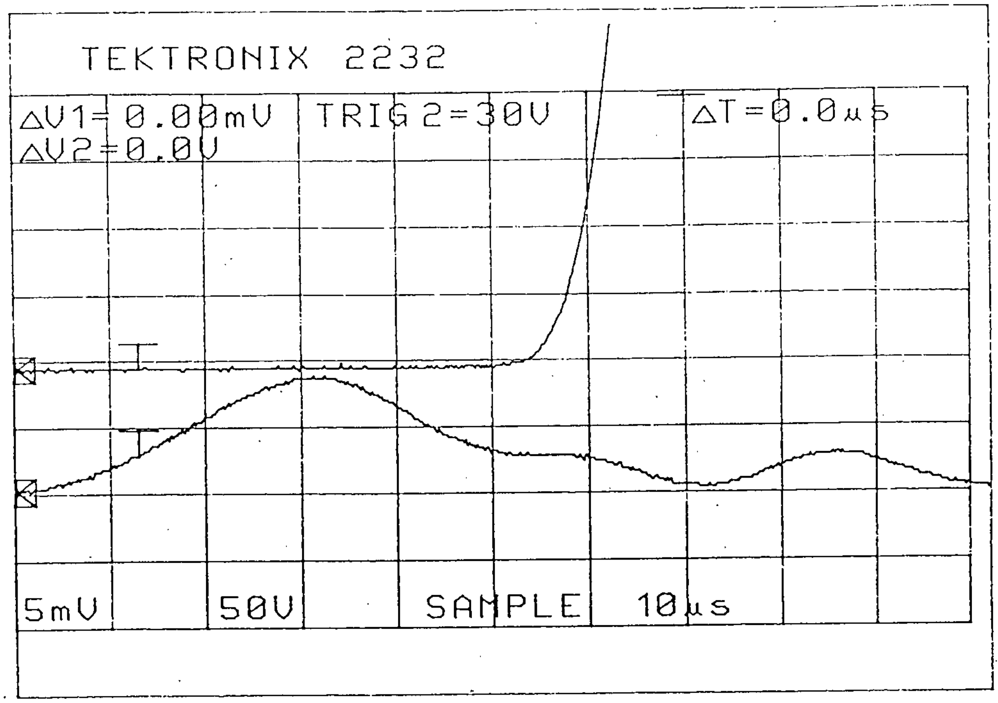

a) Knots-free (point 7, timing 52 μs)

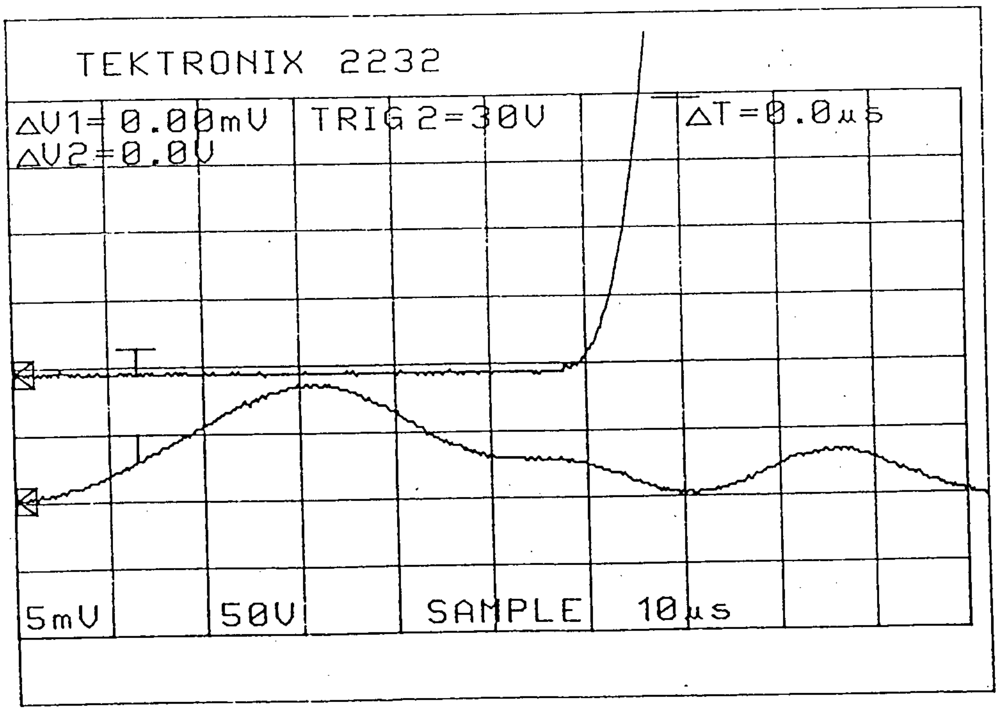

b) Knots (point 6, timing 57 μs)

Fig. 27. Knots effect on timing in the parallel to grain direction (specimen 10)

a) Original waveform

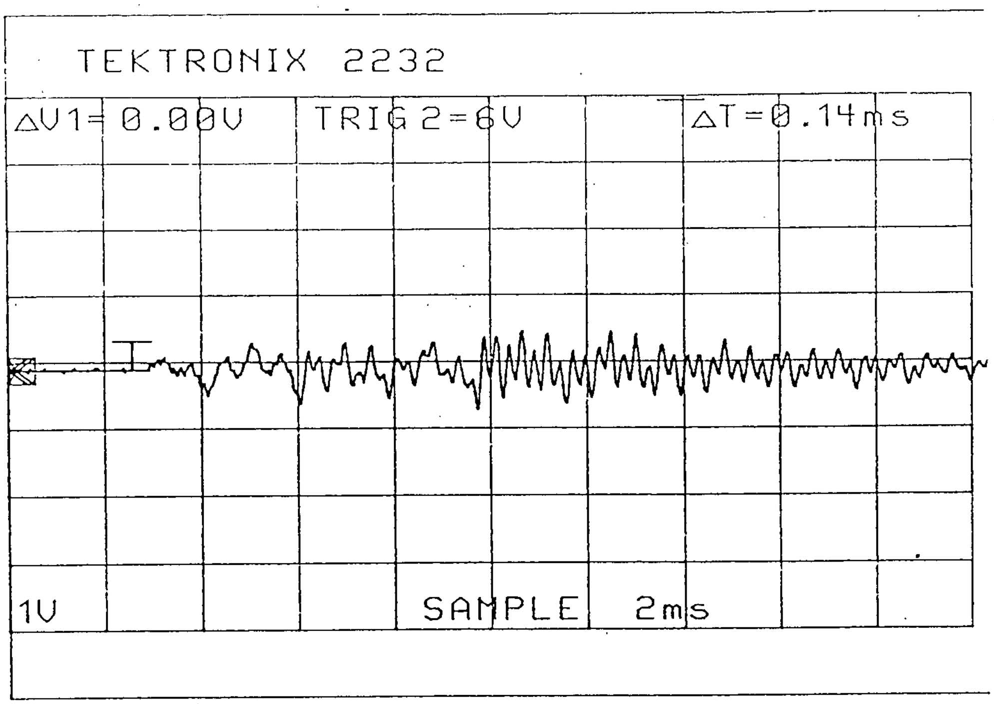

b) Waveform after introducing 5 artificial checks (depth 80%)

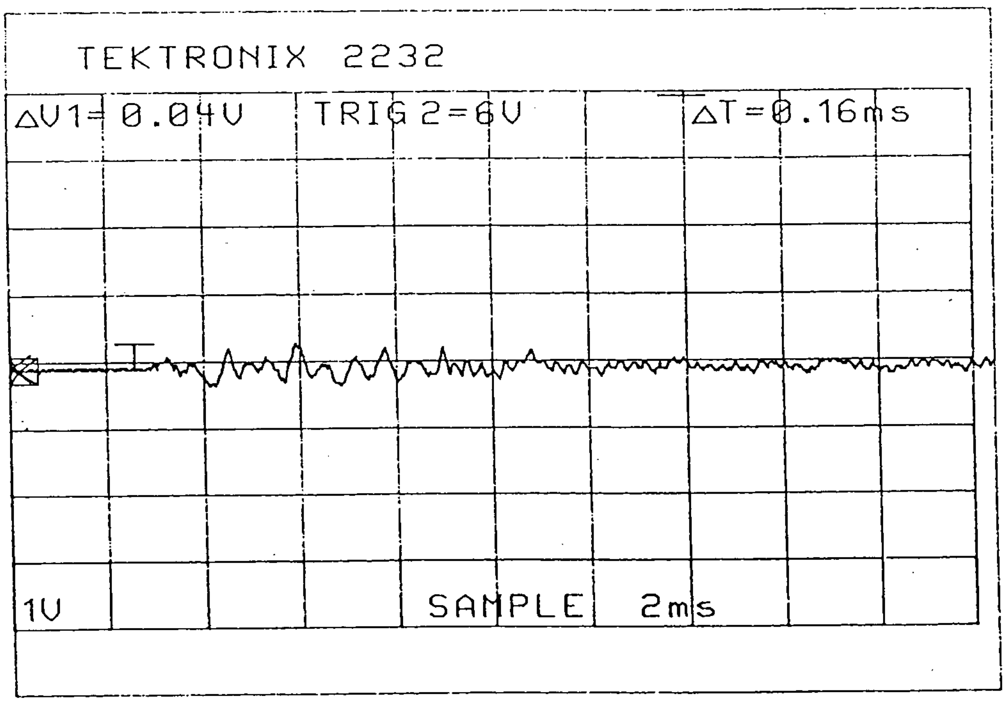

Fig. 28. Artificial check effects on waveforms in the perpendicular to grain direction (specimen 1, point 4, averaged lathe check depth 65.5%)

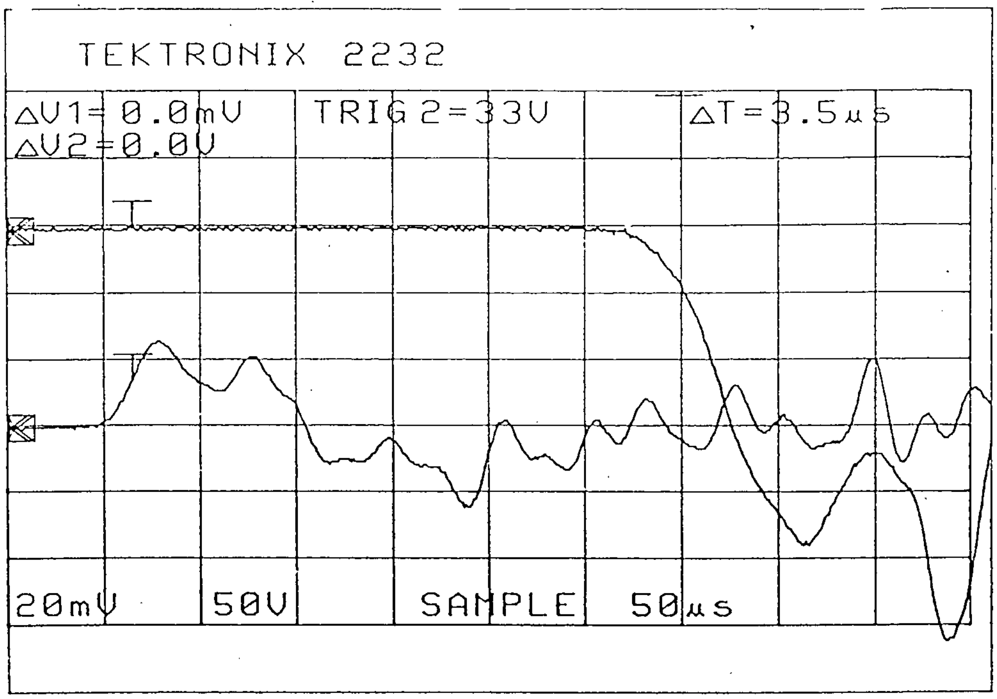

a) Original timing (272 μs, 95 mv)

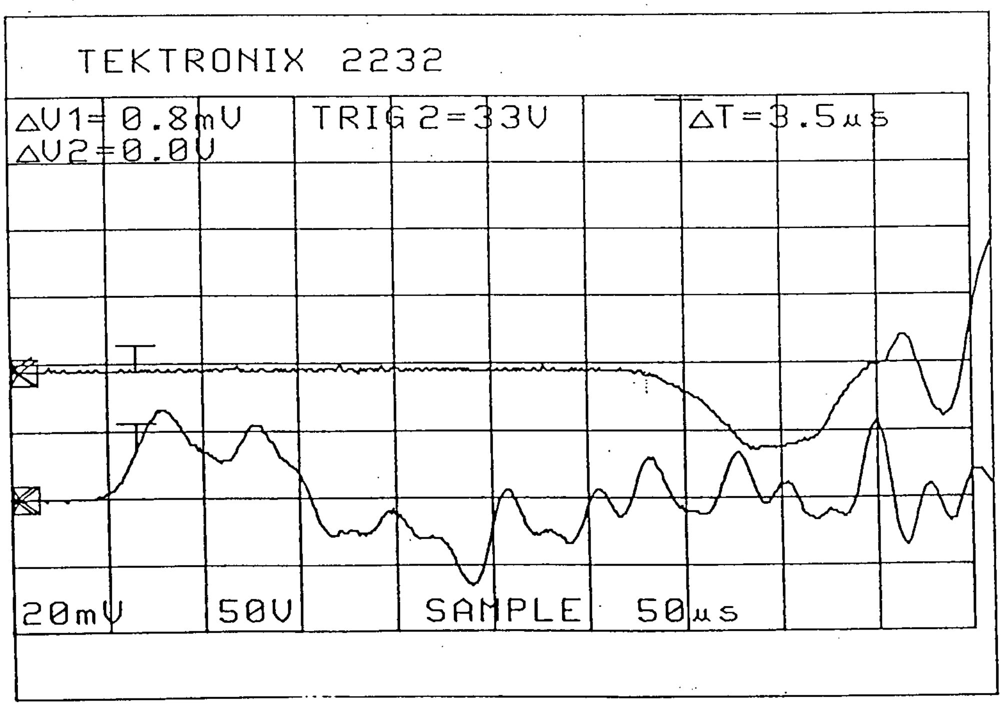

b) Timing after introducing 5 artificial checks

(depth 80%, timing 282 μs, 25 mv)

Fig. 29. Artificial check effects on timings and first peak amplitude in the perpendicular to grain direction (specimen 1, point 1)

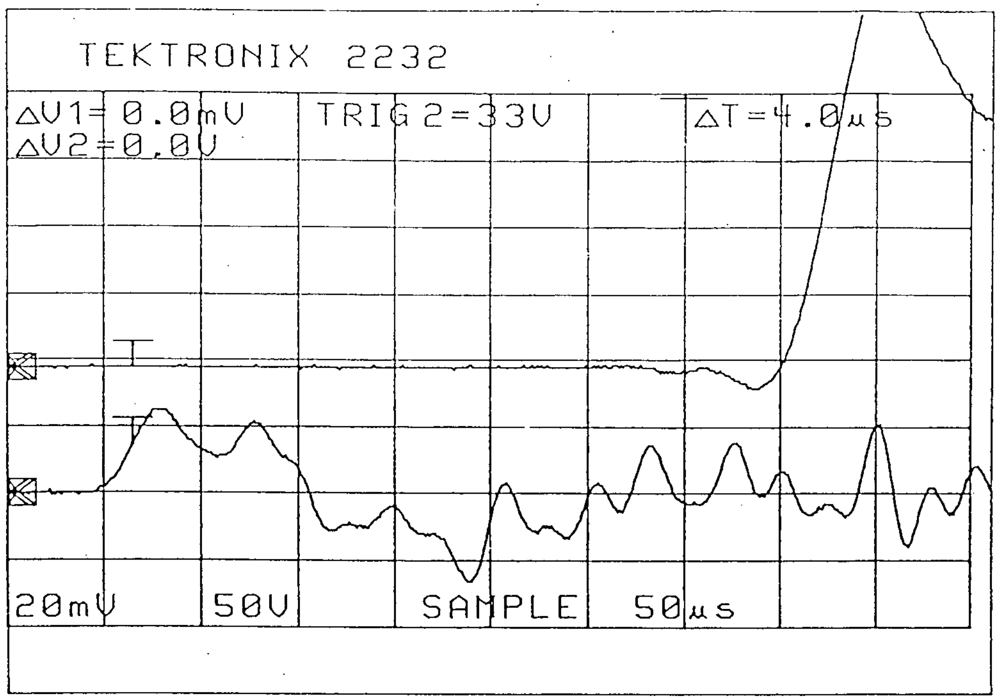

a) 5 artificial checks (322 μs, 7.5 mv)

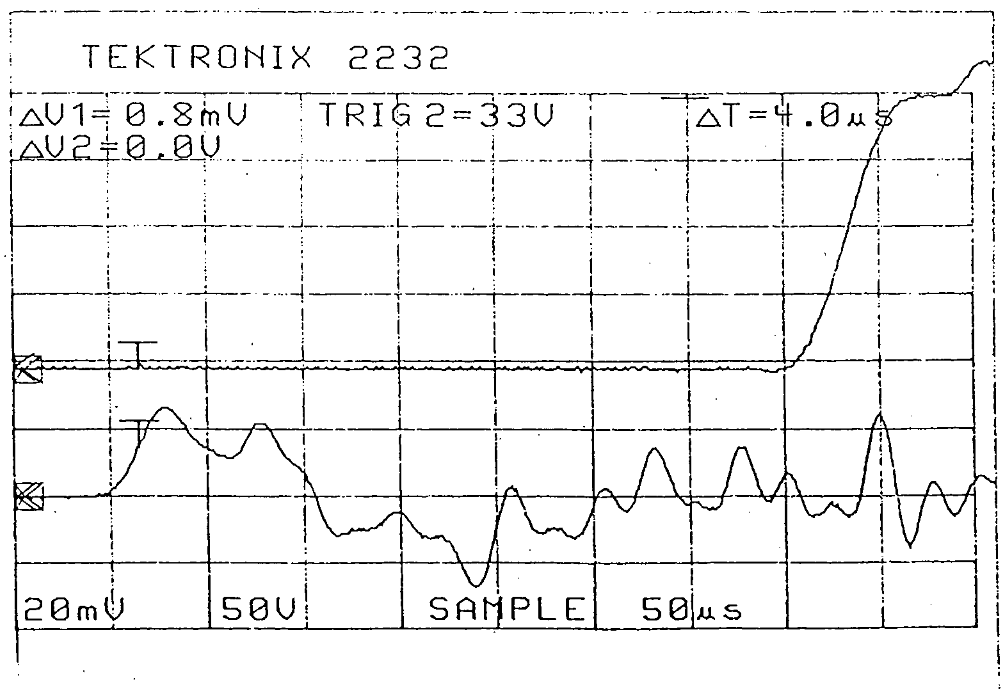

b) 10 artificial checks (355 μs, 88 mv)

Fig. 30. Artificial check effects on timings and first peak amplitude in the perpendicular to grain direction (specimen 1, point 5)

Appendix C

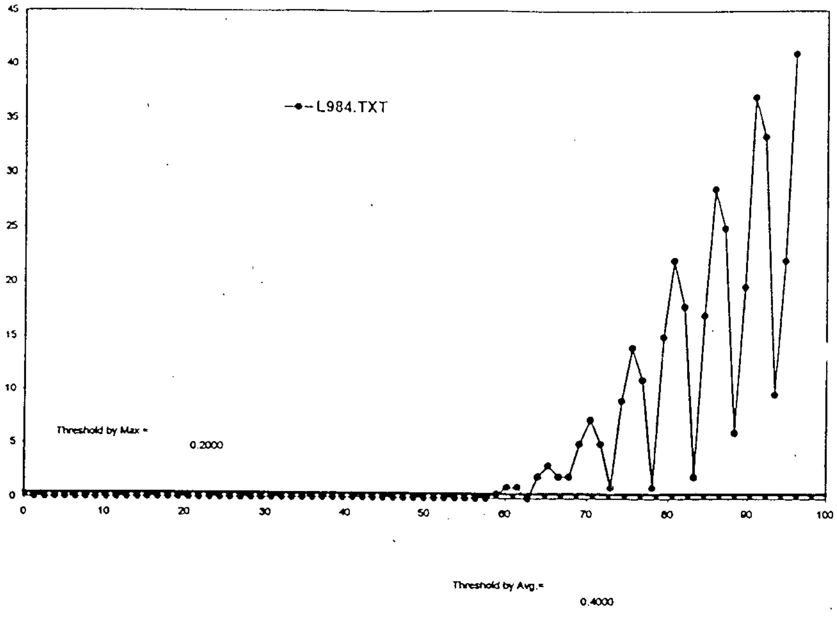

a) L984 (without noise at first 40 points)

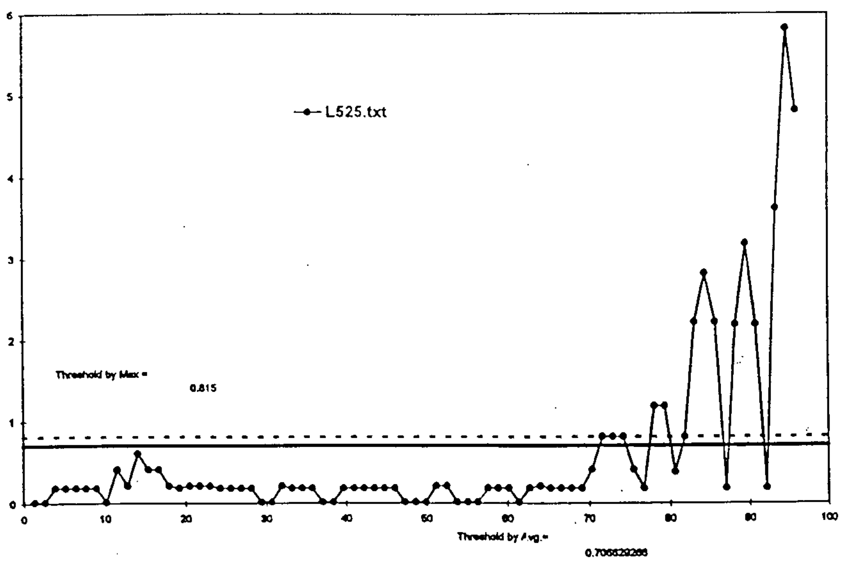

b) L525 (with noise at first 40 points)

Fig. 31. Thresholds set for AU timings in the parallel to grain direction

Appendix D

Lathe check influence on time domain waveform and power spectrum

a. Parallel to grain direction

Significant amplitude differences existed in waveforms of three specimens parallel to grain at sampling point 4 as shown in Figures 32a, 32b and 32c. The amplitude of the specimen 56 or 96 were almost 5 times that of the specimen 29. The descending order based on voltage levels was specimen 56 → specimen 96→ specimen 29, which was not in accordance with the specimen order based on LCD or mass density. Therefore, the waveform and amplitude parallel to grain were not significantly affected by lathe checks and mass density.

Note that from Figures 32a, 32b and 32c, pronounced differences existed in RMS voltages of three specimens. The ascending order based on RMS voltages of an entire waveform was specimen 29 (12.95 mV) → specimen 96 (30.53 mV) → specimen 56 (52.73 mV), whereas the ascending order based on RMS voltages of first 100 points was specimen 29 (17.00 mV) → specimen 56 (72.00 mV) → specimen 96 (87.10 mV). Both orders again violated the specimen ascending order based on LCD. This demonstrated that: 1) wave attenuation characteristics parallel to grain were not apparently affected by the seriousness of lathe checks and 2) the RMS voltages were dependent on the number of data points selected and the shape of a waveform. To better characterize the wave attenuation characteristics in veneer, it was suggested that the RMS voltage be calculated based on an entire waveform.

Note also that from Figures 32a, 32b and 32c, the frequency components were centered on two clearly defined zones, *i.e.*, 25 kHz and 95 kHz in this direction regardless of LCD and mass density.

b. **Perpendicular to grain direction**

Note that from Figures 33a, 33b and 33c, remarkable differences in three waveforms or amplitudes were observed. The descending order based on voltage levels was specimen 56 → specimen 29 → specimen 96, which did agree with the specimen ascending order based on LCD. This suggested that LCD might have a potent influence on the waveform and amplitude perpendicular to grain.

Note also that from Figures 33a, 33b and 33c, there existed differences in RMS voltages of three specimens. The descending order based on RMS voltages was specimen 56 (2.89 mV)→ specimen 29 (0.95 mV) → specimen 96 (0.91 mV), which conformed with the specimen ascending order based on LCD. Therefore, wave attenuation characteristics perpendicular to grain could also be affected by lathe checks.

Note again that from Figures 33a, 33b and 33c, the frequency components were again located in two clearly defined zones, *i.e.*, 25 kHz and 95 kHz regardless of LCD and mass density, and the signal energy would mainly concentrated on the lower frequency zone with the increase of LCD.

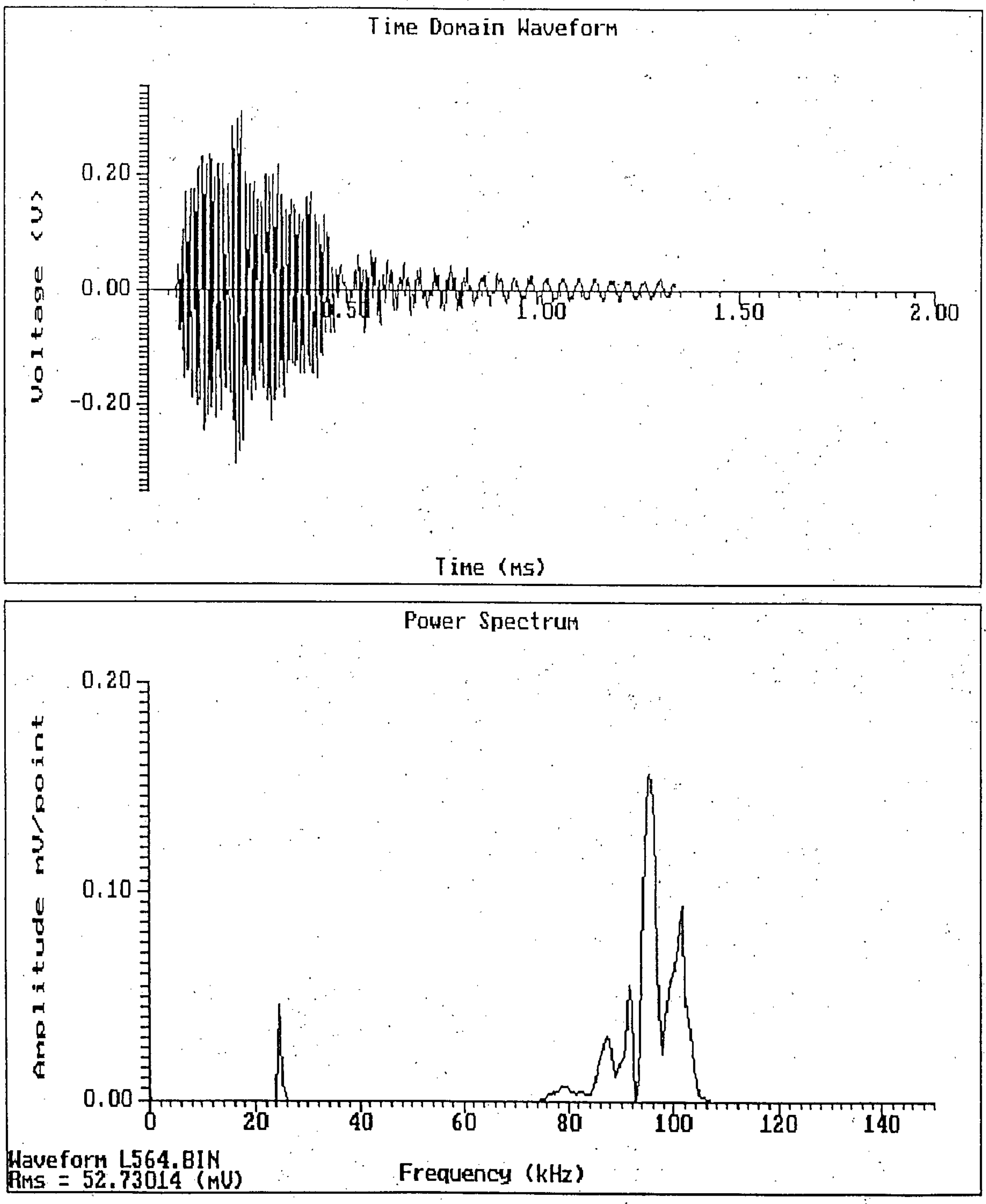

Fig. 32a. Lathe check influences on time domain waveform and power spectrum

(Parallel, specimen 56, point 4, averaged lathe check depth 23.6%, PKA 0.26%)

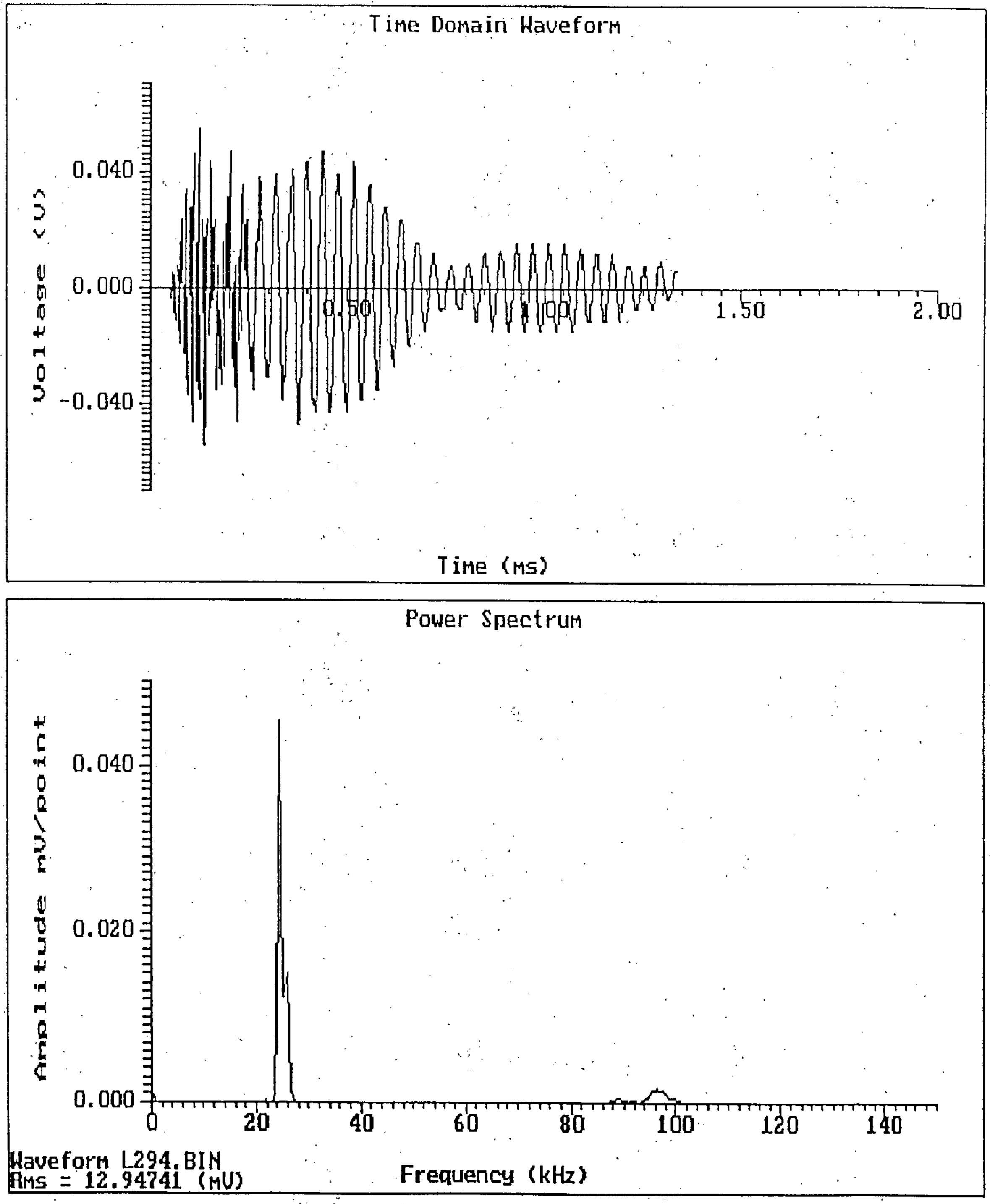

Fig. 32b. Lathe check influences on time domain waveform and power spectrum

(Parallel, specimen 29, point 4, averaged lathe check depth 51.1%, PKA 0%)

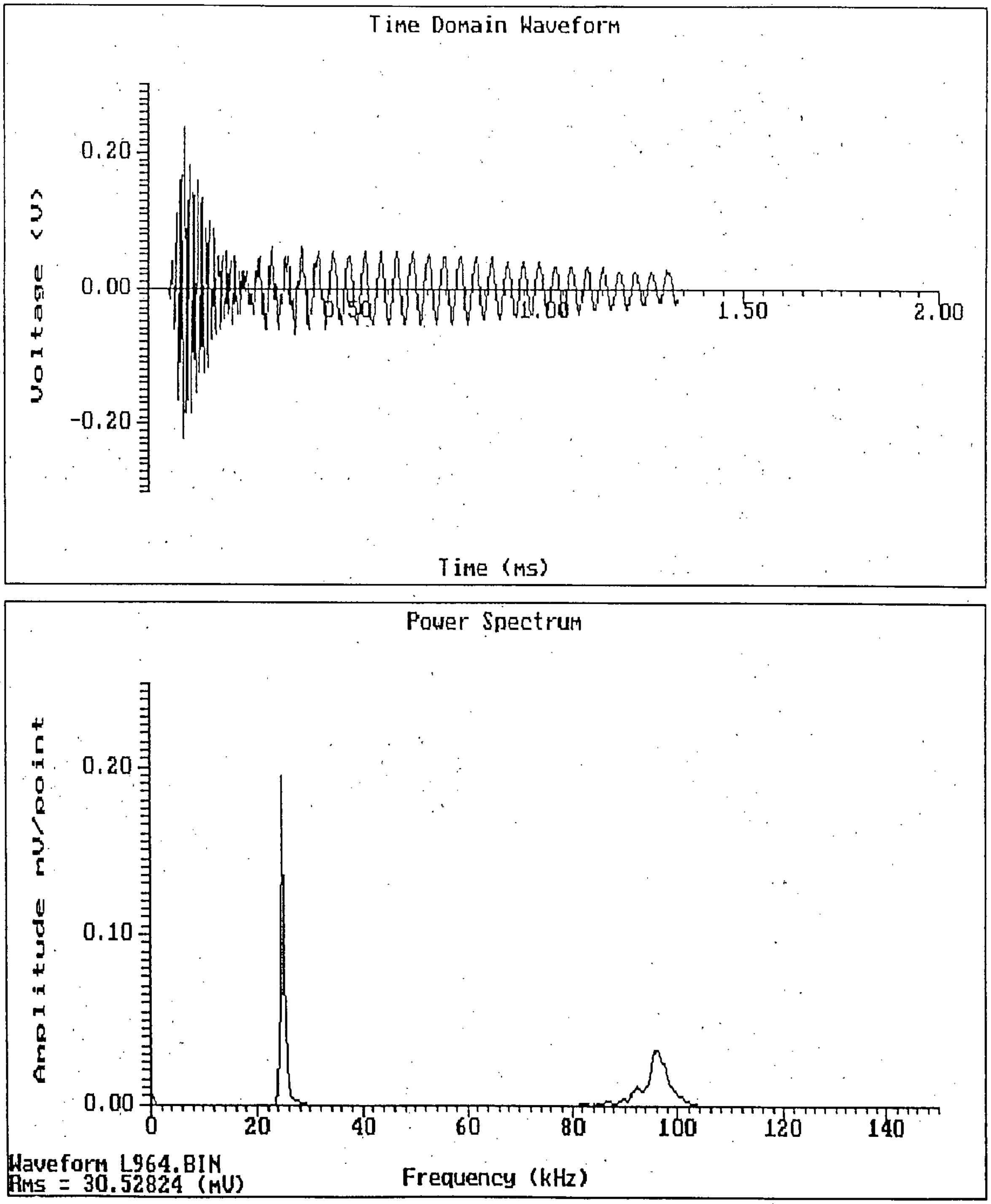

Fig. 32c. Lathe check influences on time domain waveform and power spectrum

(Parallel, specimen 96, point 4, averaged lathe check depth 76.1%, PKA 0.47%)

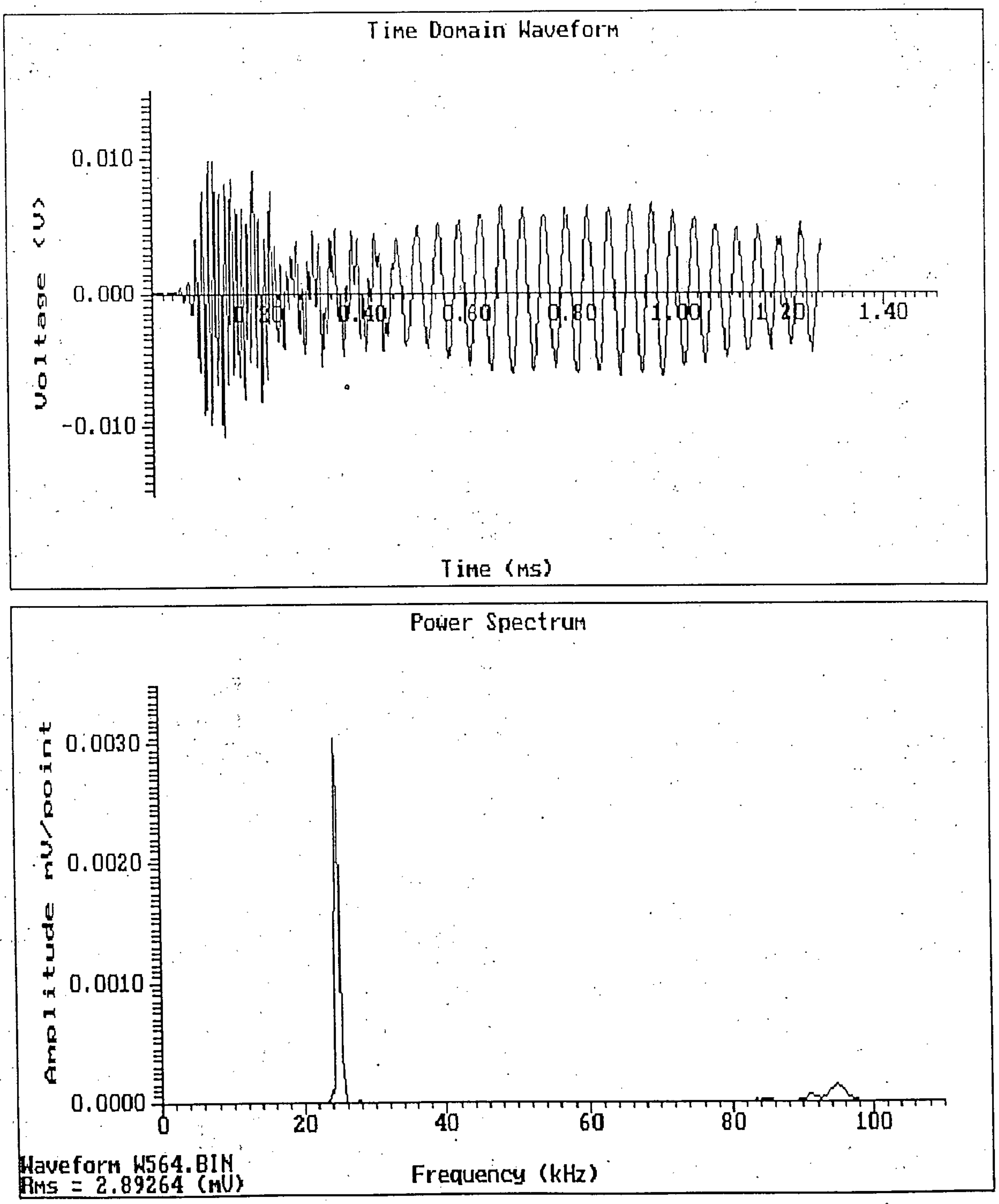

Fig. 33a. Lathe check influences on time domain waveform and power spectrum (Perpendicular, specimen 56, point 4, averaged lathe check depth 23.6%, PKA 0.26%)

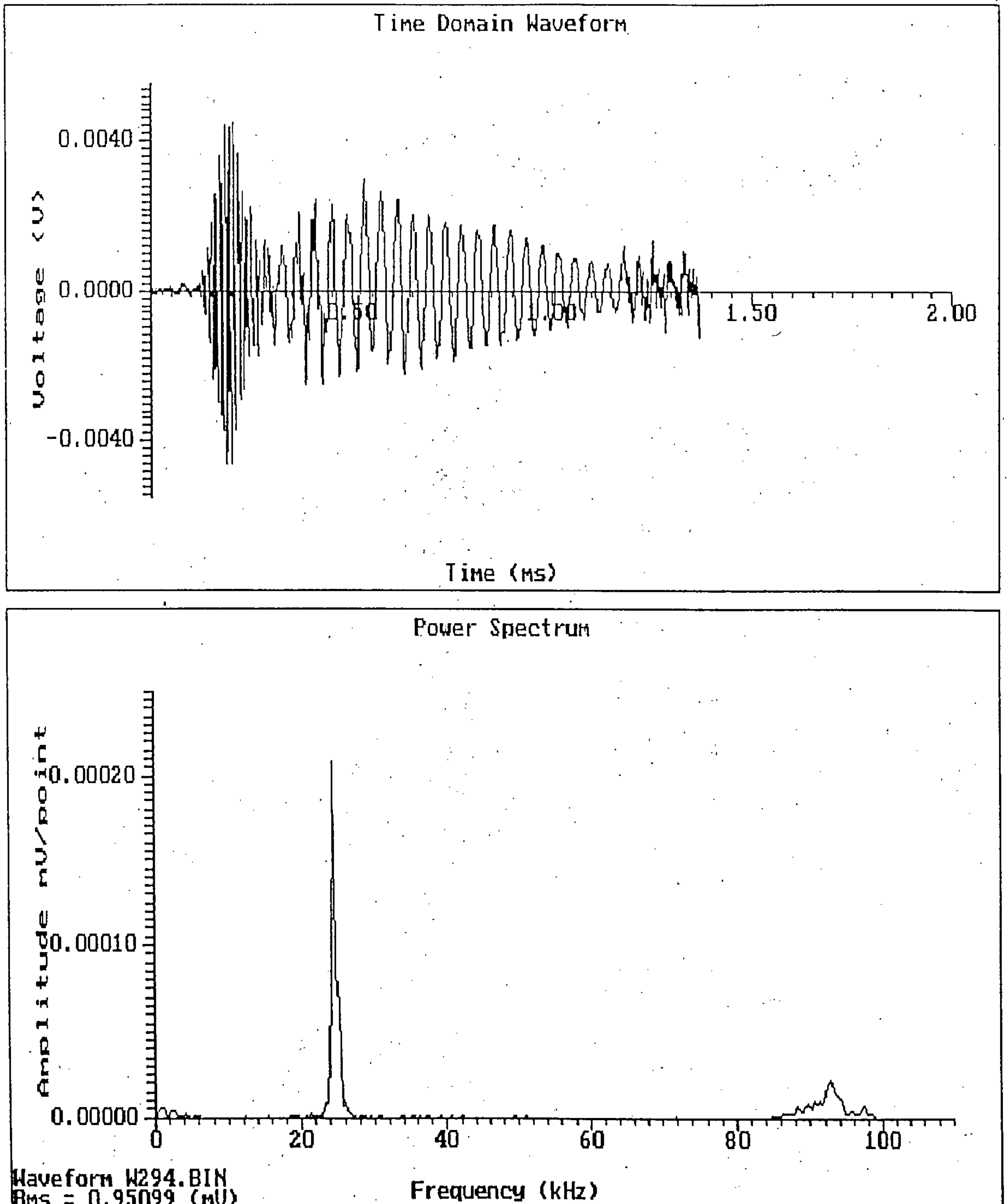

Fig. 33b. Lathe check influences on time domain waveform and power spectrum (Perpendicular, specimen 29, point 4, averaged lathe check depth 51.1%, PKA 0%)

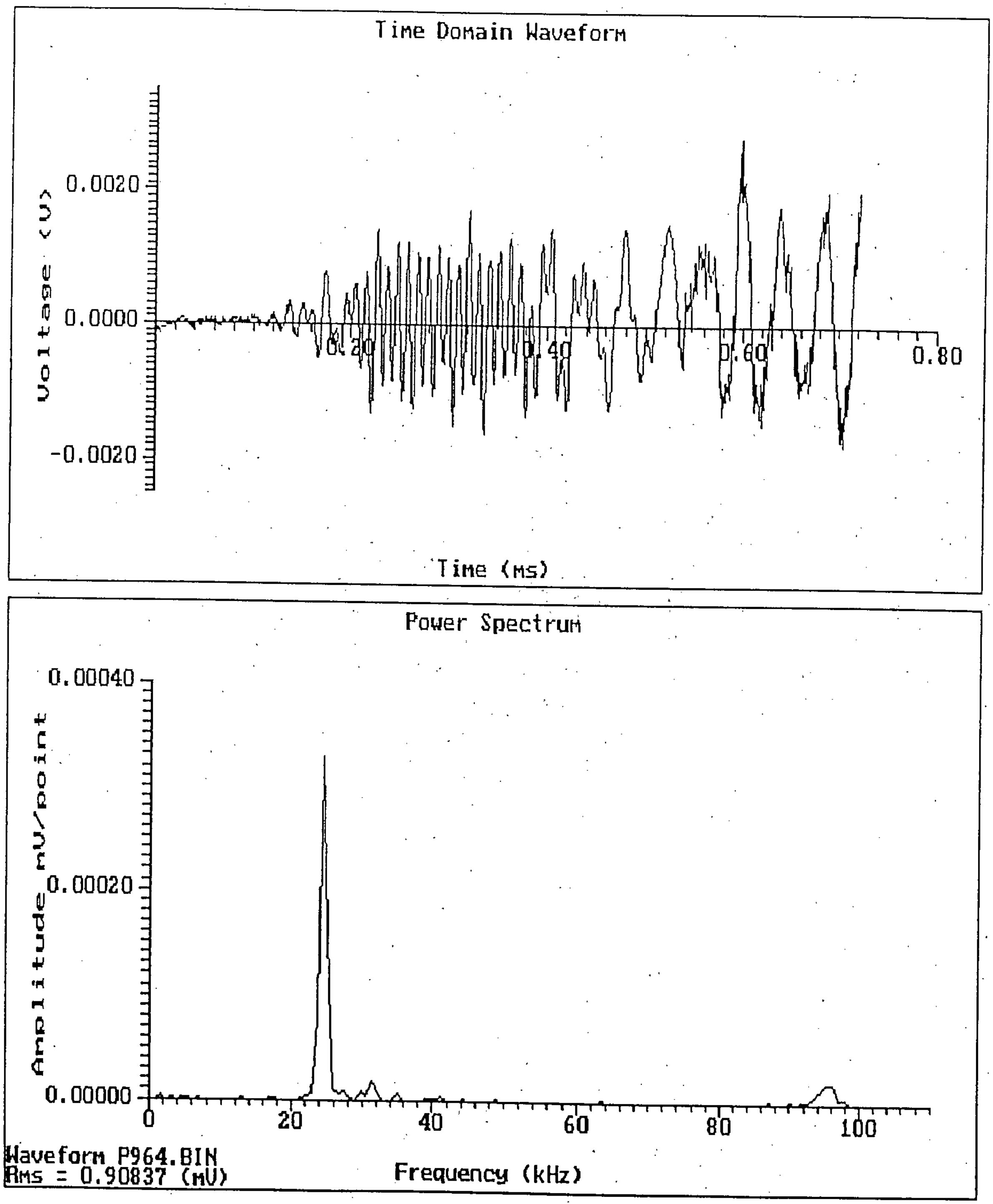

Fig. 33c. Lathe check influences on time domain waveform and power spectrum (Perpendicular, specimen 96, point 4, averaged lathe check depth 76.1%, PKA 0.47%)

Appendix E

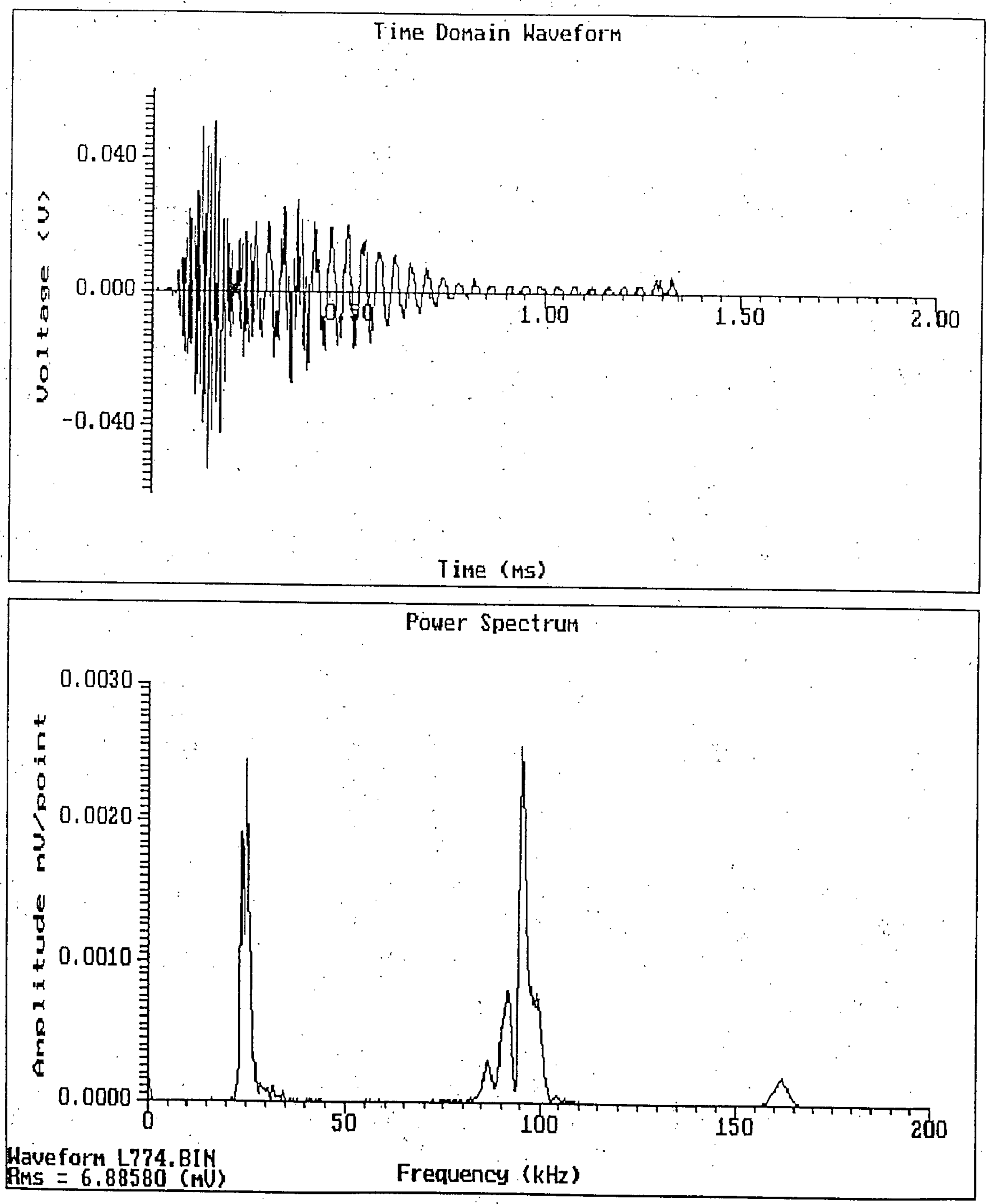

Fig. 34a. Knots influences on time domain waveform and power spectrum

(Parallel, specimen 77, point 4, averaged lathe check depth 77.65%, PKA 1.66%, propagation line through knots)

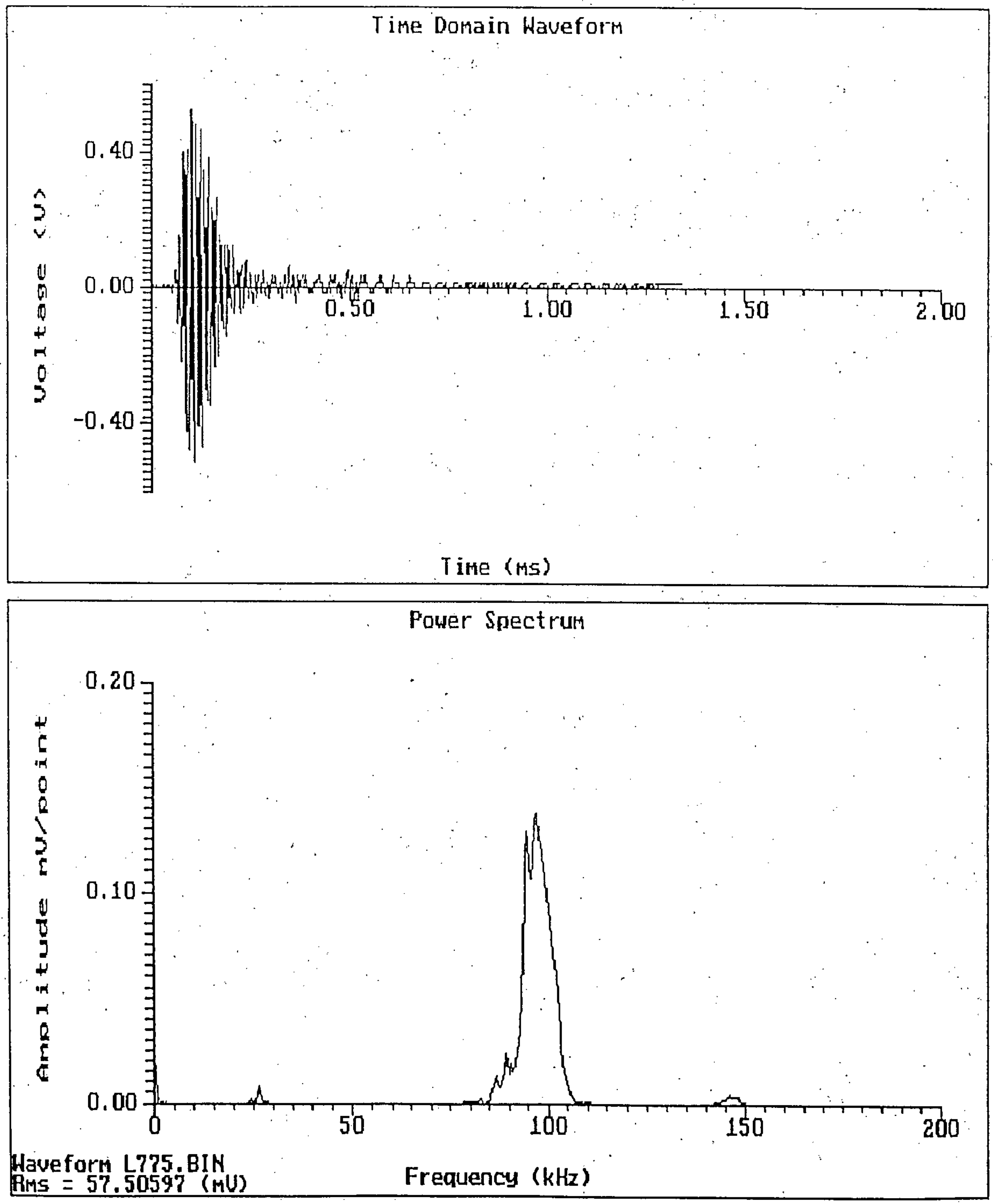

Fig. 34b. Knots influences on time domain waveform and power spectrum

(Parallel, specimen 77, point 5, averaged lathe check depth 77.65%, PKA 1.66%, knots-free propagation line)

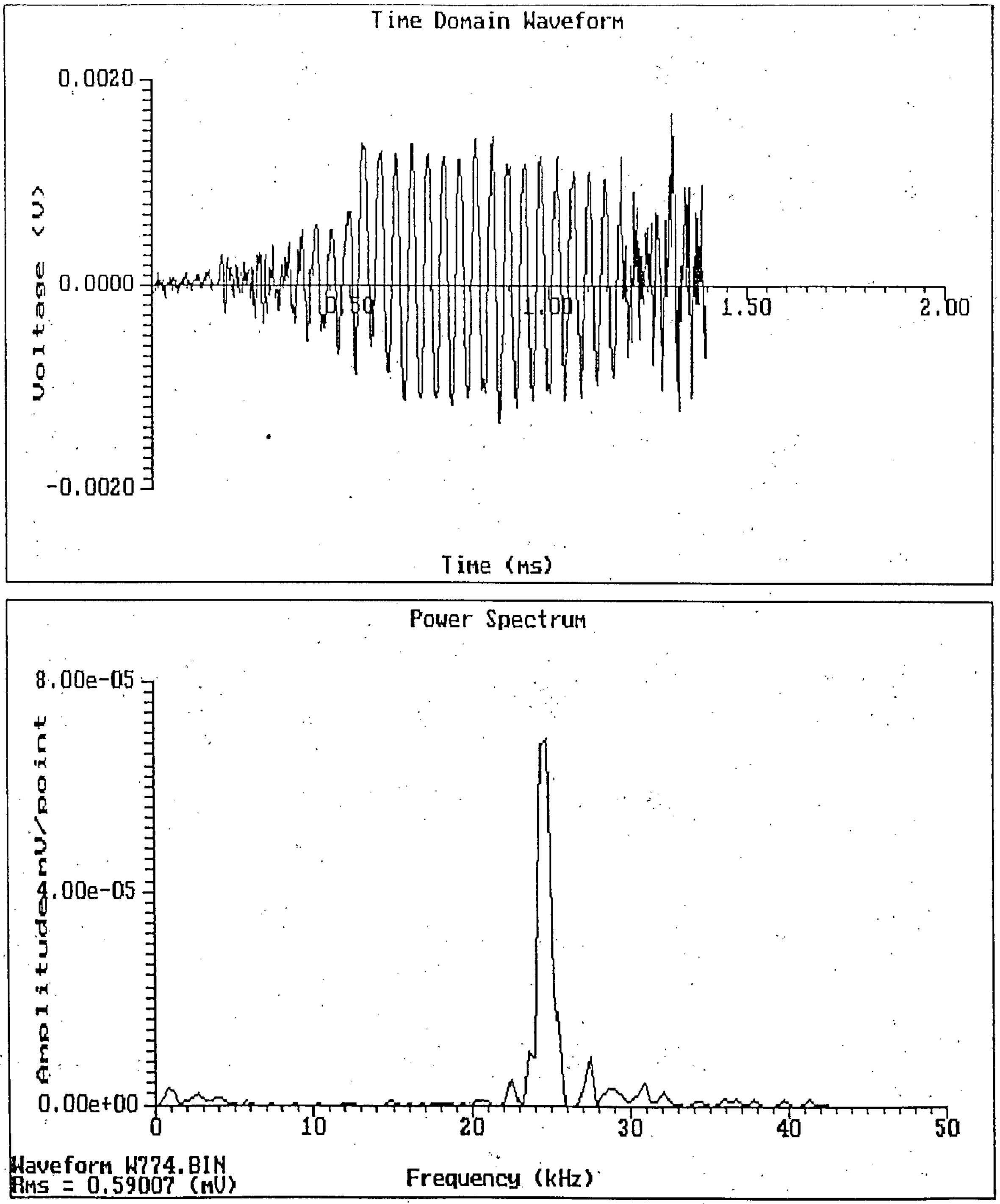

Fig. 35a. Knots influences on time domain waveform and power spectrum

(Perpendicular, specimen 77, point 4, averaged lathe check depth 77.65%, PKA 1.66%, propagation line through knots)

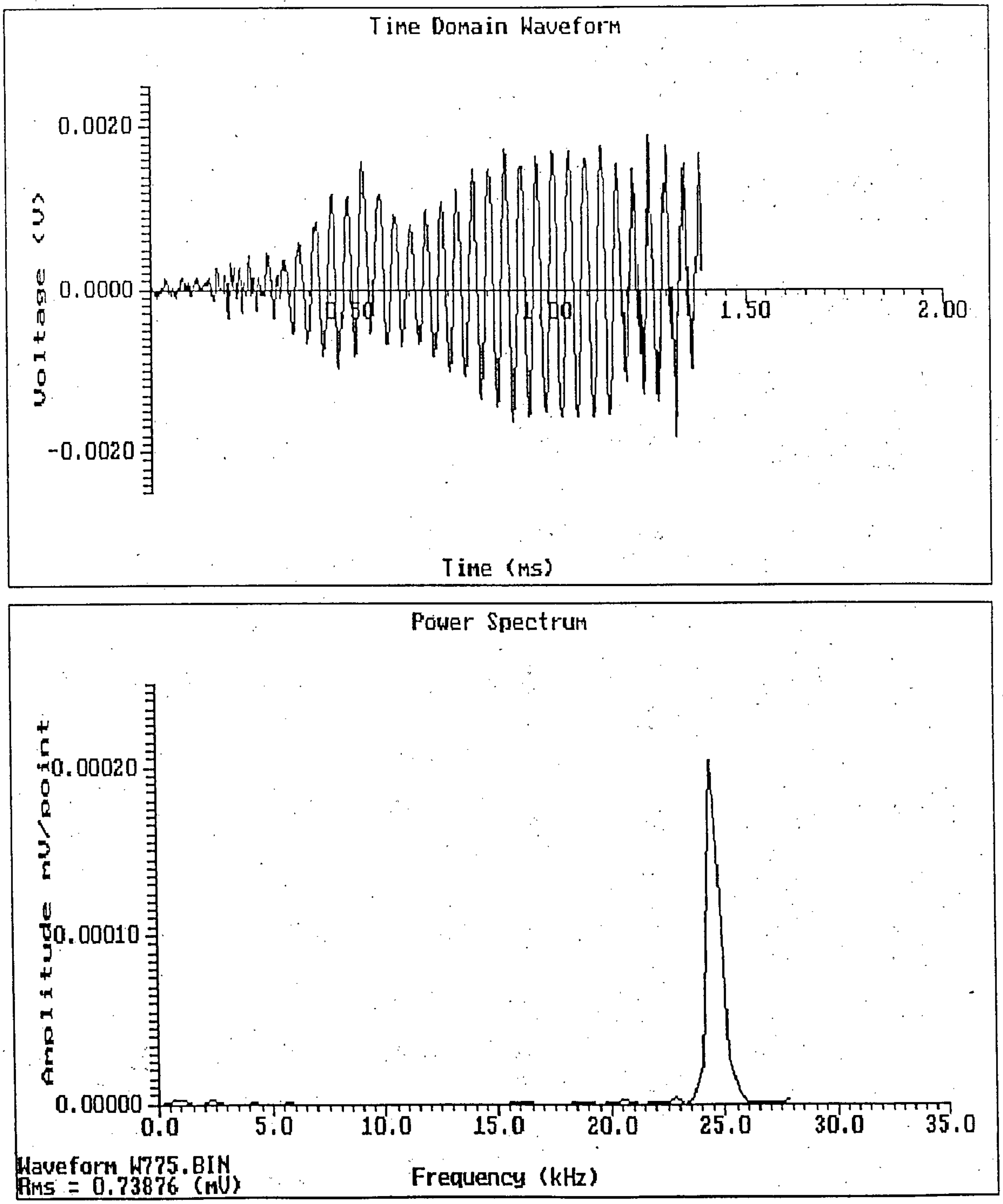

Fig. 35b. Knots influences on time domain waveform and power spectrum (Perpendicular, specimen 77, point 5, averaged lathe check depth 77.65%, PKA 1.66%, knots-free propagation line)

Appendix F

Table 2. Experimental results of stress wave parameters and veneer quality criterion

Specimen	Wave parameters (Parallel)			Wave parameters (Perpendicular)				Observed	Predicted
No	Timing	Stdev	Velocity (V_1)	Timing	Stdev	Velocity (V_2)	Attenuation	Q	Q
	(μs)		(m/s)	(μs)		(m/s)	(1 / mv)	w1=w2=1	
1	45.2	1.32	6195	276.5	6.22	1013	0.893	0.797	0.778
2	45.4	2.12	6167	254.8	15.50	1099	0.367	0.492	0.639
3	44.8	0.46	6250	297.0	23.90	943	0.341	0.917	0.886
4	47.1	4.14	5945	308.9	18.70	906	0.143	0.787	0.996
5	45.4	1.32	6167	268.2	3.89	1044	0.314	0.677	0.731
6	45.7	3.67	6127	279.6	30.91	1001	0.272	0.458	0.808
7	50.8	2.17	5512	236.1	18.74	1186	0.803	0.935	0.599
8	45.5	0.94	6154	248.5	15.11	1127	0.319	0.856	0.594
9	46.9	4.05	5970	287.1	11.60	975	0.493	0.855	0.877
10	55.5	3.08	5045	299.9	6.64	934	0.758	0.960	1.096
11	51.4	3.82	5447	243.1	7.43	1152	0.547	0.832	0.667
12	54.8	2.45	5109	229.2	10.31	1222	0.324	0.773	0.604
13	51.7	3.11	5416	246.0	12.20	1138	0.433	0.792	0.694
14	49.3	1.54	5680	232.6	10.50	1204	0.432	0.607	0.542
15	49.1	3.58	5703	245.1	3.54	1142	0.593	0.898	0.641
16	59.8	2.64	4682	216.8	15.96	1292	0.103	0.078	0.557
17	53.4	4.31	5243	269.2	14.83	1040	0.315	1.137	0.886
18	45.8	1.43	6114	228.4	8.01	1226	0.125	0.391	0.435
19	48.4	1.04	5785	243.2	26.74	1151	0.335	0.432	0.613
20	45.7	1.49	6127	294.1	15.02	952	0.727	0.975	0.891
21	44.5	2.01	6292	265.6	12.84	1054	0.706	0.697	0.693
22	43.7	0.53	6407	244.1	15.86	1147	0.23	0.749	0.520
23	41.0	1.48	6829	262.1	9.96	1068	0.681	0.826	0.583
24	45.2	2.25	6195	253.1	11.14	1106	0.197	0.678	0.622
25	42.8	0.88	6542	278.6	16.65	1005	0.71	0.823	0.735
26	45.5	1.35	6154	276.3	14.48	1013	0.551	0.856	0.784
27	52.8	2.79	5303	251.7	27.52	1112	0.035	0.285	0.756
28	42.9	1.53	6527	247.2	22.03	1133	0.334	0.639	0.524
29	45.9	1.43	6100	234.6	7.11	1194	0.402	0.393	0.491
30	44.8	1.41	6250	285.6	19.54	980	0.31	0.769	0.824
31	52.1	1.16	5374	241.1	7.17	1161	0.381	0.752	0.662
32	45.3	1.05	6181	345.8	19.51	810	0.092	1.000	1.120
33	51.6	4.79	5426	247.2	12.63	1133	0.368	0.365	0.702
34	47.1	0.61	5945	232.4	12.69	1205	0.512	0.522	0.498
35	61.1	2.73	4583	200.6	11.33	1396	0.085	0.233	0.398
36	46.3	1.67	6048	300.0	21.19	933	0.349	0.742	0.935
37	54.1	2.94	5176	269.7	16.76	1038	0.537	0.970	0.900
38	44.9	0.76	6236	243.9	10.64	1148	0.573	0.445	0.546
39	48.4	4.01	5785	266.6	14.08	1050	0.444	0.665	0.782
40	50.0	2.00	5600	227.6	15.67	1230	0.243	0.363	0.511
41	46.3	1.42	6048	276.6	2.99	1012	0.934	0.774	0.803
42	43.5	0.53	6437	253.1	30.32	1106	0.041	0.452	0.583
43	44.7	1.10	6264	294.9	11.08	949	0.361	0.837	0.873
44	43.3	0.89	6467	297.3	34.84	942	0.418	0.640	0.853
45	47.7	2.24	5870	264.1	9.55	1060	0.291	0.805	0.751
46	54.7	3.55	5119	255.9	11.15	1094	0.332	0.348	0.816
47	52.2	4.20	5364	255.8	16.32	1095	0.529	0.986	0.776
48	50.7	2.11	5523	256.8	23.13	1090	0.71	0.880	0.757
49	42.5	0.77	6588	310.4	16.00	902	0.397	0.812	0.900
50	43.7	1.24	6407	265.9	2.56	1053	0.4	0.723	0.677
51	48.1	2.75	5821	275.9	12.62	1015	0.428	0.832	0.835
52	59.9	3.09	4674	221.1	13.83	1266	0.15	0.722	0.600

Appendix F

Table 2. Experimental results of stress wave parameters and veneer quality criterion

Specimen	Wave parameters (Parallel)			Wave parameters (Perpendicular)				Observed	Predicted
No	Timing	Stdev	Velocity (V_1)	Timing	Stdev	Velocity (V_2)	Attenuation	Q	Q
	(μs)		(m/s)	(μs)		(m/s)	(1 / mv)	w1=w2=1	
53	46.9	1.77	5970	272.9	11.23	1026	0.256	0.906	0.792
54	46.3	1.25	6048	261.5	17.53	1071	0.441	0.777	0.705
55	45.8	0.66	6114	264.5	11.94	1059	0.285	0.795	0.715
56	59.1	3.13	4738	198.1	12.03	1413	0.262	0.045	0.344
57	53.1	4.05	5273	283.1	16.68	989	0.082	1.093	0.967
58	47.5	1.49	5895	231.5	10.78	1210	0.115	0.532	0.498
59	50.2	1.63	5578	229.7	9.05	1219	0.344	0.304	0.533
60	44.5	0.41	6292	269.1	13.30	1041	0.588	0.856	0.716
61	45.2	1.13	6195	260.9	12.70	1073	0.265	0.672	0.677
62	48.4	3.17	5785	210.4	6.21	1331	0.319	0.157	0.313
63	46.2	4.30	6061	256.1	15.16	1093	0.203	1.155	0.665
64	42.7	1.08	6557	248.7	3.34	1126	0.274	0.564	0.531
65	44.5	0.91	6292	274.4	21.63	1020	0.49	0.878	0.750
66	46.3	0.95	6048	268.1	9.97	1044	0.391	0.764	0.749
67	52.3	0.85	5354	207.4	3.24	1350	0.104	0.188	0.350
68	44.5	0.70	6292	254.6	14.07	1100	0.658	0.661	0.617
69	47.0	0.93	5957	233.9	8.87	1197	0.56	0.321	0.509
70	46.4	0.93	6034	284.1	9.03	986	0.231	0.788	0.850
71	52.9	0.71	5293	248.4	12.26	1127	0.19	0.650	0.733
72	50.0	1.46	5600	287.2	19.24	975	0.411	0.891	0.938
73	47.1	3.34	5945	284.0	25.70	986	0.309	0.785	0.864
74	47.7	1.39	5870	242.1	17.64	1157	0.335	0.515	0.590
75	58.2	1.75	4811	205.9	6.31	1360	0.207	0.307	0.422
76	46.3	1.03	6048	293.1	13.70	955	0.112	0.847	0.898
77	53.0	2.83	5283	273.1	14.35	1025	0.282	1.005	0.905
78	49.5	5.24	5657	258.6	12.68	1083	0.231	0.596	0.748
79	44.0	1.04	6364	281.9	15.92	993	0.188	0.692	0.784
80	53.4	2.31	5243	240.0	20.83	1167	0.054	0.753	0.675
81	50.3	2.06	5567	287.6	11.56	974	0.239	0.763	0.945
82	45.7	0.78	6127	247.1	18.65	1133	0.478	0.516	0.588
83	45.3	0.61	6181	238.8	15.26	1173	0.18	0.558	0.514
84	54.2	2.47	5166	211.6	10.58	1323	0.113	0.427	0.425
85	45.1	2.61	6208	267.3	17.85	1048	0.166	0.587	0.718
86	59.1	9.14	4738	252.3	14.20	1110	0.301	1.733	0.851
87	47.6	1.41	5882	246.4	9.59	1136	0.513	0.526	0.622
88	47.2	3.78	5932	266.8	14.59	1049	0.179	0.582	0.759
89	51.1	3.63	5479	230.1	12.19	1217	0.083	1.216	0.553
90	47.8	2.45	5858	254.9	10.00	1098	0.252	0.673	0.690
91	51.8	5.37	5405	249.6	7.76	1122	0.33	0.959	0.724
92	43.3	1.17	6467	267.7	15.74	1046	0.123	0.603	0.679
93	53.4	0.62	5243	211.2	6.16	1326	0.388	0.558	0.409
94	44.7	1.89	6264	255.5	11.06	1096	0.246	0.509	0.628
95	50.7	0.75	5523	239.4	18.91	1170	0.259	0.458	0.625
96	49.8	2.22	5622	245.7	4.83	1140	0.298	0.811	0.659
97	46.6	2.93	6009	258.7	18.49	1082	0.205	0.966	0.692
98	53.9	1.67	5195	249.4	15.75	1123	0.384	0.846	0.756
Average	48.5	2.10	5815	257.2	13.85	1100	0.350	0.694	0.694
Stdev	4.42	1.41	497.33	26.30	6.23	114.02	0.195	0.262	0.164

Appendix G

Table 3.1. AU testing results in the parallel to grain direction

Specimen No.	Original Speci. No.	Density	PKA	Parallel timings		Attenuation*	
				Average	Stdev.	Average	Stdev.
		(g/mm^3)	(%)	(μs)		(1/ mv)	
1	3	0.436	0.00	52.48	0.00	0.0420	0.0234
2	5	0.525	0.00	55.59	2.07	0.0226	0.0169
3	6	0.517	0.28	54.31	2.75	0.0181	0.0107
4	27	0.432	0.19	70.03	2.64	0.1114	0.0551
5	28	0.578	0.15	55.22	2.81	0.0429	0.0182
6	29	0.419	0.00	54.31	1.25	0.0164	0.0208
7	51	0.555	0.00	56.50	3.42	0.0114	0.0052
8	52	0.684	0.00	68.75	4.35	0.0349	0.0400
9	54	0.574	0.00	54.31	1.01	0.0122	0.0137
10	56	0.456	0.26	67.11	2.32	0.0260	0.0181
11	57	0.435	2.07	63.45	4.17	0.0600	0.0496
12	58	0.546	0.15	59.61	4.04	0.0640	0.0287
13	59	0.458	0.15	63.63	4.23	0.0737	0.0674
14	60	0.543	0.10	53.21	0.68	0.0089	0.0042
15	61	0.413	0.00	53.94	1.56	0.0158	0.0087
16	62	0.553	0.00	57.78	4.87	0.0041	0.0026
17	63	0.487	2.30	54.67	3.82	0.0237	0.0240
18	64	0.535	0.36	54.86	1.56	0.1190	0.0922
19	65	0.527	0.97	53.03	1.45	0.0118	0.0093
20	66	0.491	0.29	55.95	2.53	0.0304	0.0404
21	74	0.581	0.05	56.87	2.65	0.0106	0.0108
22	75	0.588	0.00	65.65	2.30	0.0167	0.0175
23	76	0.466	0.14	53.58	0.88	0.0133	0.0081
24	77	0.58	1.66	60.71	3.61	0.0206	0.0367
25	78	0.533	0.20	59.43	3.45	0.0158	0.0084
26	79	0.496	0.00	53.39	1.22	0.0330	0.0173

Note: * Attenuation is defined as 1/ RMS of first 100 points.

Table 3.2. AU testing results in the perpendicular to the grain direction

Specimen No.	Original Speci. No.	Density	Averaged Lathe check depth	Perpendicular timings Average	Perpendicular timings Stdev.	RMS Average	RMS Stdev.	ATT(1/ RMS)
		(g/mm^3)	(100*%)	(μs)		(mv)		(1/ mv)
1	3	0.4360	0.8860	309.8	72.50	0.6013	0.4095	1.6632
2	5	0.5250	0.7145	309.6	50.98	0.6061	0.2745	1.6500
3	6	0.5170	0.5285	247.0	135.50	0.5755	0.1086	1.7375
4	7	0.4790	0.6785	259.8	35.10	1.0421	0.6349	0.9596
5	8	0.5730	0.7750	263.5	23.00	0.7514	0.2967	1.3308
6	10	0.5450	0.8605	390.4	134.30	0.4580	0.1081	2.1834
7	14	0.5330	0.6645	219.6	7.70	1.0700	0.3335	0.9350
8	15	0.5550	0.8720	240.0	22.67	1.1265	0.5806	0.8877
9	16	0.4510	0.2305	200.9	11.12	2.1012	1.2912	0.4759
10	27	0.4320	0.4145	252.9	44.90	1.0384	0.3646	0.9630
11	28	0.5780	0.6715	295.3	32.20	0.8091	0.2972	1.2359
12	29	0.4190	0.5110	236.1	16.00	0.9842	0.4449	1.0160
13	51	0.5550	0.8250	297.0	36.82	0.5158	0.1222	1.9387
14	52	0.6840	0.7465	223.8	29.90	0.8996	0.2947	1.1116
15	54	0.5740	0.7855	256.0	12.70	0.8586	0.2640	1.1676
16	55	0.5440	0.7930	269.3	18.35	0.7493	0.1553	1.3346
17	56	0.4560	0.2360	194.9	11.35	2.3868	0.7904	0.4190
18	57	0.4350	0.7965	268.6	39.70	0.5862	0.0757	1.7059
19	58	0.5460	0.5950	235.0	17.22	1.3495	0.3830	0.7410
20	59	0.4580	0.4320	235.5	18.07	1.3283	0.6954	0.7529
21	60	0.5430	0.8320	312.7	25.97	0.8343	0.3313	1.1986
22	61	0.4130	0.7105	286.5	29.40	1.8726	0.8782	0.5340
23	62	0.5530	0.3425	209.2	10.98	1.3022	0.6133	0.7679
24	63	0.4870	0.8175	274.6	13.80	0.7895	0.2673	1.2666
25	64	0.5350	0.5965	294.0	27.03	0.9070	0.4825	1.1026
26	65	0.5270	0.7570	311.8	43.09	0.7498	0.2952	1.3337
27	66	0.4910	0.7460	346.9	32.95	0.7373	0.3029	1.3563
28	68	0.5500	0.6965	249.9	9.20	0.9466	0.3639	1.0564
29	74	0.5810	0.5930	231.3	14.21	0.5628	0.0809	1.7770
30	75	0.5880	0.4500	190.9	3.00	2.9915	1.1300	0.3343
31	76	0.4660	0.8215	307.6	24.30	0.5889	0.1291	1.6980
32	77	0.5800	0.7765	300.8	47.90	0.5976	0.1337	1.6735
33	78	0.5330	0.6355	257.6	25.30	0.9857	0.4337	1.0146
34	79	0.4960	0.7250	323.1	30.90	0.6030	0.1210	1.6583
35	84	0.5800	0.5140	194.5	3.13	3.3357	1.2318	0.2998
36	85	0.4930	0.6500	253.8	12.37	0.7215	0.1801	1.3861
37	86	0.5750	0.7540	298.0	60.82	0.5577	0.1640	1.7931
38	88	0.5230	0.6465	237.1	19.44	0.9325	0.4366	1.0724
39	91	0.4960	0.7290	283.5	35.20	1.0020	0.4260	0.9979
40	93	0.5300	0.6290	206.4	12.02	2.2876	0.6978	0.4371
41	94	0.5860	0.5945	246.8	21.83	1.0638	0.5341	0.9400
42	95	0.4930	0.5575	222.1	7.85	1.3309	0.5893	0.7514
43	96	0.5440	0.7610	251.0	34.72	0.8364	0.1781	1.1955
44	97	0.5160	0.5465	239.7	13.76	0.8905	0.6037	1.1230
45	98	0.4930	0.8350	232.8	16.53	0.7579	0.5520	1.3195
46	71	0.4840	0.6890	246.6	N/A	0.7118	N/A	1.4049
47	81	0.4720	0.7675	439.0	N/A	0.3936	N/A	2.5206
48	87	0.5230	0.5645	256.9	N/A	0.5567	N/A	1.7964
49	89	0.5030	0.6430	230.0	N/A	0.6401	N/A	1.5622
50	90	0.4990	0.6790	270.9	N/A	0.5287	N/A	1.8916

Note: N/A means not applicable since specimens 46-50 only had 3 sampling points each.